SOLUTION OF THE GENERAL BOUNDARY-LAYER EQUATIONS FOR COMPRESSIBLE LAMINAR FLOW, INCLUDING TRANSVERSE CURVATURE

By

DARWIN W. CLUTTER and A. M. O. SMITH

Report No. LB 31088

15 February 1963

PREPARED UNDER NAVY, BUREAU OF NAVAL WEAPONS, CONTRACT NOw 60-0533c.

DOUGLAS AIRCRAFT DIVISION

SOLUTION OF THE GENERAL BOUNDARY-LAYER EQUATIONS FOR COMPRESSIBLE LAMINAR FLOW, INCLUDING TRANSVERSE CURVATURE

By

DARWIN W. CLUTTER and A. M. O. SMITH

Report No. LB 31088

15 February 1963

PREPARED UNDER NAVY CONTRACT NOw 60-0553c,
ADMINISTERED UNDER TECHNICAL DIRECTION
OF THE BUREAU OF NAVAL WEAPONS FLUID
MECHANICS AND FLIGHT DYNAMICS BRANCH, RRRE-4.

Douglas Aircraft Co., Inc. ■ Aircraft Division ■ Long Beach, California

1.0 SUMMARY

An accurate and rapid method is presented for solution of the general equations of compressible, steady, laminar-boundary-layer flow. The method allows arbitrary conditions on all of the following: pressure gradient, surface temperature and its gradient, heat transfer, mass transfer, and fluid properties. Also, the method can calculate the second-order effect of transverse curvature. The only restrictions on the method are that the body be axially symmetric or two-dimensional and that no dissociation of the fluid occurs.

The equations that are solved are developed from the Navier-Stokes and energy equations by an order-of-magnitude analysis. They differ from the conventional boundary-layer equations of Prandtl only in that the second-order terms that include transverse curvature are retained.

The method of solution consists of replacing the partial derivatives with respect to the flow direction by finite differences, while retaining the derivatives in a direction normal to the boundary, so that the partial differential equations become approximated by ordinary differential equations. Reasons for choosing this method rather than the more conventional finite-difference methods are discussed.

Arbitrary fluid properties may be used in the method of solution, that is, they are inputs in the computer program in the form of formulas or tables as functions of local enthalpy and pressure. Results obtained with the method using exact fluid properties for air are compared with those using simpler fluid-property laws. These simpler laws, which often have been used in the past in boundary-layer investigations, are shown often to give poor predictions of heat transfer and skin friction at high speeds.

The method has been programmed on the IBM 7090 computer, and solutions for a wide variety of flows are presented. Comparisons are made with other exact and approximate methods of solutions. The flows include cases of heat transfer, mass transfer, and discontinuities in the boundary conditions over a large range in Mach number (Mach 0.0 to 10.0). Some comparison with ex-

perimental measurement is also made. Also a study of the effect of transverse curvature on the flow over cones is presented. The large number of calculations and comparisons establish that the method is rapid, highly accurate, and powerful. It appears capable of solving any flow problem for which the boundary-layer equations themselves remain valid.

2.0 TABLE OF CONTENTS

3.0 INDEX OF FIGURES

4.0 PRINCIPAL NOTATION

a	local velocity of sound
$a_1, a_2, \ldots$ $b_1, b_2, \ldots$ $c_1, c_2, \ldots$	constants defined where applicable
$A_1, A_2, \ldots$ $B_1, B_2, \ldots$ $C_1, C_2, \ldots$	constant coefficients defined where applicable
c	chord length
c_f	local skin-friction coefficient, eq.(6.114)
c_f^*	skin-friction parameter, eq.(6.116)
c_p	specific heat at constant pressure
C	$\frac{\rho \mu}{\rho_e \mu_e}$
f	nondimensional stream function, defined by eq.(6.7)
$\overline{F}$	body force
g	nondimensional total enthalpy ratio = H/H_e
h	local enthalpy
h_{ref}	reference enthalpy used in fluid property relation from Ref. 7, = 2.119×10^8 ft^2/sec^2
H	total enthalpy = $h + \frac{1}{2} u^2$
i	count of successive tries in procedure for solving momentum equation (Appendix B)
$\overline{i}, \overline{j}$	unit vector, eq.(A-5)
k	thermal conductivity
K	bound in computer program on values of φ'
L	count of successive solutions of the energy equation and fluid properties in the procedure of solution
m	the exponent in the free stream velocity variation, $U = c_1 x^m$

M	Mach number
n	count of the number of steps in the x-direction
N	$\frac{P+1}{2} + R$
p	pressure
P	$\frac{x}{u_e}\frac{du_e}{dx}$
Pr	Prandtl number
q	heat transfer
Q	count of successive solutions of the momentum equation in the procedure of solution
r	radial distance from axis of revolution
r_o	radius of body of revolution
r_f	recovery factor, defined by eq.(7.10)
R	$\frac{x}{r}\frac{dr}{dx}$
Re	Reynolds number = $\frac{\rho_e u_e x}{\mu_e}$
St	Stanton number, defined by eq.(6.120)
T	transverse curvature term defined by Eq.(6.32) except in Sections 7.3 and 7.4 where it is absolute temperature
u	x component of velocity, $\frac{u}{u_e} = f'$
v	y component of velocity
$\overline{V}$	vector velocity, eq.(A-5)
x	distance along body surface measured from stagnation point
X	axial or chordwise distance
$\overline{X}$	body force in x-direction
y	distance normal to x
Y	nondimensional normal distance, eq.(6.106)
$\overline{Y}$	body force in y-direction

α	angle between normal to the surface y and the radius r
β	Hartree's measure of free-stream velocity distribution in similar flow, $\beta = \frac{2m}{m+1}$
γ	ratio of specific heats, c_p/c_v
δ	thickness of boundary layer
δ^*	displacement thickness
Δ^*	dimensionless displacement thickness, eq.(6.103)
ϵ	specified accuracy in program
η	transformed y coordinate, eq.(6.4)
η_∞	either a very large η, that is, outside the boundary layer or η at the edge of the boundary layer, i.e., $= \eta_e$
θ	momentum thickness
θ	dimensionless momentum thickness, eq.(6.110)
μ	dynamic viscosity
ν	kinematic viscosity
ξ	variable of integration, or in Section 7.9, a transverse curvature parameter
π	function in energy equation defined by eq.(6.50)
ρ	density
τ	shear stress
φ	transformed stream function $= f - \eta$, see eq.(6.36)
ψ	in Section 6.1, a stream function defined by eqs.(6.5 and 6.7); in all other Sections, the enthalpy function $g - 1$, eq.(6.45)

SUBSCRIPTS

ad	evaluated at adiabatic wall
e	evaluated at outer edge of boundary layer

n	evaluated at station n
rec	evaluated at recovery temperature, $T_{rec} = T_{ad}$
ref	evaluated ar reference enthalpy
stag	evaluated at stagnation point
t	evaluated at total temperature
w	evaluated at wall
oo	evaluated at a reference condition, or see η_{∞}
o	usually means evaluated at initial condition, $x = 0$. One exception is r_o

Primes denote differentiation with respect to η. $\frac{\partial f}{\partial \eta} = f'$, etc.

5.0 INTRODUCTION

The present work was started because there were many problems of laminar boundary-layer flow for which no satisfactory solutions had been found. Among them were questions on high-speed heat transfer and the effects of heat transfer and wall mass transfer on drag. Answers to these questions require an exact general method for solving the boundary-layer equations. Available methods for solving the boundary-layer equations appeared inadequate. Integral methods can treat general flows, but they give only approximate solutions. Similar-flow methods are accurate but are restricted to special pressure distributions. When the work was started, finite-difference methods appeared to require unreasonably long computing times for accuracy. Therefore, studies were made to develop a practical method for solving "exactly" the complete equations of compressible boundary-layer flow in two-dimensions. The sense of "exactly" as used here is that the solution approaches the exact as the step length in the calculation procedure approaches zero. The objective of the studies was to find a method capable of obtaining solutions for arbitrary values of (1) pressure distribution. (2) wall mass-transfer distribution, (3) gas properties, and (4) wall temperature distribution. The only restriction on the flow was that it be two-dimensional or axially symmetric.

The problem was approached by first finding a method that gave an accurate solution for the general incompressible boundary-layer equation. An accurate and rapid method was developed and is presented in References 1, 2, and 3. The method is a modification of the Hartree-Womersley technique. It consists of replacing the partial derivatives with respect to the flow direction by finite differences, while retaining the derivatives in a direction normal to the boundary, so that the partial differential equation becomes approximated by an ordinary differential equation. The method was programed on an electronic computer, and solutions for a wide variety of flows were calculated and are presented in References 1 and 2. The large number of calculations and their comparison with other exact and approximate solutions establish that the method is rapid, highly accurate, and powerful. It is capable of solving any flow problem for which the incompressible boundary-layer equations themselves are valid. The mathematics of the solution, that

is, the behavior of the process of solution, the nature of solution, its difficulties, etc., are reported in Reference 3. Also, the reasons for choosing the present method rather than the more conventional finite-difference methods are discussed.

After the method of solution had proved successful for incompressible flow it was extended and modified to solve the fully general laminar boundary-layer equations for compressible flow. The only restrictions are that the flow be two-dimensional or axially symmetric and that no dissociation occur .

The purpose of this report is to describe this method for solving the compressible flow equations and establish its validity. Section 6.0 develops the equations, by starting with the Navier-Stokes equations. The second-order effect of transverse curvature is retained. Steps in the procedure for solving the equations are described, and the reasons for choosing them over other possibilities are discussed. Section 7.0 consists of the results of calculations of a wide variety of flows. They establish the accuracy of the method. Wherever possible comparisons of the calculations are made with other methods and with experiment.

6.0 DESCRIPTION OF METHOD OF SOLUTION

6.1 Boundary-Layer Equations

The problem to be considered is axisymmetric, steady, equilibrium flow about a body of revolution. The equations necessary to describe such a flow are those of continuity, momentum, and energy. Also the equation of state and relations describing the fluid properties such as viscosity and specific heat are required.

The problem will be restricted to high Reynolds number, so that the Navier-Stokes and energy equations are simplified to essentially the form of the boundary-layer equations as originally developed by Prandtl in 1904. The second-order effect of transverse curvature that was neglected by Prandtl will be considered here. Van Dyke considered all second-order effects identified as: transverse curvature, longitudinal curvature, slip, temperature jump, entropy gradient, stagnation enthalpy gradient and displacement in a recent article for the special case of a blunt body (Reference 4). As pointed out by Van Dyke, logically, all second-order effects should be considered concurrently, but consideration of all these effects is beyond the scope of the present work. The effect of transverse curvature is included because of its importance in predicting boundary-layer growth on long slender bodies, such as certain missiles.

The basic notation and scheme of coordinates are shown in figure 1, where u_∞ is a reference velocity and $u_e(x)$ is the velocity of the main flow just outside the boundary layer. The term H_e represents the total enthalpy outside the boundary layer and is constant. Local enthalpy outside the boundary layer h_e is given from the relation

$$H_e = h_e + \frac{1}{2} u_e^2 = h_\infty + \frac{1}{2} u_\infty^2$$

The coordinates are a curvilinear system in which x is distance along the surface measured from the stagnation point. The dimension y is measured normal to the surface. Within the boundary layer the velocity components are u and v, being, respectively, in the x and y directions. The body radius is r_o.

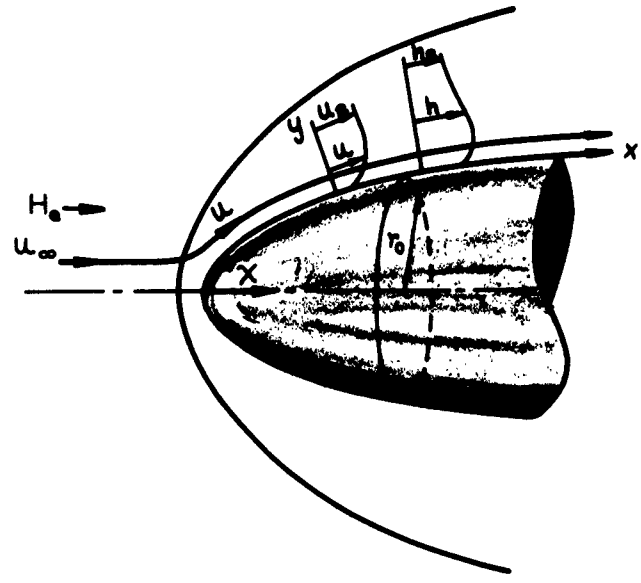

Figure 1.- Boundary layer on a body of revolution. Coordinate system.

The basic steady-flow equations for a laminar boundary layer in the above coordinate system are developed in Appendix A. They are, including the transverse-curvature terms:

CONTINUITY

$$\frac{1}{r}\left[\frac{\partial}{\partial x}(r\,\rho\,u) + \frac{\partial}{\partial y}(r\,\rho\,v)\right] = 0 \tag{6.1}$$

MOMENTUM

$$\rho\left[u\frac{\partial u}{\partial x} + v\frac{\partial u}{\partial y}\right] = -\frac{dp}{dx} + \frac{\mu}{r}\frac{\partial r}{\partial y}\frac{\partial u}{\partial y} + \frac{\partial}{\partial y}\left(\mu\frac{\partial u}{\partial y}\right) \tag{6.2}$$

ENERGY

$$\rho\left[u\frac{\partial H}{\partial x} + v\frac{\partial H}{\partial y}\right] = \frac{1}{r}\frac{\partial r}{\partial y}\left[\frac{\mu}{Pr}\frac{\partial H}{\partial y} + \mu\left(1-\frac{1}{Pr}\right)u\frac{\partial u}{\partial y}\right]$$

$$+ \frac{\partial}{\partial y}\left[\frac{\mu}{Pr}\frac{\partial H}{\partial y} + \mu\left(1-\frac{1}{Pr}\right)u\frac{\partial u}{\partial y}\right] \tag{6.3}$$

Equations (6.2) and (6.3) differ from the forms usually obtained when the Prandtl boundary-layer approximations are made, because they contain the transverse curvature terms:

$$\frac{\mu}{r}\frac{\partial r}{\partial y}\frac{\partial u}{\partial y} \qquad \text{in (6.2)}$$

and

$$\frac{1}{r}\frac{\partial r}{\partial y}\left[\frac{\mu}{Pr}\frac{\partial H}{\partial y} + \mu\left(1 - \frac{1}{Pr}\right) u \frac{\partial u}{\partial y}\right] \qquad \text{in (6.3)}$$

6.2 Transformed Boundary-Layer Equations

Whereas the above equations could perhaps be solved by the method to be presented, they will be transformed to a more convenient coordinate system. Flügge-Lotz and Blottner have solved the above equations essentially as they are written, though simplified relations for the fluid properties—viscosity and Prandtl number—were used (Reference 6). The equations as written have several disadvantages; for example, they may be singular at $x = 0$, and the boundary-layer thickness varies greatly with distance.

These difficulties can be overcome by stretching of the coordinate normal to the wall y. The transformation that has proven most effective for accomplishing the stretching is that of Howarth-Dorodnitsyn, where

$$\eta_H = \int_0^y \rho \, dy$$

$$\xi = x$$

It is felt that a second requirement of the transformation of the y-coordinate be that it should reduce to the incompressible transformation that was studied extensively by the authors in References 1, 2, and 3. Therefore, consider the transformation

$$\left.\begin{aligned} \eta &= \sqrt{\frac{u_e}{\rho_\infty \mu_\infty x}} \int_0^y \rho \, dy \\ x &= x \end{aligned}\right\} \qquad (6.4)$$

Also, it is convenient to describe a stream function ψ such that

$$\left.\begin{aligned} \rho\, r\, u &= \frac{\partial(\psi r)}{\partial y} \\ \rho\, r\, v &= -\frac{\partial(\psi r)}{\partial x} \end{aligned}\right\} \tag{6.5}$$

Furthermore, as was done in incompressible flow, it is convenient to introduce a dimensionless stream function f such that

$$\frac{\partial f}{\partial \eta} = f' = \frac{u}{u_e} \tag{6.6}$$

The relation between f and ψ is

$$\psi = \sqrt{\rho_\infty \mu_\infty x\, u_e}\; f \tag{6.7}$$

In order to transform the boundary-layer equations above to x, η - coordinates, the following relations are used:

$$\begin{aligned} \left(\frac{\partial}{\partial x}\right)_y &= \left(\frac{\partial x}{\partial x}\right)_y \left(\frac{\partial}{\partial x}\right)_\eta + \left(\frac{\partial \eta}{\partial x}\right)_y \left(\frac{\partial}{\partial \eta}\right)_x \\ &= \frac{\partial}{\partial x} - \frac{1}{2}\,\frac{\eta}{x}\,\frac{\partial}{\partial \eta} + \frac{1}{2}\,\frac{\eta}{u_e}\,\frac{du_e}{dx}\,\frac{\partial}{\partial \eta} + \eta\,\frac{\int_0^y \frac{\partial \rho}{\partial x}\,dy}{\int_0^y \rho\, dy}\,\frac{\partial}{\partial \eta} \end{aligned} \tag{6.8}$$

$$\begin{aligned} \left(\frac{\partial}{\partial y}\right)_x &= \left(\frac{\partial x}{\partial y}\right)_x \left(\frac{\partial}{\partial x}\right)_\eta + \left(\frac{\partial \eta}{\partial y}\right)_x \left(\frac{\partial}{\partial \eta}\right)_x \\ &= \sqrt{\frac{u_e}{\rho_\infty\, \mu_\infty\, x}}\;\rho\;\frac{\partial}{\partial \eta} \end{aligned} \tag{6.9}$$

The continuity equation is automatically satisfied by the definition of the stream function.

The momentum equation (6.2) becomes the following in the transformed plane:

$$\frac{1}{C_\infty}\,\frac{1}{r}\,\frac{\partial}{\partial\eta}\,(C\,r\,f'') + P\left(\frac{\rho_e}{\rho} - f'^2\right) + \left[\frac{P+1}{2} + R\right] ff''$$

$$- x\left[f'\,\frac{\partial f'}{\partial x} - f''\,\frac{\partial f}{\partial x}\right] = 0 \qquad (6.10)$$

where:

primes denote differentiation with respect to η,

$$C \equiv \frac{\rho\,\mu}{\rho_e\,\mu_e} \qquad (6.11)$$

$$C_\infty \equiv \frac{\rho_\infty\,\mu_\infty}{\rho_e\,\mu_e} \qquad (6.12)$$

$$P \equiv \frac{x}{u_e}\,\frac{du_e}{dx} = \text{Pressure gradient parameter}^* \qquad (6.13)$$

$$R \equiv \frac{x}{r}\,\frac{dr}{dx} \quad = \text{Radius parameter} \qquad (6.14)$$

For equation (6.10) the boundary conditions are:

$$\eta = 0: \quad f'(0) = f'_w = 0, \quad f(0) = f_w \qquad (6.15)$$

If the wall is impermeable, $f_w = 0$; but with flow through the surface

$$(\rho\,r\,v)_w = -\frac{\partial(\psi r)_w}{\partial x}$$

Then

$$(\psi r)_w = -\int_0^x \rho_w(\xi)\,v_w(\xi)\,r_w(\xi)\,d\xi$$

---

* In the incompressible reports (References 1, 2, and 3) M was used for the pressure gradient parameter but it is changed here to prevent any confusion with Mach number.

$$f_w = \frac{\psi_w}{\sqrt{\rho_\infty \mu_\infty x u_e}} = -\frac{\sqrt{\frac{\rho_\infty u_\infty}{\mu_\infty}}}{r_w \sqrt{x \frac{u_e}{u_\infty}}} \int_0^x \frac{\rho_w v_w}{\rho_\infty u_\infty} r_w \, dx \qquad (6.16)$$

Note that v_w positive corresponds to blowing; negative to suction. The outer boundary conditions are

$$\eta \longrightarrow \infty: \qquad f' \longrightarrow 1$$

$$f'' \longrightarrow 0$$

A few of the more important properties of eq.(6.10) are noted. If the edge velocity is of the form $u_e = c_1 x^P$, $(x/u_e)(du_e/dx)$ is identically P. If $r = c_1 x^R$, $R = (x/r)(dr/dx)$. If P and R are constants it can be shown that the equation is independent of x and provides the so-called similar solutions.

Equation (6.10) has several advantages over other possible forms. Other forms are singular at $x = 0$ and require that an initial profile be specified, usually some distance from the leading edge; but in (6.10) the term containing the x-derivatives disappears at the start of the flow, and the solution can be started with a similar flow. Finally, the equation reduces to the incompressible form which was studied extensively in References 1, 2, and 3. Thus, not only does form (6.10) have the advantages that are discussed in these references for incompressible flow, but also the large number of flows studied there may be used as a check on the present method.

To transform the energy equation (6.3) to the x, η -plane, first define the enthalpy ratio g

$$g = \frac{H}{H_e} \qquad (6.17)$$

and let

$$\frac{\partial g}{\partial \eta} = g' \qquad (6.18)$$

Then (6.3) becomes

$$\frac{1}{C_\infty}\,\frac{1}{r}\,\frac{\partial}{\partial\eta}\left\{r\left[\frac{C}{Pr}\,g' + \frac{u_e^2}{H_e}\,C\left(1-\frac{1}{Pr}\right)f'f''\right]\right\}$$

$$= -\left[\frac{P+1}{2} + R\right] f\,g' + x\left[f'\,\frac{\partial g}{\partial x} - g'\,\frac{\partial f}{\partial x}\right] \qquad (6.19)$$

In the solution of (6.19) either the wall temperature or the heat transfer at the wall, corresponding, respectively, to g_w and g_w' will be specified. The outer boundary condition is

$$g(\eta) \longrightarrow 1 \qquad \text{as} \qquad \eta \longrightarrow \infty \qquad (6.20)$$

6.3 Fluid Properties

Fluid properties that appear in the momentum and energy equations are density ρ, viscosity μ, and Prandtl number Pr. These equations were developed to be valid so long as the fluid is in equilibrium, that is, the fluid properties are functions only of local conditions — pressure and enthalpy. Previous investigators have usually used simplified laws for these properties, such as, a power law or Sutherland's law for viscosity and a constant value of the Prandtl number. Whereas it is known that these laws do not accurately represent the properties over the entire flight regime of interest, the effect of these inaccuracies on the solution of the boundary-layer equations has never been investigated. The present method of solution has been developed so that arbitrary fluid properties may be used. That is, they are inputs in the program in the form of formulas or tables as functions of local enthalpy and pressure. There is no restriction on the fluid to be considered, that is, the flow may be in either air, helium, water, or some other medium. All that is required is that the fluid be in equilibrium and its properties be specified in the proper form.

All of the flows to be presented in this report are for air without dissociation. Relations for fluid properties that will be used have been chosen

from Reference 7. Reasons for this choice are: (1) The relations correlate well with the known properties of air throughout the sensible flight regime, up to velocities of 29,000 ft/sec and an altitude of 250,000 ft. (2) The relations are presented as functions of local enthalpy and pressure, whereas most other reports present the properties as function of temperature and pressure. (3) The reference also considers equilibrium dissociating air and the relations presented are compatible when either dissociation or no dissociation occurs. Whereas the present report is restricted to nondissociating gases, it is planned to extend the method presented here to dissociating gases in equilibrium. Thus the relations of reference 7 would be consistent for such an extension to flow in air.

Cohen (Reference 7) presents formulas for density and the product of density and viscosity and a table of Prandtl numbers all as functions of a local enthalpy ratio h/h_{ref} and static pressure p. He chose h_{ref} to be about the average value of total enthalpy encountered in the sensible flight regime

$$h_{ref} = 2.119 \times 10^{8} \text{ ft}^2/\text{sec}^2 \tag{6.21}$$

The enthalpy ratio can be obtained from the functions of f and g of the momentum and energy equations from the relations:

$$H = h + \frac{u^2}{2} \tag{6.22}$$

$$\frac{h}{h_{ref}} = \frac{H}{h_{ref}} - \frac{1}{2}\frac{u^2}{h_{ref}}$$

$$= g\frac{H_e}{h_{ref}} - f'^2 \frac{u_e^2}{u_\infty^2}\frac{u_\infty^2}{2h_{ref}} \tag{6.23}$$

Note that H_e/h_{ref} and u_∞^2/h_{ref} are constants for the flow, u_e^2/u_∞^2 is a function of x only, and g and f' are functions of both η and x.

Cohen's formulas for the variation of density with enthalpy in the boundary layer (recall that there is no pressure change in the boundary layer) can be written as

$$\frac{\rho_e}{\rho} = \frac{(h/h_{ref})^{0.6123} - 0.0455283}{(h_e/h_{ref})^{0.6123} - 0.0455283} \tag{6.24}$$

With regard to the accuracy of (6.24), Cohen states "the function fits the data reasonably well over the range $0.0152 \leq h/h_{ref} \leq 2.0$" for pressures in the range 10^{-4} to 10 atmospheres. "The maximum deviation in this range is about ± 25 percent at low enthalpy and the average deviation for all data is about ± 5 percent. Agreement is best in the range $0.2 < h/h_{ref} < 1.6$".

Viscosity appears in the boundary-layer equations as the product of viscosity and density. This product is a function of enthalpy only across the boundary layer , and its ratio C according to Reference 7 is

$$C = \frac{\rho\,\mu}{\rho_e \mu_e} = \frac{(h_e/h_{ref})^{0.3329} - 0.020856}{(h/h_{ref})^{0.3329} - 0.020856} \tag{6.25}$$

The variation of C outside the boundary layer is also required and is given by

$$C_\infty = \frac{\rho_\infty \mu_\infty}{\rho_e \mu_e} = \frac{(h_e/h_{ref})^{0.3329} - 0.020856}{(h_\infty/h_{ref})^{0.3329} - 0.020856} \left(\frac{p_\infty}{p_e}\right)^{0.992} \tag{6.26}$$

where

$$\frac{h_\infty}{h_{ref}} = \frac{H_e}{h_{ref}} - \frac{u_\infty^2}{2h_{ref}}$$

With regard to the accuracy with which (6.25) and (6.26) agree with data, Cohen states:" Maximum deviation is about ± 8 percent and the average deviation in the entire range $0.0152 \leq h/h_{ref} \leq 2.0$ is about ± 3 percent." For flows where h/h_{ref} is less than 0.015, a linear viscosity law is used and the density is taken as inversely proportional to local enthalpy.

Reference 7 presents the variation of Prandtl number with enthalpy in table form (Table 1, page 26 of Ref.7). Whereas it is possible to use this

table as an input in the computer program for solving the boundary-layer equations, a simpler and more accurate method is to fit relations to the tabular values. It has been found that the following three least-square relations fit the tabular values with an error of less than 0.22 percent over the range of data.

For $0.005 \leq h/h_{ref} \leq 0.075$,

$$Pr = 0.77 + \sum_{n=1}^{6} a_n \left(\frac{h}{h_{ref}} - 0.005\right)^n \tag{6.27a}$$

where

$$a_1 = -\ 6.18253 \qquad a_4 = -\ 642822.0$$
$$a_2 = -\ 147.9245 \qquad a_5 = +\ 8.00559 \times 10^6$$
$$a_3 = +\ 21609.81 \qquad a_6 = -\ 3.66200 \times 10^7$$

For $0.075 \leq h/h_{ref} \leq 0.30$,

$$Pr = 0.7374 + \sum_{n=1}^{6} b_n (h/h_{ref} - 0.075)^n \tag{6.27b}$$

where

$$b_1 = +\ 2.009 \qquad b_4 = -\ 3319.69$$
$$b_2 = -\ 45.112 \qquad b_5 = +\ 10613.04$$
$$b_3 = +\ 524.907 \qquad b_6 = -\ 13410.82$$

For $0.30 \leq h/h_{ref} \leq 2.0$,

$$Pr = 0.755 + \sum_{n=1}^{3} c_n (h/h_{ref} - 0.30)^n \tag{6.27c}$$

where

$$c_1 = -\ 0.1299$$
$$c_2 = +\ 0.05757$$
$$c_3 = +\ 0.001323$$

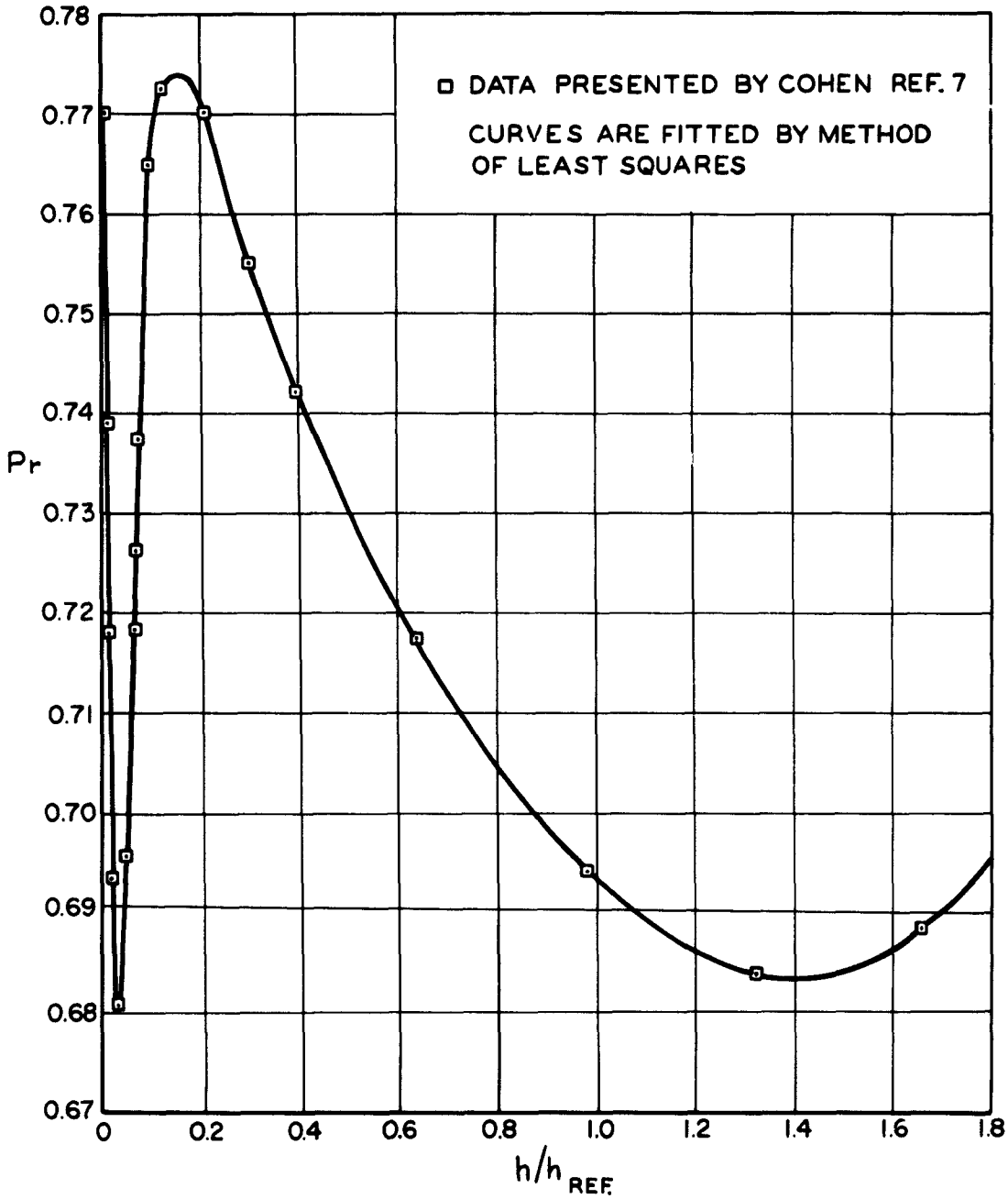

Figure 2.– Variation of Prandtl number with enthalpy. Cohen's data of Reference 7 and fitted curve.

These relations and the tabular values from Reference 7 are plotted in figure 2. At very low enthalpies, it is seen that the Prandtl number, both Cohen's data and the fitted curves, increases rapidly as enthalpy decreases. It is believed that Prandtl number should have a value of 0.72 at the lower enthalpies. Therefore, if $h/h_{ref} < 0.015$, this value is used in the program.

Boundary layer in flows of fluids other than air or in air with other fluid-property laws can be handled by replacing the relations of this section by ones appropriate to the flow being studied.

6.4 Choice of Procedure for Solution of Boundary-Layer Equations

The method of solution will be similar to that used in the study of the incompressible boundary layer (References 2 and 3). The x-derivatives in the momentum and energy equations are replaced by finite differences, so that the partial differential equations are approximated by ordinary differential equations. Then the problem of solution is essentially to find the unknown boundary conditions at the wall that satisfy the known outer boundary conditions. This is done by a cut-and-try procedure, which is described in Sections 6.5 and 6.6. The momentum equation (6.10) and the energy equation (6.19) are interdependent and must be solved simultaneously.

Several procedures for solving the equations simultaneously are possible. Three are:

I. Starting with assumed boundary conditions at the wall, solve the two equations simultaneously with the appropriate fluid properties. A cut-and-try procedure would be used on the wall values until the outer boundary conditions are satisfied.

II. To get started, assume an enthalpy distribution (and thus the fluid properties) and calculate the momentum equation. Again a cut-and-try procedure would be required. Values of the stream function f and the velocity f' from the first solution of the momentum equation would be used in the solution of the energy equation and the fluid properties. The new fluid properties would be used again to solve the momentum equation. This iterative procedure would be continued until convergence of the solution is obtained. A diagram of

the procedure is sketched below.

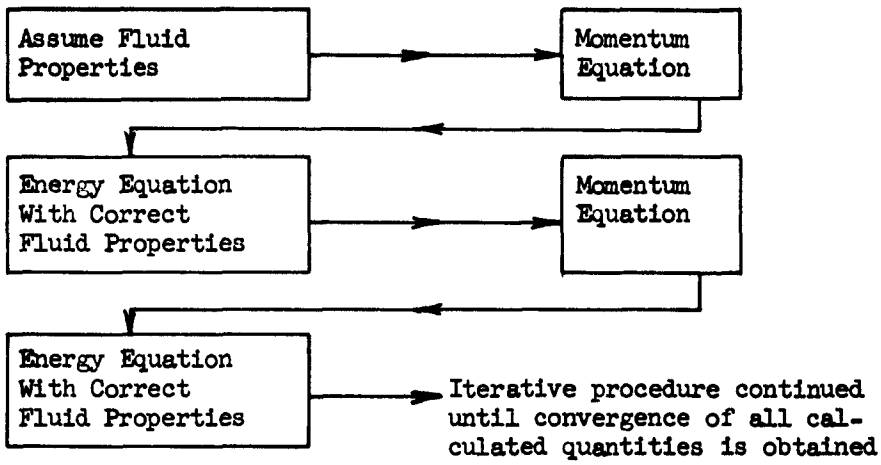

III. Again,to get started, the fluid properties are assumed to get a first solution of the momentum equation. The energy equation is then calculated, but by using the assumed fluid properties. By use of this assumption, the energy equation is linear, and thus its solution is considerably simplified. Then the calculated enthalpies are used to determine new fluid properties,which are used to solve anew the energy equation. Once convergence of the fluid properties is obtained, the momentum equation is solved a second time. This double-iteration procedure is continued until convergence of both the momentum and energy equations is obtained. The procedure is diagramed on the next page.

Studies indicate that the solution will be simpler and probably more accurate if derivatives of the fluid properties, such as $\partial C/\partial\eta$, $\partial(\rho_e/\rho)/\partial\eta$, etc., do not have to be evaluated in the solution. This forces the use of Procedure III above, for consider the energy equation (6.19)

III. PROCEDURE FOR SOLVING EQUATIONS SIMULTANEOUSLY

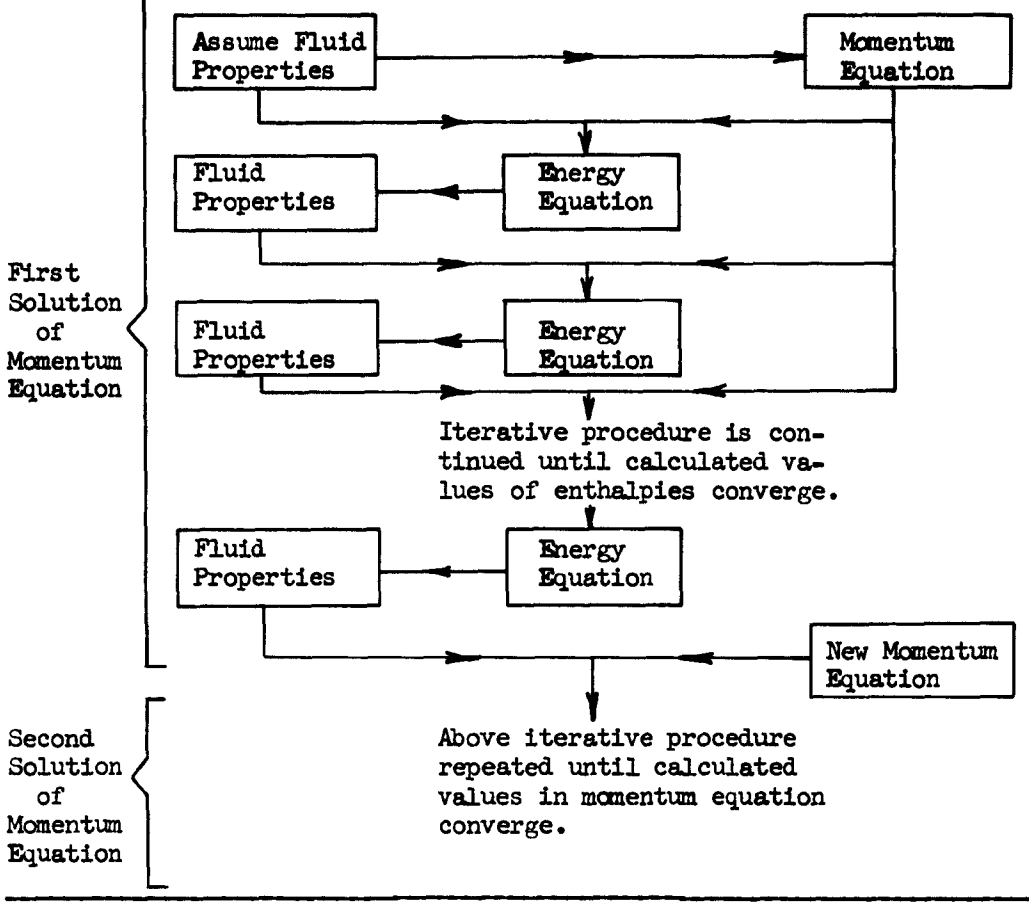

$$\frac{1}{C_\infty}\frac{1}{r}\frac{\partial}{\partial\eta}\left\{r\left[\frac{C}{Pr}\,g' + \frac{u_e^2}{H_e}\,C\left(1-\frac{1}{Pr}\right)f'f''\right]\right\}$$

$$= x\left[f'\frac{\partial g}{\partial x} - g'\frac{\partial f}{\partial x}\right] - \left[\frac{P+1}{2} + R\right] f\,g' \qquad (6.19)$$

To keep from using values of $\partial C/\partial\eta$ one must solve

$$\left\{r\left[\frac{C}{Pr}\,g' + \frac{u_e^2}{H_e}\,C\left(1-\frac{1}{Pr}\right)f'f''\right]\right\}_{\eta_1}$$

$$= C_\infty \int_0^{\eta_1} r\left\{x\left[f'\frac{\partial g}{\partial x} - g'\frac{\partial f}{\partial x}\right] - \left[\frac{P+1}{2} + R\right] f\,g'\right\} d\eta + K \qquad (6.28)$$

Thus the left-hand side of (6.28) can be determined, but the values of C and Pr depend on g, which must be determined by integrating g'. An iterative procedure could be used to determine the value of C, Pr and g', but this can be avoided by using Procedure III.

Detailed steps in the procedure of solution are given in Section 6.9 and Appendix B.

6.5 Method of Solution of Momentum Equation

Before attempting its solution, equation (6.10) will be rewritten for simplification. First, consider the first term in (6.10)

$$\frac{1}{C_\infty}\,\frac{1}{r}\,\frac{\partial}{\partial \eta}\,(C\,r\,f'')$$

The radius r is a function of both x and η, being defined by

$$r = r_o + y\cos\alpha = r_o + \cos\alpha\left[\sqrt{\frac{\rho_\infty\,\mu_\infty x}{u_e}}\int \frac{1}{\rho}\,d\eta\right] \qquad (6.29)$$

where r_o is the local radius of the axisymmetric body

α is the angle between the normal to the surface and the radius r (see Fig. A1).

It would be difficult to handle the integral in (6.29) within the differential in equation (6.10). Therefore rewrite the first term of (6.10) as

$$\frac{1}{C_\infty}\,\frac{1}{r}\,\frac{\partial}{\partial \eta}\,(C\,r\,f'') = \frac{1}{C_\infty}\,\frac{\partial}{\partial \eta}\,(C\,f'') + \frac{C}{C_\infty}\,f''\,\frac{1}{r}\,\frac{\partial r}{\partial \eta} \qquad (6.30)$$

The second term on the right-hand side is the transverse-curvature term and is negligible when the boundary-layer thickness is small compared to the body radius. Thus there is a second advantage to writing the first term of (6.10) in two parts, in that the transverse-curvature term stands by itself. For further simplification introduce T, a transverse curvature parameter, defined such that

$$\frac{1}{r}\,\frac{\partial r}{\partial \eta} = T\,\frac{\rho_e}{\rho}$$

Substitution of the value of r given in (6.29) gives

$$\frac{1}{r}\frac{\partial r}{\partial \eta} = T\frac{\rho_e}{\rho} = \frac{\cos\alpha}{r_o + y\cos\alpha}\sqrt{\frac{\rho_\infty \mu_\infty x}{u_e}}\ \frac{1}{\rho}$$

$$= \frac{\cos\alpha}{\frac{r_o}{x}\sqrt{\frac{u_e}{u_\infty}}\sqrt{\frac{\rho_\infty u_\infty x}{\mu_\infty}} + \left(\int_0^\eta \frac{\rho_\infty}{\rho}\,d\eta\right)\cos\alpha}\ \frac{\rho_\infty}{\rho} \qquad (6.31)$$

Now T may be written as

$$T = \frac{\cos\alpha}{\frac{r_o}{x}\sqrt{\frac{u_e}{u_\infty}}\sqrt{\frac{\rho_\infty u_\infty x}{\mu_\infty}} + \left(\int_0^\eta \frac{\rho_\infty}{\rho}\,d\eta\right)\cos\alpha}\ \frac{\rho_\infty}{\rho_e} \qquad (6.32)$$

For simplicity, introduce T_w which is a function of x only

$$T_w = T(\eta = 0) = \frac{\cos\alpha}{\frac{r_o}{x}\sqrt{\frac{u_e}{u_\infty}}\sqrt{\frac{\rho_\infty u_\infty x}{\mu_\infty}}}\ \frac{\rho_\infty}{\rho_e} \qquad (6.32a)$$

Then (6.32) can be written as

$$T = \frac{T_w}{1 + T_w\int_0^\eta \frac{\rho_e}{\rho}\,d\eta} \qquad (6.32b)$$

Effects of transverse curvature for particular flows are presented in Section 7.9.

The radius parameter R may be written as

$$R = \frac{x}{r}\frac{dr}{dx} = \frac{x}{r_o + y\cos\alpha}\left[\frac{dr_o}{dx} + y\frac{d\cos\alpha}{dx}\right] \qquad (6.33)$$

Now if the boundary layer is small with respect to the body radius, as is usually assumed in boundary-layer flow, R is simply

$$R \simeq \frac{x}{r_o} \frac{dr_o}{dx} \tag{6.33a}$$

But if it is not, the y terms in (6.33) may affect the solution of the momentum equation. The last term in (6.33) is

$$\frac{dr_o}{dx} + y \frac{d \cos \alpha}{dx} = \left[\frac{dr_o}{dx} - y \sin \alpha \frac{d\alpha}{dx} \right]$$

$$= \frac{dr_o}{dx} \left[1 - y \frac{d\alpha}{dx} \right]$$

since $\sin \alpha = dr_o/dx$. But $d\alpha/dx$ is the reciprocal of the local longitudinal radius of curvature, and this radius must be large with respect to y if the boundary-layer approximation used in developing the momentum and energy equations is to hold. That is, if the local radius of curvature is small with respect to y, the second-order effect of longitudinal curvature becomes of importance, and the approximation of no pressure change across the boundary layer is no longer true. Therefore $y(d\alpha/dx) << 1$ and (6.33) may be written as

$$R = \frac{x}{r} \frac{dr}{dx} \simeq \frac{\frac{x}{r_o} \frac{dr_o}{dx}}{1 + \frac{y}{r_o} \cos \alpha} = \frac{\frac{x}{r_o} \frac{dr_o}{dx}}{1 + \frac{\cos \alpha}{r_o} \sqrt{\frac{\rho_\infty \mu_\infty x}{u_e}} \int_0^\eta \frac{1}{\rho} d\eta}$$

$$= \frac{\frac{x}{r_o} \frac{dr_o}{dx}}{1 + T_w \int_0^\eta \frac{\rho_e}{\rho} d\eta} \tag{6.33b}$$

Also for simplicity the symbol N is introduced, defined as

$$N = \frac{P + 1}{2} + R \tag{6.34}$$

The momentum equation can now be written

$$\frac{\partial}{\partial\eta}(C\,f'') = -T\frac{\rho_e}{\rho}C\,f'' - C_\infty P\left(\frac{\rho_e}{\rho} - f'^2\right) - C_\infty N\,ff'' + C_\infty x\left[f'\frac{\partial f'}{\partial x} - f''\frac{\partial f}{\partial x}\right] \tag{6.35}$$

It will be solved in the same manner as the incompressible equation was in References 2 and 3. Values of the fluid properties C and ρ_e/ρ, which of course were not needed in the incompressible problem, are assumed here to be given by the most recent solution of the energy equation. For the very first solution they are assumed.

In the authors' studies of the incompressible boundary layer it was found that round-off errors in the computer program could be reduced by substitution of $\varphi' = f' - 1$ into the momentum equation (Reference 3). The same substitution will be made here. The reason that round-off errors are reduced by the substitution is that in equation (6.35) all terms approach zero as η approaches ∞; both ρ_e/ρ and f'^2 approach unity and the round-off error is primarily introduced when taking their difference. The substitution is

$$\left.\begin{aligned} \varphi &= f - \eta \\ \varphi' &= f' - 1 \\ \varphi'' &= f'' \\ \varphi''' &= f''' \end{aligned}\right\} \tag{6.36}$$

Introduction into (6.35) gives

$$\frac{\partial}{\partial\eta}(C\,\varphi'') = -T\frac{\rho_e}{\rho}C\,\varphi'' + C_\infty P\left[\varphi'^2 + 2\varphi' + 1 - \frac{\rho_e}{\rho}\right]$$

$$- C_\infty N(\varphi + \eta)\varphi'' + C_\infty x\left[(\varphi' + 1)\frac{\partial\varphi'}{\partial x} - \varphi''\frac{\partial\varphi}{\partial x}\right] \tag{6.37}$$

The boundary conditions are now:

$\eta = 0$:

$$\left.\begin{aligned} \varphi_w &= f_w \\ \varphi_w' &= -1 \\ \varphi_w'' &= \text{unknown, to be solved for} \end{aligned}\right\} \tag{6.38a}$$

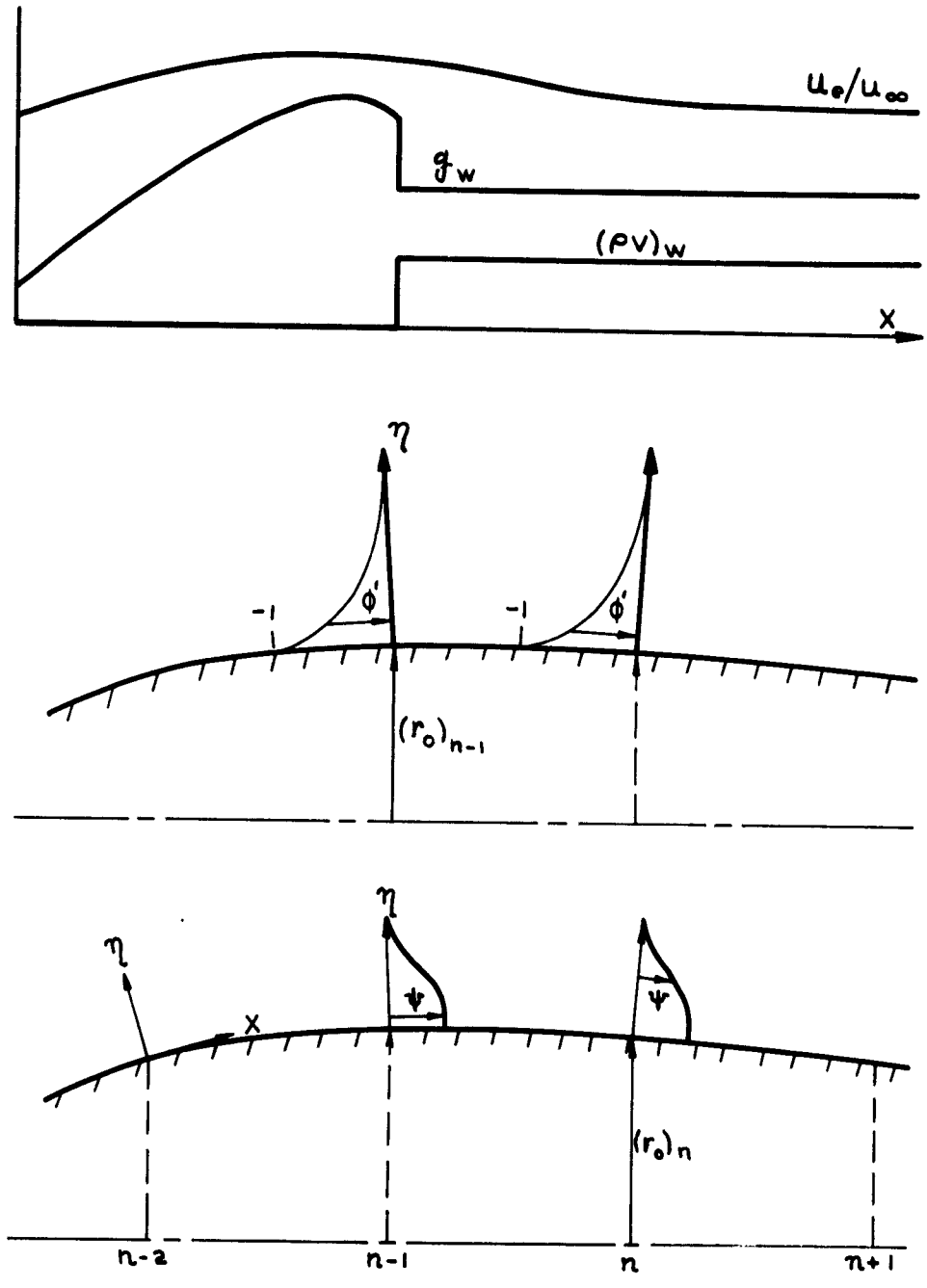

Figure 3.- Notation system for velocity and enthalpy profiles in the boundary layer on a body of revolution.

$\eta \rightarrow \infty$:

$$\varphi' \rightarrow 0$$
$$\varphi'' \rightarrow 0 \qquad (6.38b)$$

The region of solution will be divided into x-wise stations as shown in figure 3. At each station the x-derivatives will be replaced by finite differences. The finite-difference representation is described in Section 6.7. This replacement of the partial derivative with respect to x by finite differences results in an ordinary differential equation at each x-station for the momentum equation. Each equation must be solved step by step as the calculation proceeds in the x-direction. The equation is third order and nonlinear. Solution of the equation is made difficult by both the nonlinearity and the fact that one boundary is at $\eta = \infty$. Ample work in the past has proved the existence of a solution; therefore it is sufficient to search for the correct solution. A positive method for doing this is to solve (6.37) as an initial value problem using arbitrary values of φ_w'' as a third boundary condition. It is then necessary to search through the possible values of φ_w'' to find the one that satisfies the outer boundary condition — that φ' approaches zero asymptotically as η approaches infinity. The procedure for performing the search is described below but first consider the solution of tne equation as an initial value problem. First determine

$$C\,\varphi'' = \int_0^{\eta} \frac{\partial}{\partial \eta} (C\,\varphi'')\, d\eta + C_w\,\varphi_w'' \qquad (6.39)$$

where $\frac{\partial}{\partial \eta} (C\,\varphi'')$ is given by the right hand side of (6.37). C_w is known or assumed but φ_w'' is not. It will be found by the searching procedure described in the following paragraph. The method of integration to be used in (6.39) is described in Section 6.8. Other quantities needed in the solution of (6.39) are given by

$$\varphi'' = \frac{(C\,\varphi')}{C} \qquad (6.40)$$

$$\varphi' = \int_0^{\eta} \varphi''\, d\eta - 1 \qquad (6.41)$$

$$\varphi = \int_0^{\eta} \varphi' \, d\eta + \varphi_w \tag{6.42}$$

Briefly, the procedure for searching for the correct value of φ_w'' is to first try values of φ_w'' until the solutions for φ' are bounded in a specified region. Then an interpolation method is used to obtain the value of φ_w'' that satisfies the outer boundary condition. The steps in the procedure are:

1. Try $\varphi_w'' = (\varphi_w'')_{input}$, where the latter is an input to the program or, more conveniently, is the value at the previous station. Compute outward to determine if the trial solution exceeds $\varphi' = 0$ or not. Because of the transformation used, the value of φ_w'' will generally remain between 0 and 4. A value of $\varphi_w'' = 0$ corresponds to separation.
2. If φ' exceeds 0, the trial value of φ_w'' is high and a second solution is computed with a reduced φ_w''. This procedure is continued until both a high and a low value of φ_w'' are known.
3. Once both a high and a low value of φ_w'' are known, the bounds on the correct value of φ_w'' can be further narrowed by splitting the difference between the upper and lower bounds, and computing again.
4. This splitting the difference can be continued until φ_w'' for a high solution and φ_w'' for a low solution agree to a specified number of decimal places. This procedure is positive but costly in computing time. Studies have shown that the searching procedure can be speeded up considerably with no loss in accuracy by the following: the splitting-the-difference procedure is used until three solutions are obtained such that φ' at $\eta_{max} = \eta_\infty$ is between the bounds of $-K \leq \varphi'(\eta_\infty) \leq K$. (Both η_∞ and K are inputs in the computer program.) At least one of the three solutions must be high and one low. A three-point-interpolation procedure is then used to determine the solution that satisfies the outer boundary condition $\varphi'(\eta_\infty) = 0$. This is the same procedure that was used in the solution of the incompressible-boundary-layer equations and reported on in Reference 3.

The interpolation procedure is as follows. Consider the typical set of trial runs shown in figure 4. The runs are for incompressible stagnation-point

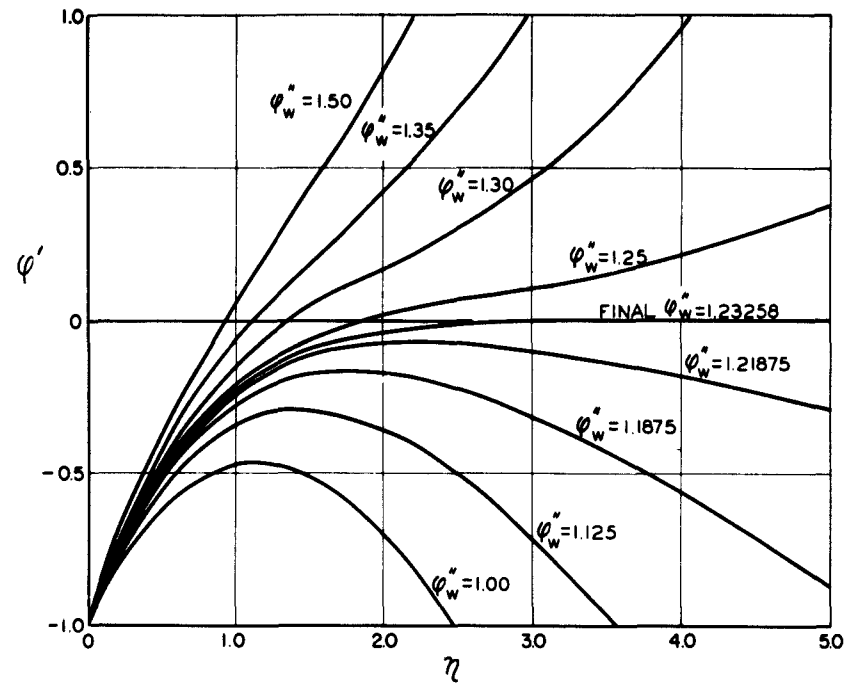

Figure 4.- Trial solutions for various values of φ''_w. Stagnation-point flow, P = 1.0, R = 0.

flow. The tries were:

Try	φ''_w	Nature	Tries used for interpolation	η_{MAX}
1st	1.0	Low		2.50
2nd	1.5	High		1.95
3rd	1.25	High	1st	5.0
4th	1.125	Low		3.55
5th	1.1875	Low	2nd	5.0
6th	1.21875	Low	3rd	5.0
Interpolated	1.232587			

The program first tried φ''_w= 1.0, which it found to be low. The second try of 1.5 was high. It then proceeded to split the difference between the last high and low tries until it had three solutions that extended all the way to η_∞ within the bounds of $\varphi'(\eta_\infty) \pm 1$. These three solutions were the 3rd,

5th, and 6th tries. Denote them as

$$\begin{array}{llllll} \text{1st solution} & \varphi_1 & \varphi_1' & \varphi_1'' & (C\,\varphi'')_1' \\ \text{2nd solution} & \varphi_2 & \varphi_2' & \varphi_2'' & (C\,\varphi'')_2' \\ \text{3rd solution} & \varphi_3 & \varphi_3' & \varphi_3'' & (C\,\varphi'')_3' \end{array}$$

Lagrangian three-point interpolation is used to determine the solution which meets the outer boundary condition $\varphi'(\eta_\infty) = 0$. The interpolated solution is given by

$$\left.\begin{aligned} \varphi(\eta) &= A_1\,\varphi_1(\eta) + A_2\,\varphi_2(\eta) + A_3\,\varphi_3(\eta) \\ \varphi'(\eta) &= A_1\,\varphi_1'(\eta) + A_2\,\varphi_2'(\eta) + A_3\,\varphi_3'(\eta) \end{aligned}\right\} \qquad (6.43)$$

and a similar relation for $\varphi''(\eta)$ and $(C\,\varphi'')'$ where the coefficients are given by

$$\left.\begin{aligned} A_1 &= \frac{\varphi_2'(\eta_\infty)\;\;\varphi_3'(\eta_\infty)}{[\varphi_1'(\eta_\infty) - \varphi_2'(\eta_\infty)][\varphi_1'(\eta_\infty) - \varphi_3'(\eta_\infty)]} \\ A_2 &= \frac{\varphi_1'(\eta_\infty)\;\;\varphi_3'(\eta_\infty)}{[\varphi_2'(\eta_\infty) - \varphi_1'(\eta_\infty)][\varphi_2'(\eta_\infty) - \varphi_3'(\eta_\infty)]} \\ A_3 &= \frac{\varphi_1'(\eta_\infty)\;\;\varphi_2'(\eta_\infty)}{[\varphi_3'(\eta_\infty) - \varphi_1'(\eta_\infty)][\varphi_3'(\eta_\infty) - \varphi_2'(\eta_\infty)]} \end{aligned}\right\} \qquad (6.44)$$

The solution can be made as accurate as desired by restricting the values of the bounds K. Effect of K on the accuracy of solution is discussed in Section 7.2. Typically K would have a value of 1 for five-place accuracy. Computing time required to obtain this accuracy with the interpolation method is about one fourth the time required if just splitting the difference between the high and low tries were used. A study showed the three-point form of interpolation to be considerably more accurate than the two-point form, but no great gains in accuracy were obtained by using more than three points.

6.6 Method of Solution of Energy Equation

Before solving the energy equation (6.19) it is convenient to substitute the functions T and φ introduced in the preceding Section and to also introduce the function ψ defined as

$$\psi = g - 1 \tag{6.45}$$

for the same reasons that φ was introduced in the momentum equation. Substitution of the functions in (6.19) gives

$$\frac{\partial}{\partial\eta}\left[\frac{C}{Pr}\psi' + \frac{u_e^2}{H_e}\, C\left(1 - \frac{1}{Pr}\right)(\varphi' + 1)\,\varphi''\right]$$

$$= -T\left(\frac{\rho_e}{\rho}\right)\left[\frac{C}{Pr}\psi' + \frac{u_e^2}{H_e}C\left(1 - \frac{1}{Pr}\right)(\varphi' + 1)\,\varphi''\right]$$

$$- C_\infty N(\varphi + \eta)\psi' + C_\infty x\left[(\varphi' + 1)\frac{\partial\psi}{\partial x} - \psi'\frac{\partial\varphi}{\partial x}\right] \tag{6.46}$$

The wall boundary condition are:

at $\eta = 0$:

$$\begin{aligned} \psi_w &= g_w - 1 \\ \psi_w' &= g_w' \end{aligned} \tag{6.47}$$

A more general boundary condition could be defined by

$$\Omega = g_w + k\, g_w'$$

but usually either g_w or g_w', corresponding respectively to wall temperature and wall heat transfer, would be known.

The third boundary condition is, as $\eta \longrightarrow \infty$;

$$\begin{aligned} \psi &\longrightarrow 0 \\ \psi' &\longrightarrow 0 \end{aligned} \tag{6.48}$$

The method of solution of (6.46) is similar to that of the momentum equation. The region of solution is divided into x-wise stations as indicated in figure 3. Again the x-derivatives are replaced by finite differences, which are defined in the next section of this report. When solving (6.46) values of φ and its derivatives that were determined from the previous solution of the momentum equation and fluid properties that were determined from the previous solution of the energy equation are used. Once a solution has been obtained the fluid properties are re-evaluated and the energy equation is solved again. This iterative procedure is continued until convergence of the solution is obtained. Details of the iterative procedures for solving both the momentum and energy equations are given in Section 6.9. With these procedures ψ and ψ' are the only unknowns in the solution of (6.46) and the equation is linear.

The solution of (6.46) is as follows. Rewrite it as

$$\frac{\partial}{\partial\eta}(\pi) \equiv \pi' = -T\frac{\rho_e}{\rho}\pi - C_\infty N(\varphi+\eta)\psi' + C_\infty x\left[(\varphi'+1)\frac{\partial\psi}{\partial x} - \psi'\frac{\partial\varphi}{\partial x}\right] \tag{6.49}$$

where for simplicity

$$\pi \equiv \frac{C}{Pr}\psi' + \frac{u_e^2}{H_e}C\left(1-\frac{1}{Pr}\right)(\varphi'+1)\varphi'' \tag{6.50}$$

Equation (6.49) is integrated to determine π :

$$\pi = \int_0^\eta \pi'\,d\eta + \pi_w \tag{6.51}$$

The method of integration is the same as for the momentum equation and is described in Section 6.5. From (6.50)

$$\psi' = \frac{Pr}{C}\left[\pi - \frac{u_e^2}{H_e}C\left(1-\frac{1}{Pr}\right)(\varphi'+1)\varphi''\right] \tag{6.52}$$

which may be integrated to determine ψ :

$$\psi = \int_0^\eta \psi'\,d\eta + \psi_w \tag{6.53}$$

Since equation (6.49) is treated as linear, its solutions may be linearly combined. It will be solved twice, and the two solutions combined to meet the outer boundary condition. The exact procedure will depend on whether g_w or g_w' is known.

Case 1: g_w is known. Both solutions begin with the same value of ψ_w, the one imposed by the boundary condition

$$\psi(0) = \psi_w = g_w - 1$$

First equation (6.49) is solved by using a trial value of $\psi_w' = g_w'$. The solution is denoted as

$$\psi_1(\eta)$$

If $\psi_1(\eta_\infty)$ is greater than zero, a lower value of ψ_w' is tried; if it is less, a higher value of ψ_w'. The second try is denoted as

$$\psi_2(\eta)$$

The two solutions can be added to produce the most general solution, which can be made to meet the boundary conditions. The general solution is

$$\psi(\eta) = A\,\psi_1(\eta) + B\,\psi_2(\eta) \tag{6.54}$$

The outer boundary conditions are

$$\begin{aligned} \psi(\eta_\infty) &= A\,\psi_1(\eta_\infty) + B\,\psi_2(\eta_\infty) = 0 \\ \psi'(\eta_\infty) &= A\,\psi_1'(\eta_\infty) + B\,\psi_2'(\eta_\infty) = 0 \end{aligned} \tag{6.55}$$

and also

$$\psi_w = A\,\psi_{w_1} + B\,\psi_{w_2}$$

But

$$\psi_w = \psi_{w_1} = \psi_{w_2}$$

so that

$$A + B = 1$$

Equation (6.55) gives

$$A = \frac{-\psi_2(\eta_\infty)}{\psi_1(\eta_\infty) - \psi_2(\eta_\infty)} \tag{6.56}$$

and the correct solution is for all η's

$$\psi(\eta) = A\,\psi_1(\eta) + (1 - A)\,\psi_2(\eta) \tag{6.57a}$$

and also

$$\psi'(\eta) = A\,\psi_1'(\eta) + (1 - A)\,\psi_2'(\eta) \tag{6.57b}$$

Case 2: g_w' is known.

The procedure is similar to Case 1, but now the energy equation is solved with two trial values of g_w instead of g_w'. Again, the two trial solutions are denoted as $\psi_1(\eta)$ and $\psi_2(\eta)$. Relations (6.56), (6.57a), and (6.57b) then may be used to give the correct solution.

6.7 Finite-Difference Representation of x-Derivatives.

The fundamental idea for the method of solution — that of replacing the x-derivatives by finite differences to approximate the partial differential equation by an ordinary differential equation — was advanced by Hartree and Womersley (Reference 8). The idea was applied to the incompressible boundary layer by Hartree (References 9 and 10) and the authors in References 1, 2, and 3.

Two treatments within the scheme are possible. One is to deal in terms of the differential equation at a point; in particular, the x-derivatives at a point are replaced by their finite-difference equivalents. Another treatment is to deal in terms of mean values of the variable φ or ψ for a region of finite extent. Both methods are described in Reference 3. Within both of the methods there are many possible representations of a derivative by finite differences, for example, two, three, or more points may be used. Note that all of the x-derivatives that appear in the momentum and energy equations are only of first order.

In reference 3 the authors made an extensive study of the use of two-point, three-point, and four-point finite differences in solving the incompressible-boundary-layer equations. Both the concept of the point form and of the mean form were studied. The investigation showed that whereas the two-point mean representation was more accurate than the two-point point form, the use of three and four points proved the point forms to be more accurate. Solutions obtained by the mean method with the higher number of points diverged wildly as the step length became small. The same type of divergence appeared in Reference 1 where the two-point mean form was used, but occurred there at much smaller step sizes in x. The investigation also showed that whereas the use of three points in the point form of finite differences gave a much more accurate solution than the use of two points, further increase of the number of points to four gave no great increase in accuracy. As a result of the investigation, the three-point point form of representing the derivatives was chosen in the present method. In addition to being freer of oscillations as the step size becomes very small, the point form has the advantages of being simpler conceptually and simpler to program on the computer.

The basic scheme of the finite-difference representation is diagramed in figure 5. The space is divided into a number of regions bounded by lines x_n, x_{n-1}, x_{n-2}, x_{n-3}. The spacing Δx need not be constant. Because the momentum equation and energy equation are parabolic in x, the problem must be solved by proceeding in the direction of positive x. It is assumed that the solution has been found at all previous stations up to and including x_{n-1}, which of course means that $\varphi(\eta)$ and $\psi(\eta)$ and their derivatives are fully known at these stations. The quantity $\varphi'(\eta)$ typically has the appearance shown in figure 5. The problem is to find the solution $\varphi(\eta)$ and $\psi(\eta)$ at the new station x_n.

Whereas usually three-point finite differences will be used, at the start of a solution only two points are available and the two-point form must be used. Also, when there are discontinuities in the boundary conditions, it may be more accurate to use the two-point form. The finite difference representations are:

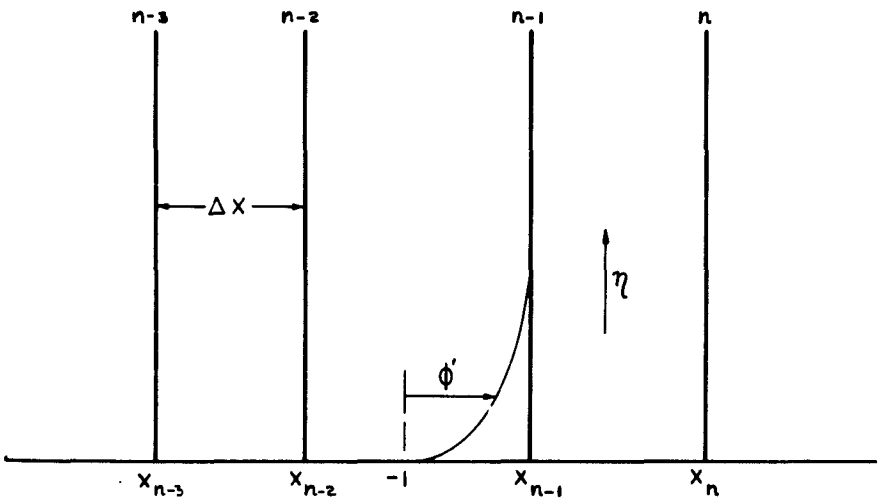

Figure 5.– Notation system for finite-difference representation of x-derivatives.

For two points:

$$\frac{\partial \varphi_n}{\partial x} = \frac{\varphi_n - \varphi_{n-1}}{x_n - x_{n-1}} \tag{6.58}$$

The error in this expression is

$$\frac{(x_n - x_{n-1})}{2} \quad \frac{\partial^2 \varphi(\xi)}{\partial x^2}$$

where ξ is some value of x in the interval $x_n - x_{n-1}$.

For three points:

$$\frac{\partial \varphi_n}{\partial x} = \left[\frac{1}{(x_n - x_{n-1})} + \frac{1}{(x_n - x_{n-2})} \right] \varphi_n - \frac{(x_n - x_{n-2})}{(x_n - x_{n-1})(x_{n-1} - x_{n-2})} \varphi_{n-1} + \frac{(x_n - x_{n-1})}{(x_n - x_{n-2})(x_{n-1} - x_{n-2})} \varphi_{n-2} \tag{6.59}$$

The error here is

$$\frac{(x_n - x_{n-1})(x_n - x_{n-2})}{6} \frac{\partial^3 \varphi(\xi)}{\partial x^3}$$

where here ξ is some value of x in the interval $x_n - x_{n-2}$.

In solving the boundary-layer equations the quantity $\partial\varphi/\partial x$ in both the momentum equation (6.37) and the energy equation (6.46) is replaced by either (6.58) or (6.59). The other x-derivatives $\partial\varphi'/\partial x$ and $\partial\psi/\partial x$ are replaced by similar expressions. When these substitutions are made, it is assumed that all of the other quantities in the boundary-layer equations are evaluated at x_n. The equations are then ordinary differential equations in η with the variable quantities φ, φ', and ψ at the n-1 and n-2 stations. Step length Δx is not a primary parameter; instead, $x/\Delta x$ is.

In solving the boundary-layer equations the calculation must start at $x = 0$. For the $x = 0$ station the terms with x-derivatives in both the momentum and energy equations disappear. At the second station the two-point form of the finite differences is used, but, at all stations farther downstream the three-point form may be used. The error in the three-point form is like

$$\frac{(\Delta}{3} \quad \frac{\partial^3 \varphi}{\partial x^3}$$

as compared to

$$\frac{\Delta x}{2} \quad \frac{\partial^2 \varphi}{\partial x^2}$$

for the two-point form. Therefore in order to have the same accuracy in the solution at all stations the step size at the second station must be suitably reduced. In practice these errors near the leading edge will probably be small due to the fact that the flow is nearly similar there, and thus the x-derivatives are small. But in any case Δx can be kept small here, in order to keep accuracy high.

For further discussion of application of Hartree-Womersley's method for solution of the boundary-layer equations and the associated errors, see References 1 and 3.

6.8 Method of Integration

The overall method of solution of both the momentum and energy equations is outlined in Sections 6.5 and 6.6. The problem of solution is essentially one of integration. There are several methods for performing the integration that are available as subroutines on the computer, for example, Milne's fourth-order predictor-corrector method, but because of their generality, they require long computing times to solve the present problem. Therefore the authors made a study of various techniques that were available for performing the integration as applied to the incompressible problem. The results of this study are reported in Reference 3. A method was developed there that appears to be both highly accurate and rapid. It uses the Falkner extrapolation formulas and the Adams interpolation formulas which are described on pages 116-131 of Reference 11. Furthermore, as a result of the study, the four-point form of these formulas appears most appropriate for the present problem.

First consider the general situation where the solution is known up to η_r and the problem is to find the values of φ and ψ and their derivatives at $\eta_r + \Delta\eta = \eta_{r+1}$ by use of equations (6.39 to 6.42) and equations (6.49, 6.51 and 6.53). A special procedure will be required to get started near the wall, and it is described in succeeding paragraphs. Considering first the momentum equation, the integration indicated in equations (6.39, 6.41, 6.42) will be approximated by the extrapolation and interpolation formulas. First the extrapolation formulas use values of $(C\,\varphi'')'$ and φ'' at the r, r-1, r-2, r-3 stations to determine values of φ, φ', φ'' and $(C\,\varphi'')'$ at the r+1 station. The formulas are

$$(C\,\varphi'')_{r+1)_E} = (C\,\varphi'')_r + \frac{\Delta\eta}{24}\Big[55(C\,\varphi'')'_r - 59(C\,\varphi'')'_{r-1} + 37(C\,\varphi'')'_{r-2} - 9(C\,\varphi'')'_{r-3}\Big] \quad (6.60)$$

where the subscript E is used to denote extrapolation. The step length $\Delta\eta$ is a constant in the solution. The error in (6.60) is

$$E_1 \leq + \frac{251}{720}(\Delta\eta)^5\,[C\,\varphi''(\xi)]^V$$

The extrapolation formulas for φ' and φ are:

$$\varphi'_{r+1)_E} = \varphi'_r + \frac{\Delta\eta}{24}\left(55\,\varphi''_r - 59\,\varphi''_{r-1} + 37\,\varphi''_{r-2} - 9\,\varphi''_{r-3}\right) \tag{6.61}$$

with an error of

$$E_2 \leq + \frac{251}{720}(\Delta\eta)^5\,\varphi^{VI}(\xi)$$

and

$$\varphi_{r+1)_E} = \varphi_r + \Delta\eta\,\varphi'_r + \frac{(\Delta\eta)^2}{360}\left[323\,\varphi''_r - 264\,\varphi''_{r-1} + 159\,\varphi''_{r-2} - 38\,\varphi''_{r-3}\right] \tag{6.62}$$

with an error of

$$E_3 \leq + \frac{3}{32}(\Delta\eta)^6\,\varphi^{VI}(\xi)$$

The value of $(C\,\varphi'')'$ at r+1 can now be determined by using the momentum equation (6.37) and the extrapolated values of φ'', φ', and φ. It will be denoted by

$$(C\,\varphi'')'_{r+1)_E} = F_1(\varphi''_E,\ \varphi'_E,\ \varphi_E)_{r+1}$$

The interpolation formulas can now be used to determine more exact values of φ'', φ', φ and $(C\,\varphi'')'$ at the r+1 station. The formulas are

$$(C\,\varphi'')_{r+1} = (C\,\varphi'')_r + \frac{\Delta\eta}{24}\left[9(C\,\varphi'')'_{r+1)_E} + 19(C\,\varphi'')'_r - 5(C\,\varphi'')'_{r-1} + (C\,\varphi'')'_{r-2}\right] \tag{6.63}$$

with an error of

$$E_4 \leq -\frac{19}{720}(\Delta\eta)^5\,[C\,\varphi''(\xi)]^V$$

and

$$\varphi'_{r+1} = \varphi'_r + \frac{\Delta\eta}{24}\left[9\,\varphi''_{r+1} + 19\,\varphi''_r - 5\varphi''_{r-1} + \varphi''_{r-2}\right] \tag{6.64}$$

with an error of

$$E_5 \leq -\frac{19}{720}(\Delta\eta)^5\,\varphi^{VI}(\xi)$$

and

$$\varphi_{r+1} = \varphi_r + \Delta\eta\ \varphi'_r + \frac{(\Delta\eta)^2}{360}\left[38\ \varphi''_{r+1} + 171\ \varphi''_r - 36\ \varphi''_{r-1} + 7\ \varphi''_{r-2}\right] \tag{6.65}$$

with an error or

$$E_6 \leq -\frac{17}{1440}\ (\Delta\eta)^6\ \varphi^{VI}(\xi)$$

Finally the value of $(C\ \varphi'')'_{r+1}$ is obtained by again using the basic momentum equation (6.37) and the interpolated values above

$$(C\ \varphi'')' = F_1(\varphi'', \varphi', \varphi)$$

A comparison of the error terms for the extrapolated and interpolated values shows that not only are the interpolation errors much less than the extrapolation, they are also opposite in sign. Therefore the exact value of the quantity in question, say φ', must lie in the bounds of the extrapolated and interpolated values. Thus there is a check on the accuracy of the procedure. This method of checking is the concept used in all predictor-corrector methods of numerical analysis (for example, Milne's methods described in Reference 12, pages 199-202). The method developed here, using the Falkner and Adams formulas, was chosen over the more established predictor-corrector methods because its use of higher derivatives gives much smaller errors. It is particularly well suited to solving high-order ordinary differential equations. The solution can be made as exact as desired by choosing a small enough step size $\Delta\eta$.

The use of both the extrapolation and interpolation formulas does essentially mean that the integration over each step length is being performed twice. In the interest of saving computing time, a study was made to see if use of only the extrapolation formulas would give accurate solutions. In some flows it was found that the extrapolation gave oscillating values of φ'' and φ' at the outer edge of the boundary layer. These oscillations disappeared when both the extrapolation and interpolation formulas were used.

The formulas for performing the integrations required in solution of the energy equation are similar to the above. They are:

for equation (6.51)

$$\pi_{r+1)_E} = \pi_r + \frac{\Delta\eta}{24}\left[55\,\pi'_r - 59\,\pi'_{r-1} + 37\,\pi'_{r-2} - 9\,\pi'_{r-3}\right] \tag{6.66}$$

for equation (6.53)

$$\psi_{r+1)_E} = \psi_r + \frac{\Delta\eta}{24}\left[55\,\psi'_r - 59\,\psi'_{r-1} + 37\,\psi'_{r-2} - 9\,\psi'_{r-3}\right] \tag{6.67}$$

and from equation (6.49)

$$\pi'_{r+1)_E} = F_2(\pi_E,\ \psi_E)_{r+1}$$

The interpolated values are given by

$$\pi_{r+1} = \pi_r + \frac{\Delta\eta}{24}\left[(9\,\pi'_{r+1})_E + 19\,\pi'_r - 5\,\pi'_{r-1} + \pi'_{r-2}\right] \tag{6.68}$$

$$\psi_{r+1} = \psi_r + \frac{\Delta\eta}{24}\left[9\,\psi'_{r+1} + 19\,\psi'_r - 5\,\psi'_{r-1} + \psi'_{r-2}\right] \tag{6.69}$$

and finally from equation (6.49)

$$\pi'_{r+1} = F_2(\pi,\ \psi)_{r+1}$$

The Starting Procedure.

The extrapolation-interpolation formulas above require values of the variables at four previous η stations. To get started at the wall Taylor's series will be used. Consider the Taylor's series for $C\,\varphi''$

$$(C\,\varphi'')_{\Delta\eta} = (C\,\varphi'')_w + \Delta\eta(C\,\varphi'')'_w + \frac{(\Delta\eta)^2}{2}(C\,\varphi'')''_w + \ldots$$

The use of high-order terms in the expansion would require values of the derivatives of C at the wall, for example, the use of the third term requires the value of

$$(C\,\varphi'')''_w = (C''\varphi'')_w + 2(C'\varphi''')_w + (C\,\varphi^{IV})_w$$

Derivatives of C are not known from the method of solution, and it would be difficult to obtain their values accurately. Therefore only two terms will be used in the Taylor's series expansion. Error studies show that if the same accuracy is to be maintained in the expansion as in the extrapolation — interpolation formulas above, much shorter steps in η are required in the Taylor's series. The study shows that for about five-place accuracy in the values of φ and ψ, a step size of $\Delta\eta \approx 0.1$ is sufficient in the extrapolation — interpolation formulas but that the Taylor's series expansion requires a step length of about 0.008. The accuracy can be held by using the Taylor's series to obtain the values at only $\eta = \frac{\Delta\eta}{16}$ from the wall. Here $\Delta\eta$ is used to denote the step size used in the four-point extrapolation — interpolation formulas above. Values are then built up to the full length step $\Delta\eta$ by using two-point and three-point extrapolation formulas. Accuracy requires a step size of $\Delta\eta/4$ for the two-point form, and a step size of $\Delta\eta/2$ for the three-point form. The steps in the procedure are outlined in Table I and are sketched in figure 6. The equations to be used are:

TAYLOR' SERIES — STEP SIZE $\Delta\eta/16$

$$(C\,\varphi'')_{\Delta\eta/16} = (C\,\varphi'')_w + \frac{\Delta\eta}{16}(C\,\varphi'')'_w \tag{6.70}$$

$$\varphi'_{\Delta\eta/16} = -1 + \frac{\Delta\eta}{16}\varphi''_w \tag{6.71}$$

$$\varphi_{\Delta\eta/16} = \varphi_w - \frac{\Delta\eta}{16} + \frac{(\Delta\eta)^2}{512}\varphi''_w \tag{6.72}$$

$$T_{\Delta\eta/16} = T_w + \frac{\Delta\eta}{16}T'_w \tag{6.73}$$

$$\psi_{\Delta\eta/16} = \psi_w + \frac{\Delta\eta}{16}\psi'_w \tag{6.74}$$

TWO-POINT FORMULAS — STEP SIZE $\Delta\eta/16$

$$(C\,\varphi'')_{\Delta\eta/8} = (C\,\varphi'')_{\Delta\eta/16} + \frac{\Delta\eta}{32}\left[3(C\,\varphi'')'_{\Delta\eta/16} - (C\,\varphi'')'_{w}\right] \tag{6.75}$$

$$\varphi'_{\Delta\eta/8} = \varphi'_{\Delta\eta/16} + \frac{\Delta\eta}{32}\left[3\,\varphi''_{\Delta\eta/16} - \varphi''_{w}\right] \tag{6.76}$$

$$\varphi_{\Delta\eta/8} = \varphi_{\Delta\eta/16} + \frac{\Delta\eta}{16}\varphi'_{\Delta\eta/16} + \frac{(\Delta\eta)^2}{1536}\left[4\,\varphi''_{\Delta\eta/16} - \varphi''_{w}\right] \tag{6.77}$$

$$\pi_{\Delta\eta/8} = \pi_{\Delta\eta/16} + \frac{\Delta\eta}{32}\left[3\,\pi'_{\Delta\eta/16} - \pi'_{w}\right] \tag{6.78}$$

$$\psi_{\Delta\eta/8} = \psi_{\Delta\eta/16} + \frac{\Delta\eta}{32}\left[3\,\psi'_{\Delta\eta/16} - \psi'_{w}\right] \tag{6.79}$$

TWO-POINT FORMULAS — STEP SIZE $\Delta\eta/8$

$$(C\,\varphi'')_{\Delta\eta/4} = (C\,\varphi'')_{\Delta\eta/8} + \frac{\Delta\eta}{16}\left[3(C\,\varphi'')'_{\Delta\eta/8} - (C\,\varphi'')'_{w}\right] \tag{6.80}$$

$$\varphi'_{\Delta\eta/4} = \varphi'_{\Delta\eta/8} + \frac{\Delta\eta}{16}\left[3\,\varphi''_{\Delta\eta/8} - \varphi''_{w}\right] \tag{6.81}$$

$$\varphi_{\Delta\eta/4} = \varphi_{\Delta\eta/8} + \frac{\Delta\eta}{8}\varphi'_{\Delta\eta/8} + \frac{(\Delta\eta)^2}{384}\left[4\,\varphi''_{\Delta\eta/8} - \varphi''_{w}\right] \tag{6.82}$$

$$\pi_{\Delta\eta/4} = \pi_{\Delta\eta/8} + \frac{\Delta\eta}{16}\left[3\,\pi'_{\Delta\eta/8} - \pi'_{w}\right] \tag{6.83}$$

$$\psi_{\Delta\eta/4} = \psi_{\Delta\eta/8} + \frac{\Delta\eta}{16}\left[3\,\psi'_{\Delta\eta/8} - \psi'_{w}\right] \tag{6.84}$$

TWO-POINT FORMULAS — STEP SIZE $\Delta\eta/4$

$$(C\,\varphi'')_{r+1} = (C\,\varphi'')_r + \frac{\Delta\eta}{8}\left[3(C\,\varphi'')'_r - (C\,\varphi'')'_{r-1}\right] \tag{6.85}$$

$$\varphi'_{r+1} = \varphi'_r + \frac{\Delta\eta}{8}\left[3\,\varphi''_r - \varphi''_{r-1}\right] \tag{6.86}$$

$$\varphi_{r+1} = \varphi_r + \frac{\Delta\eta}{4}\,\varphi'_r + \frac{(\Delta\eta)^2}{96}\left[4\,\varphi''_r - \varphi''_{r-1}\right] \tag{6.87}$$

$$\pi_{r+1} = \pi_r + \frac{\Delta\eta}{8}\left[3\,\pi'_r - \pi'_{r-1}\right] \tag{6.88}$$

$$\psi_{r+1} = \psi_r + \frac{\Delta\eta}{8}\left[3\,\psi'_r - \psi'_{r-1}\right] \tag{6.89}$$

THREE-POINT FORMULAS — STEP SIZE $\Delta\eta/2$

$$(C\,\varphi'')_{r+1} = (C\,\varphi'')_r + \frac{\Delta\eta}{24}\left[23(C\,\varphi'')'_r - 16(C\,\varphi'')'_{r-1} + 5(C\,\varphi'')'_{r-2}\right] \tag{6.90}$$

$$\varphi'_{r+1} = \varphi'_r + \frac{\Delta\eta}{24}\left[23\,\varphi''_r - 16\,\varphi''_{r-1} + 5\,\varphi''_{r-2}\right] \tag{6.91}$$

$$\varphi_{r+1} = \varphi_r + \frac{\Delta\eta}{2}\,\varphi'_r + \frac{(\Delta\eta)^2}{96}\left[19\,\varphi''_r - 10\,\varphi''_{r-1} + 3\,\varphi''_{r-2}\right] \tag{6.92}$$

$$\pi_{r+1} = \pi_r + \frac{\Delta\eta}{24}\left[23\,\pi'_r - 16\,\pi'_{r-1} + 5\,\pi'_{r-2}\right] \tag{6.93}$$

$$\psi_{r+1} = \psi_r + \frac{\Delta\eta}{24}\left[23\,\psi'_r - 16\,\psi'_{r-1} + 5\,\psi'_{r-2}\right] \tag{6.94}$$

TABLE I

STEPS IN THE PROCEDURE FOR STARTING INTEGRATION AT WALL

Step in Procedure	η	Type of Formula	Step Size	Equations
0	0	Wall Values	———	———
1	$\Delta\eta/16$	Taylor's Series	$\Delta\eta/16$	6.70 through 6.74
2	$\Delta\eta/8$	2-Point Extrapolation	$\Delta\eta/16$	6.75 " 6.79
3	$\Delta\eta/4$	" "	$\Delta\eta/8$	6.80 " 6.84
4	$\Delta\eta/2$	" "	$\Delta\eta/4$	6.85 " 6.89
5	$3\Delta\eta/4$	" "	$\Delta\eta/4$	" " "
6	$\Delta\eta$	" "	$\Delta\eta/4$	" " "
7	$3\Delta\eta/2$	3-Point Extrapolation	$\Delta\eta/2$	6.90 " 6.94
8	$2\Delta\eta$	" "	$\Delta\eta/2$	" " "
9	$5\Delta\eta/2$	" "	$\Delta\eta/2$	" " "
10	$3\Delta\eta$	" "	$\Delta\eta/2$	" " "
11	$4\Delta\eta$	4-Point Extrapolation-Interpolation	$\Delta\eta$	6.60 " 6.69
12	$5\Delta\eta$	" " "	$\Delta\eta$	" " "
↓	↓	Etc. " "	↓	↓
	η_∞			

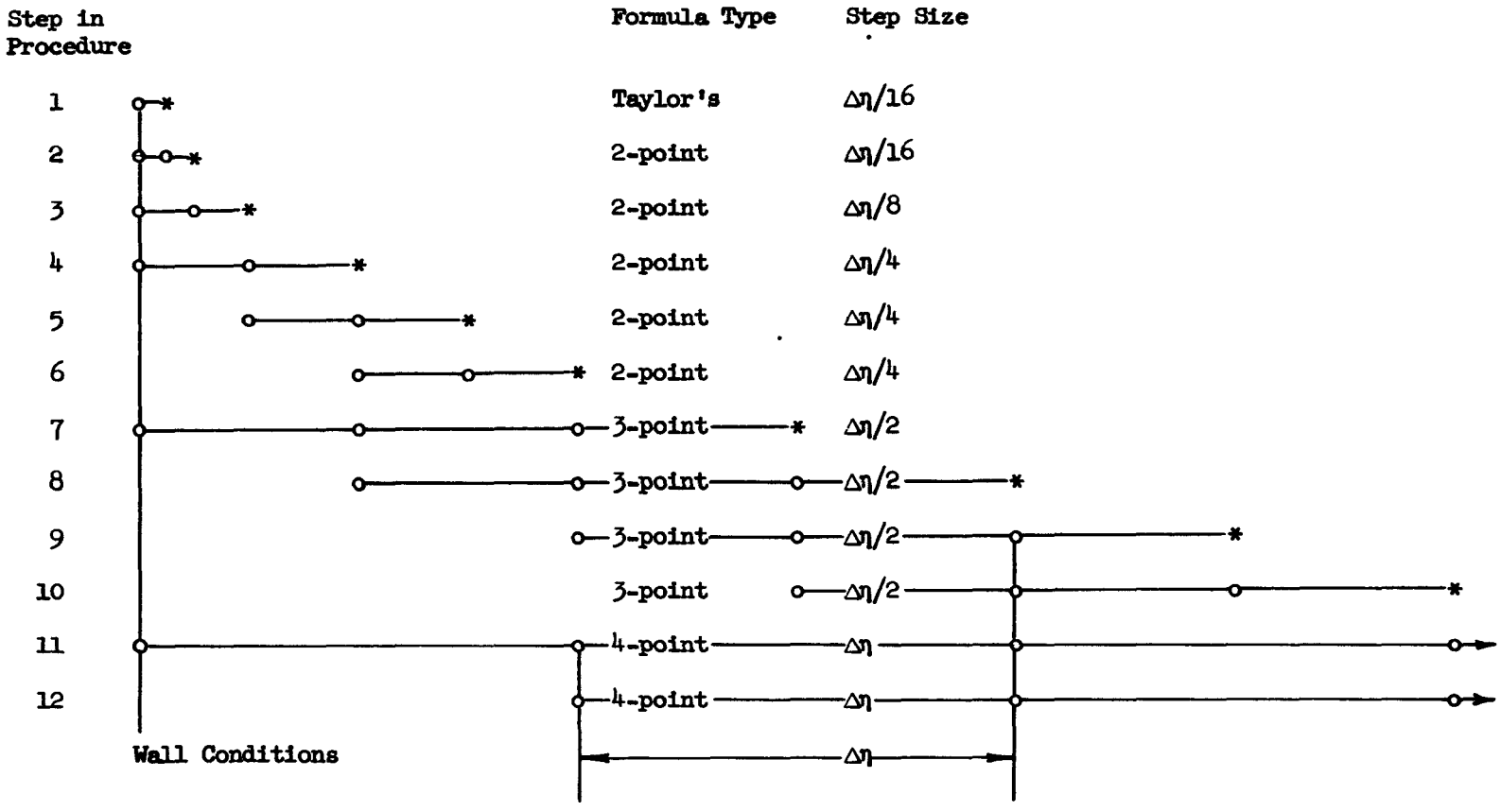

Figure 6.–Procedure for starting integration at wall.

6.9 Outline of Procedure for Solving Momentum and Energy Equations Simultaneously

The procedure for solving the momentum and energy equations is briefly described in Section 6.4, and the reason for its choice is discussed there. Details of the procedure are given in this section. Consider the general case when the program is solving the equation at the n-station. Values of φ and ψ and their derivatives at all previous stations will be known. First the momentum equation is solved using the fluid properties from the n-1 station. The values of φ's from this solution are used to solve the energy equations but still using the fluid properties from the n-1 station. Then new fluid properties are determined and an iterative procedure followed until convergence of solutions of both the momentum and energy equations is obtained. In the iterative procedure let $Q = i$ (an integer) indicate one solution of the momentum equation with the accompanying solutions for enthalpy and fluid properties. The procedure is:

$Q = 0$

(a) The momentum equation is solved by using the fluid properties from the n-1 station. It is solved by the cut-and-try and interpolating procedure described in Section 6.5. The solution is denoted as φ_o.

(b) The energy equation is solved by using the φ_o value and the n-1 fluid properties. The solution is denoted as $(\psi_o)_{L=0}$, where L is a count of successive solutions of the energy equation and fluid properties at a given Q.

(c) The solution $(\psi_o)_{L=0}$ is used to determine new fluid properties. They are denoted as $(FP_o)_{L=0}$.

(d) The fluid properties $(FP_o)_{L=0}$ and the solution φ_o are used to obtain a second solution to the energy equation $(\psi_o)_{L=1}$ and new fluid properties $(FP_o)_{L=1}$.

(e) This iterative procedure is continued until L = L-MAX. Proceed to $Q = 1$.

$Q = 1$

(a) The momentum equation is solved a second time by using fluid properties $(FP_o)_{L\text{-}MAX}$ and the solution is denoted as φ_1.

(b) Steps (b) through (e) in $Q = 0$ are repeated to obtain $(\psi_1)_{L\text{-}MAX}$.

Q > 1

(a) The procedure in $Q = 1$ is repeated, using always the latest values of (φ), (ψ), and (FP) until either

$$Q = Q_{MAX}$$

or

$$(\varphi_w'')_Q - (\varphi_w'')_{Q-1} < \epsilon$$

where ϵ is an accuracy input. If either of these conditions is satisfied, the program proceeds to the next station.

The procedure is sketched in figure 7, and further details of the computer program are given in Appendix B.

6.10 Starting the Solution

At $x = 0$ the x-dependent terms disappear in both the momentum and energy equations. The equations reduce to:

$$\frac{\partial}{\partial\eta}(C\,\varphi'') = -T\frac{\rho_e}{\rho}C\,\varphi'' + C_\infty P\left[\varphi'^2 + 2\,\varphi' + 1 - \frac{\rho_e}{\rho}\right] - C_\infty N(\varphi + \eta)\varphi'' \tag{6.95}$$

for momentum and

$$\frac{\partial}{\partial\eta}\left[\frac{C}{Pr}\psi' + \frac{u_e^2}{H_e}C\left(1 - \frac{1}{Pr}\right)(\varphi' + 1)\varphi''\right] =$$

$$-T\frac{\rho_e}{\rho}\left[\frac{C}{Pr}\psi' + \frac{u_e^2}{H_e}C\left(1 - \frac{1}{Pr}\right)(\varphi' + 1)\,\varphi''\right] - C_\infty N(\varphi + \eta)\,\psi' \tag{6.96}$$

for energy. Hence values of φ and ψ at previous stations are not required. The x-dependent terms also disappear for similar flows. Such flows occur when P, R and the wall boundary conditions are constants for all x's. They include those with constant pressure, such as flows about a flat plate and wedges. Similar flows are discussed more completely in Chapter 8 of Hayes and Probstein, Reference 13.

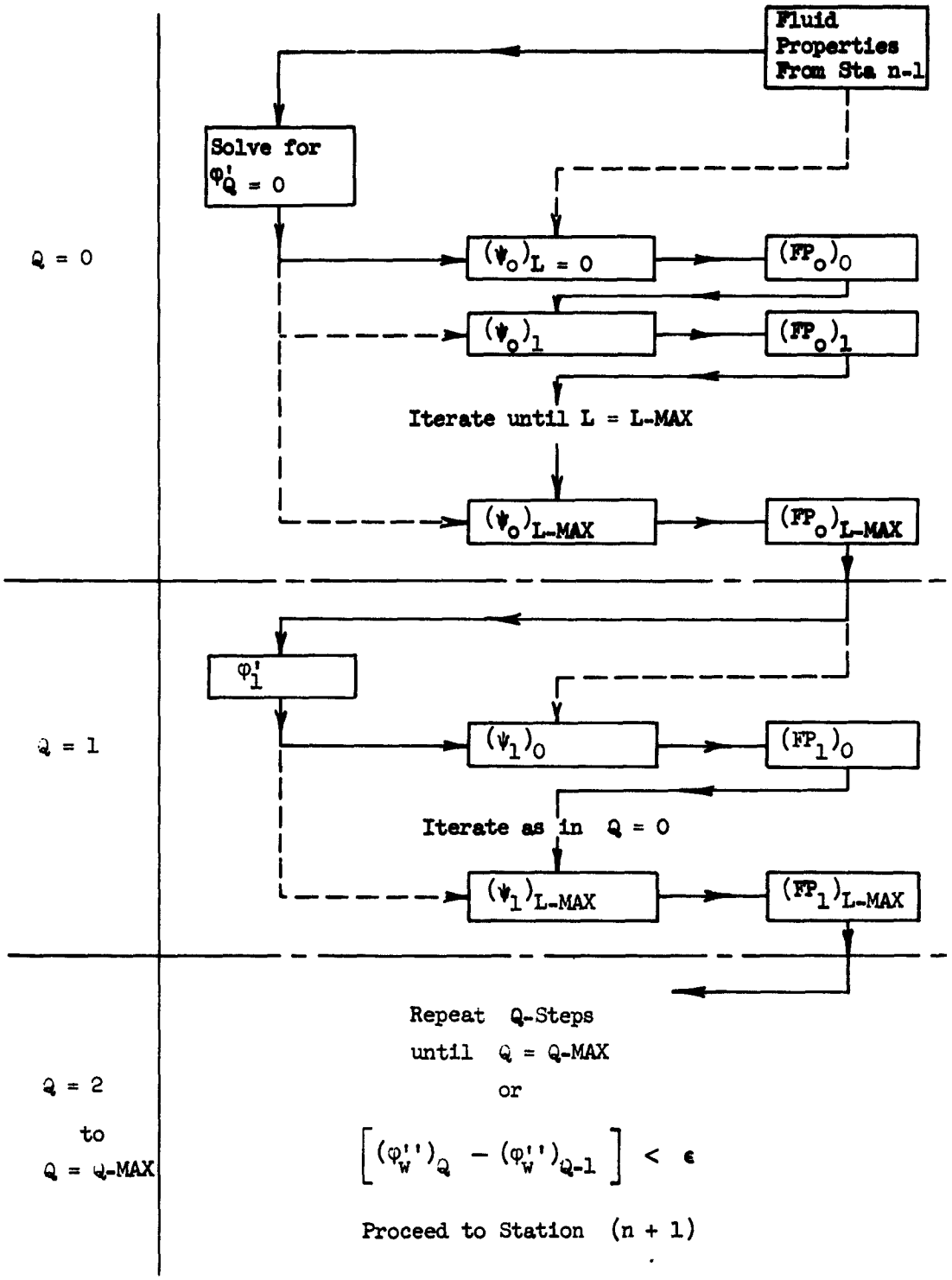

Figure 7.- Flow diagram for solving boundary-layer equations at station n.

The procedure of solution requires that the momentum equation be solved first, but to do so requires values of the fluid properties. At a downstream station the properties are approximated for the first solution of the momentum equation by assuming them to be the same as those at the previous station. To get started at the $x = 0$ station, a linear enthalpy profile that satisfies the inner and outer boundary conditions for enthalpy is assumed. The fluid properties obtained from this enthalpy profile are then used to start the solution. After the first solution of the momentum equation at any station is found, the fluid properties obtained from the latest solution of the energy equation are used for subsequent solutions of the momentum equation. The iterative procedure is presented in the preceding section of this report.

Values of P and R

The values of P and R are either inputs in the program or are calculated from the velocity distribution u_e versus x, and the radius distribution r_o versus x. They are defined by

$$P_n = \left(\frac{x}{u_e} \frac{du_e}{dx} \right)_n \tag{6.13}$$

$$R_n = \left(\frac{x}{r} \frac{dr}{dx} \right)_n$$

$$= \frac{\frac{x}{r_o} \frac{dr_o}{dx}}{1 + T \int \frac{\rho_e}{\rho} d\eta} \tag{6.14}$$

Both P_n and $(r_o/x)(dr_o/dx)$ are always inputs at $x = 0$, but may be calculated at aft stations by use of Lagrangian derivative formulae

$$\left(\frac{du_e}{dx} \right)_n = A_{n-1} u_{e_{n-1}} + A_n u_{e_n} + A_{n+1} u_{e_{n+1}} \tag{6.97}$$

and

$$\left(\frac{dr_o}{dx} \right)_n = A_{n-1} r_{o_{n-1}} + A_n r_{o_n} + A_{n+1} r_{o_{n+1}} \tag{6.98}$$

where

$$\left.\begin{aligned} A_{n-1} &= \frac{x_n - x_{n+1}}{(x_{n-1} - x_n)(x_{n-1} - x_{n+1})} \\ A_n &= \frac{2\,x_n - x_{n+1} - x_{n-1}}{(x_n - x_{n-1})(x_n - x_{n+1})} \\ A_{n+1} &= \frac{x_n - x_{n-1}}{(x_{n+1} - x_{n-1})(x_{n+1} - x_n)} \end{aligned}\right\} \qquad (6.99)$$

6.11 Boundary-Layer Parameters

Once the profiles of φ and ψ and their derivatives have been determined at an x-station, the program determines the conventional boundary-layer parameters of displacement thickness, momentum thickness, local skin friction and local heat transfer. First the profiles of φ, ψ, and their derivatives are transformed to the more conventional profiles of the stream function f, the velocity ratio f', enthalpy ratio g, etc.

The displacement thickness is calculated from the well known formula

$$\delta^* = \int_0^\infty \left(1 - \frac{\rho\, u}{\rho_e u_e}\right) dy \qquad (6.100)$$

In the true definition of a displacement thickness, equation (6.100) is exact only for two-dimensional flow. For axially symmetric flow the exact displacement thickness is given by the quadratic equation

$$\delta^*\left(1 + \frac{\delta^*}{2r_o}\cos\alpha\right) = \int_0^\infty \left(1 + \frac{y}{r_o}\cos\alpha\right)\left(1 - \frac{\rho\, u}{\rho_e u_e}\right) dy \qquad (6.101)$$

Because of difficulties in solving (6.101), the simpler expression (6.100) is used to calculate displacement thickness for all flows. Transforming to the x, η coordinates, (6.100) is

$$\delta^* = \sqrt{\frac{\rho_\infty \mu_\infty x}{u_e}} \int_0^\infty \left(1 - \frac{\rho u}{\rho_e u_e}\right) \frac{1}{\rho}\, d\eta$$

$$= \sqrt{\frac{\mu_\infty x}{\rho_\infty u_e}}\ \frac{\rho_\infty}{\rho_e} \int_0^\infty \left(\frac{\rho_e}{\rho} - \frac{u}{u_e}\right) d\eta$$

$$= \sqrt{\frac{\mu_\infty x}{u_\infty \rho_\infty}} \sqrt{\frac{u_\infty}{u_e}}\ \frac{\rho_\infty}{\rho_e} \int_0^\infty \left(\frac{\rho_e}{\rho} - f'\right) d\eta \qquad (6.102)$$

The program calculates a dimensionless displacement thickness Δ^*, which is defined by

$$\Delta^* = \sqrt{\frac{\rho_\infty u_\infty c}{\mu_\infty}}\ \frac{\delta^*}{c} = \sqrt{\frac{u_\infty}{u_e}\frac{x}{c}}\ \frac{\rho_\infty}{\rho_e}\left[\int_0^\infty \left(\frac{\rho_e}{\rho} - f'\right) d\eta\right] \qquad (6.103)$$

When comparing solutions with real flows the dimension η is not convenient, because of the transformation between it and the true physical height y. Therefore the program calculates y from η.

$$\eta = \sqrt{\frac{u_e}{\rho_\infty \mu_\infty x}} \int_0^y \rho\, dy \qquad (6.4)$$

or

$$y = \sqrt{\frac{\rho_\infty \mu_\infty x}{u_e}} \int_0^\eta \frac{1}{\rho}\, d\eta \qquad (6.104)$$

Define a dimensionless Y as

$$Y = \sqrt{\frac{\rho_\infty u_\infty c}{\mu_\infty}}\ \frac{y}{c} \qquad (6.105)$$

Then

$$Y = \frac{\int_0^\eta \frac{\rho_e}{\rho}\, d\eta}{\sqrt{\frac{u_e}{u_\infty}\frac{c}{x}}\ \frac{\rho_e}{\rho_\infty}} \qquad (6.106)$$

Introduction of Y in (6.103) gives

$$\Delta^* = \lim_{\eta \to \infty} \left[Y - \sqrt{\frac{u_\infty}{u_e} \frac{x}{c}} \frac{\rho_\infty}{\rho_e} f \right] \tag{6.107}$$

The momentum thickness is given by

$$\Theta = \int_0^\infty \frac{\rho u}{\rho_e u_e} \left(1 - \frac{u}{u_e}\right) dy \tag{6.108}$$

or in x, η coordinates by

$$\Theta = \sqrt{\frac{\mu_\infty x}{\rho_\infty u_\infty}} \sqrt{\frac{u_\infty}{u_e}} \frac{\rho_\infty}{\rho_e} \int_0^\infty f'(1 - f') \, d\eta \tag{6.109}$$

The program calculates a dimensionless momentum thickness defined as

$$\theta \equiv \sqrt{\frac{\rho_\infty u_\infty c}{\mu_\infty}} \frac{\Theta}{c} \tag{6.110}$$

or

$$\theta = \sqrt{\frac{u_\infty}{u_e} \frac{x}{c}} \frac{\rho_\infty}{\rho_e} \int_0^\infty f'(1 - f') \, d\eta \tag{6.111}$$

The shear stress at the wall is

$$\tau_w = \mu_w \left(\frac{\partial u}{\partial y}\right)_w \tag{6.112}$$

or in x, η coordinates

$$\tau_w = \sqrt{\frac{u_e}{\rho_\infty \mu_\infty x}} \mu_w \rho_w u_e f_w'' \tag{6.113}$$

Introduction of the local skin-friction coefficient defined as

$$c_f \equiv \frac{\tau_w}{\frac{1}{2}\rho_\infty u_\infty^2} \tag{6.114}$$

gives

$$c_f = 2\sqrt{\frac{\mu_\infty}{\rho_\infty u_\infty x}}\left(\frac{u_e}{u_\infty}\right)^{3/2}\frac{\rho_w\,\mu_w}{\rho_\infty\,\mu_\infty}\,f_w'' \tag{6.115}$$

A conventional shear parameter is

$$c_f^* = c_f\sqrt{\frac{\rho_\infty u_\infty c}{\mu_\infty}} = 2\left(\frac{u_e}{u_\infty}\right)^{3/2}\sqrt{\frac{c}{x}}\,\frac{\rho_w\,\mu_w}{\rho_\infty\,\mu_\infty}\,f_w'' \tag{6.116}$$

The heat transfer at the wall is

$$-q_w = \left(\frac{k}{c_p}\,\frac{\partial h}{\partial y}\right)_w \tag{6.117}$$

Now

$$\left(\frac{\partial h}{\partial y}\right)_w = \frac{\partial}{\partial y}\left[H - \frac{u^2}{2}\right]_w = \left(\frac{\partial H}{\partial y}\right)_w - \left(u\,\frac{\partial u}{\partial y}\right)_w = \left(\frac{\partial H}{\partial y}\right)_w \tag{6.118}$$

since $u_w = 0$. Heat transfer in x, η coordinates is given by

$$-q_w = \sqrt{\frac{u_e}{\rho_\infty \mu_\infty x}}\,\frac{1}{Pr_w}\,\rho_w\,\mu_w\,H_e\,g_w' \tag{6.119}$$

The Stanton number, a heat transfer parameter, is defined as*

$$St_\infty = \frac{-q_w}{\rho_\infty u_\infty (H_e - H_w)} = \sqrt{\frac{\mu_\infty}{\rho_\infty u_\infty x}}\sqrt{\frac{u_e}{u_\infty}}\,\frac{\rho_w\mu_w}{\rho_\infty\mu_\infty}\,\frac{1}{Pr_w}\,\frac{g_w'}{1-g_w} \tag{6.120}$$

The ratio of Stanton number to skin friction is given by

$$\frac{St_\infty}{c_f} = \frac{1}{2\,Pr_w}\,\frac{u_\infty}{u_e}\,\frac{1}{1-g_w}\,\frac{g_w'}{f_w''} \tag{6.121}$$

* The Stanton number is most often written in terms of $H_{rec} - H_w$ rather than $H_e - H_w$, but this is not convenient in the present method.

7.0 CHARACTER OF SOLUTION AS LEARNED FROM TRIAL RUNS

The principal purpose of this section is to establish the accuracy and character of the method of solution. It will be done by presenting a large number of flow cases that include large ranges in pressure gradient, heat transfer, transverse curvature effects, and different fluid-property laws. Whenever possible, comparisons are made with exact solutions or with experiment. Also, in some cases comparisons are made with approximate methods of other investigators. Section 7.1 discusses the accuracy for similar flows. Since these are almost the only flows for which exact solutions are available, they are used to study the effect of the various inputs in the computer program on the accuracy of the calculations in Section 7.2. Section 7.3 compares the present method of solution with that of Chapman and Rubesin for the special case of a flat plate with variable wall temperature. Effect of the various fluid-property laws on recovery factor is determined in Section 7.4. Section 7.5 compares the present method with the finite-difference method of Flügge-Lotz and Blottner. The present method is compared with experimental results for the special case of a circular cylinder in Section 7.6. An example of internal flow, the boundary layer inside a nozzle, is presented in Section 7.7. Boundary layers on a reentry-type body are presented in 7.8 showing the effect of altitude, body temperature, and the fluid-property laws on the solutions. Transverse curvature effects are studied in 7.9. Finally, in Section 7.10, discontinuities in body temperature and mass transfer are studied. This study is applicable to some types of ablation cooling.

The first — and an obvious — check of the program was simple incompressible flow. For such flow the equations reduce to the form presented in References 1 and 2, where the authors developed the present method of solution for incompressible flow. Many of the cases presented in References 1 and 2 were recalculated by the present method. Results were identical to the earlier ones and will not be repeated here. Since the energy equation is negligible and fluid properties are constants for incompressible flow, these cases afforded a check on only that portion of the program that solves the momentum equation.

7.1 Similar Flow

Since almost the only flows for which highly accurate solution are known are the similar flows calculated by Cohen and Reshotko (Reference 14), these were first used to check the programing of the equations. Similar flow occurs when the solution is a function of η only, that is, when f and g and their derivatives are independent of x. In their method Cohen and Reshotko used Stewartson's transformation to transform the compressible equation to an incompressible form. Specifically, the transformations are:

$$X = \int_0^x \lambda \frac{p_e}{p_T} \frac{a_e}{a_T} dx \tag{7.1}$$

$$Y = \frac{a_e}{a_T} \int_0^x \frac{\rho}{\rho_T} dy \tag{7.2}$$

$$U = \frac{a_T}{a_e} u \tag{7.3}$$

where here X, Y, and U are the transformed quantities, the subscript T refers to free-stream stagnation values, a is the velocity of sound, and λ is a constant in a linear viscosity-temperature relation. The transformations are restricted to the case where viscosity varies linearly with temperature and for Prandtl number 1.0. The same assumptions are used in the present method when comparing its results with those of Cohen and Reshotko. Similar flow occurs when

$$U_e = c X^m \tag{7.4}$$

Cohen and Reshotko present their results for specific values of the pressure gradient parameter β, which is related to m by

$$\beta = \frac{2m}{m + 1} \tag{7.5}$$

Results of the present method are compared with those of Cohen and Reshotko in Table II for various values of m and g_w. In the present method the calculation can be compared directly with Cohen and Reshotko's results by letting

$$u_e = U_e = c_1 x^m \tag{7.6}$$

That is, essentially low speed flow is assumed, but density does vary with enthalpy

$$\frac{\rho_e}{\rho} = \frac{h}{h_e}$$

The parameter P is identically equal to m for such flows. Results of the two methods differ by only 2 in the fourth decimal place for favorable pressure gradients. Cohen and Reshotko presented four significant figures in their results. In the present method the various inputs that affect the accuracy of the results were selected so that the calculations converged to five significant figures. These inputs are discussed in the next section. The agreement between the two methods is not so good near separation, that is, near $f_w'' = 0$. In the worst case, the difference is 2 in the second decimal place in f_w''. The present method becomes very sensitive near separation ($f_w'' < 0.08$) and its difficulties in obtaining a solution here are discussed in detail in References 2 and 3 for the case of incompressible flow. The values of g_w' and f_w'' presented in Table II for $P = 20$ and $\beta = 2.0$ should not agree exactly. A value of $\beta = 2.0$ corresponds to a value of $P = \infty$, and it is of course impossible to calculate such a flow by the present method. A value of $P = 20$ was used to convert the values of f_w'' and g_w' presented in Reference 14 for $\beta = 2.0$ to the values presented in Table II. As P becomes very large the results of the present method approach those of Cohen and Reshotko for $\beta = 2.0$.

For the case of favorable pressure gradients with heated walls, that is, the wall temperature greater than recovery temperature, the velocity within a portion of the boundary layer can exceed the local external velocity. This is known as velocity overshoot. An example is shown in figure 8, where $P = 1/3$, $g_w = h_w/H_e = 2.0$, and $M_e = 3.0$. Both enthalpy and velocity profiles are shown. The assumptions for fluid properties are the same as those used by Cohen and Reshotko; Pr = 1.0 and a viscosity proportional to temperature. By means of the Stewartson transformation the flow reduces exactly to that presented in Reference 14 for the transformed incompressible flow with $P = 1/3$ and $g_w = 2.0$.

TABLE II

COMPARISON OF SHEAR PARAMETER AND HEAT-TRANSFER PARAMETER CALCULATED BY PRESENT METHOD WITH THOSE CALCULATED BY COHEN AND RESHOTKO

β	P	g_w	f''_w		g'_w	
			Cohen and Reshotko	Present Method	Cohen and Reshotko	Present Method
1.0	1.0	1.0	1.2326	1.23259	0	0
1.0	1.0	2.0	1.7368	1.73671	-0.6154	-0.61533
0.50	0.33333	0.0	0.4741	0.47413	0.4040	0.40399
0.50	0.33333	0.2	0.5346	0.53477	0.3290	0.32922
0.50	0.33333	0.6	0.6489	0.64907	0.1706	0.17068
0.50	0.33333	1.0	0.7575	0.75745	0	0
0.50	0.33333	2.0	1.0085	1.00863	-0.4674	-0.46745
0.0	0.0	0.0	0.3321	0.332057	0.3321	0.332057
0.0	0.0	0.2	0.3321	0.332057	0.2657	0.265676
0.0	0.0	0.6	0.3321	0.332057	0.1328	0.132838
0.0	0.0	1.0	0.3321	0.332057	0.0	0.0
0.0	0.0	2.0	0.3321	0.332057	-0.3321	-0.332057
-0.10	-0.04762	2.0	0.1246	0.12478	-0.2783	-0.27826
-0.160	-0.07407	1.0	0.1296	0.12809	0.0	0.0
-0.1988	-0.09041	1.0	0.0	0.02405	0.0	0.0
-0.200	-0.09091	0.6	0.1472	0.14747	0.1096	0.10873
-0.240	-0.10714	0.6	0.0711	0.08172	0.0985	0.10304
-0.300	-0.13044	0.0	0.2098	0.21213	0.2810	0.28392
-0.300	-0.13044	0.2	0.1376	0.13843	0.2080	0.21079
-0.325	-0.13979	0.2	0.0888	0.09720	0.1910	0.19981
2.0*	20.0*	0.0	2.3917	2.33313	1.6860	1.62839
2.0	20.0	0.2	2.0719	3.01625	1.4034	1.38057
2.0	20.0	0.6	4.3191	4.23688	0.7466	0.74326
2.0	20.0	1.0	5.4666	5.34950	0	0
2.0	20.0	2.0	8.0615	7.89056	-2.1429	-2.12336

* Since $\beta = 2.0$ corresponds to $P = \infty$, the two methods can not agree exactly.

7.2 Effect of the Various Inputs on the Accuracy of the Solution

Since exact answers are available for similar flows, these flows have been used to study the accuracy of the computer program. Quantities that are inputs and that affect the accuracy of the computer results are $\Delta\eta$, η_∞, K, L, ϵ, Δx, and the trial values of either g'_w or g_w.

The step length in η affects the accuracy of the calculation because of truncation errors in the integration formulas. Effect of the step length on the calculation of f''_w is shown in Table III. Its effect on g'_w is similar. In fact the error in f''_w is typical of the maximum error that occurs in all quantities calculated, including the enthalpy profiles. In the table and in the results that follow, the various inputs that affect the accuracy have the following values, unless otherwise specified: $\Delta\eta = 0.05$, $\eta_\infty = 9.0$, $K = 0.50$, $L = 3.0$, $\epsilon = 0.000001$. The particular values of P and g_w presented in the table were chosen because exact results (4 decimal places) are available for them (Reference 14) and because they cover a large range of both pressure gradient and wall temperature. The table shows that for favorable pressure gradients a $\Delta\eta$ of 0.05 gives five-place accuracy and a $\Delta\eta$ of 0.2, three-place; but the error is larger for unfavorable pressure gradients ($P < 0$).

The maximum value of η, that is, η_∞, is an input in the program. The method of solution (see Sections 6.5 and 6.6) forces the boundary layer to satisfy the external conditions on φ' and ψ at this height. Boundary-layer thickness can vary greatly with Mach number, pressure gradient, and wall temperature, g_w. If η_∞ is chosen too small, the results will be in error. Effect of different values of η_∞ on two of the similar flows is shown in Table IV. Values of f''_w are shown, but the effect on g'_w is similar. Because η_∞ can vary greatly with the flow conditions, especially at high Mach numbers, it is not always possible to select its proper value without first making a trial run. It must be selected so that the higher derivatives of f' and g approach zero asymptotically at the outer edge of the boundary layer. In all the cases that have been calculated, it was found that the maximum value of η_∞ for five-place accuracy was about 9. For favorable pressure gradient, η_∞ can be considerably less for the same accuracy.

TABLE III

EFFECT OF STEP SIZE IN η ON ACCURACY OF SOLUTION

$\eta_\infty = 9.0$, K = 0.5, L = 3, $\epsilon = 10^{-6}$

FLOW		VALUES OF f''_w				
P	g_w	$\Delta\eta = 0.5$	$\Delta\eta = 0.2$	$\Delta\eta = 0.1$	$\Delta\eta = 0.05$	$\Delta\eta = 0.02$
1.0	1.0	1.270*	1.23270	1.232627	1.232591	1.232588
0.333333	0.2	0.540	0.53440	0.53690	0.534770	0.534786
-0.0476191	2.0	0.1905	0.1234	0.12391	0.124780	0.124703
-0.1304348	0.2	—— **	0.169	0.1391	0.138425	0.138256

*Digits underlined may not be significant

**Program unable to converge to a solution

TABLE IV

EFFECT OF INPUT η_∞ ON ACCURACY OF SOLUTION

$\Delta\eta = 0.05$, K = 0.5, L = 3, $\epsilon = 10^{-6}$

η_∞	f''_w	
	P = 1.0, g_w = 1.0	P = -0.0476191, g_w = 2.0
12	1.232588	0.124778
10	1.232588	0.124780
8	1.232588	0.12482
6	1.232591	0.1269
4	1.2328	0.1342

Digits underlined may not be significant

Selection of η_∞ much larger than necessary can affect the accuracy of the results, for, in the trial solutions of the energy equation, the values of ψ and ψ' at the outer edge of the boundary layer can grow exponentially. In cases when η_∞ was set too large, values as high as 10^{10} have been observed. In the procedure of solution, the two trial solutions are added to meet the outer boundary condition, $\psi(\eta_\infty) = 0$ (see equations 6.56 and 6.57). This process of addition can lead to large roundoff errors in the ''correct'' solution of ψ if the trial values of ψ are very large. (The computer program carries only eight significant digits.)

The bound K also affects the accuracy of the results. Its purpose is described in detail in Section 6.5; briefly, it affects the solution of the momentum equation in the following way: the correct value of f_w'' is found by trying different values of f_w''. Once three trial solutions have been found such that φ' at η_∞ is between the bounds of $-K \leq \varphi'(\eta_\infty) \leq K$, a three-point interpolation procedure is then used to determine the solution that satisfies the outer boundary condition. Effect of the bound on the solution is shown in Table V for two similar flows.

TABLE V

EFFECT OF THE BOUND K ON ACCURACY OF SOLUTION

$\Delta\eta = 0.05$, $\eta_\infty = 9.0$, L = 3, $\epsilon = 10^{-6}$

K	f_w''	
	P = 1.0 g_w = 1.0	P = -0.0476191 g_w = 2.0
0.02	1.232588	0.124780
0.2	1.232588	0.124780
0.5	1.232591	0.124786
1.0	1.23260	0.12481
2.0	1.23262	0.12489
Digits underlined may not be significant		

Results of a large number of cases show that a K of 0.5 produces values accurate to five decimal places, providing the Mach number is not so high and the wall so warm as to give large overshoot. In such extreme cases the velocity ratio $f' = 1 + \varphi'$ can exceed 1.5 in the boundary layer. In the example shown in figure 8, f' has a maximum value of 1.49. In such cases K must be chosen larger than the amount of overshoot. But in favorable pressure gradients care also must be taken that K is not too large, no more than about 2.0. For it is possible in such cases that though φ' for low trial solutions at first grows negatively, the growth can reverse; φ' then grows positively for large η, and the low trial solution can exceed a high one (see Reference 3). If this happens, the program fails to converge to an answer.

The input L determines the number of successive solutions of the energy equation used to calculate fluid properties and the enthalpy profile (see Section 6.9). Remember that in solving the energy equation, the fluid properties are first assumed and the enthalpy distribution is computed. New fluid properties are determined from the calculated enthalpy and the energy equation is solved again. This iterative procedure is continued L times. From the cases studied it has been found that for flows where the enthalpy changes by a factor of about 10 across the boundary layer an L of 3 produces values of both fluid properties and enthalpy that converge to at least four decimal places. An L of 4 gives convergence to at least six decimal places. When the enthalpy change through the boundary layer is much less, less than three times, an L of 2 gives convergence of the calculated values to at least four decimal places. The value of L necessary to give convergence of the calculated values to a specified accuracy depends mostly on the magnitude of the enthalpy change across the boundary layer and is independent of pressure gradient, Mach number, etc.

In the method of solution, once the energy equation has been solved corrected fluid properties are used to solve again the momentum equation (see Section 6.9). This iterative procedure is continued until

$$\left| (\varphi_w'')_Q - (\varphi_w'')_{Q-1} \right| < \epsilon \qquad (7.7)$$

where ϵ is an input and Q is a count of successive calculations of the momentum equation. Again, as with L, the number of times, $Q + 1$, that the momentum equation has to be solved in order to satisfy eq.(7.7), depends mostly on the enthalpy change across the boundary layer and appears to be independent of pressure gradient, Mach number, etc. Variation of Q with ϵ is shown in Table VI.

TABLE VI

NUMBER OF SUCCESSIVE CALCULATIONS $(Q + 1)$ OF MOMENTUM EQUATION NECESSARY TO SATISFY ACCURACY REQUIREMENT

$$\left|(\varphi_w'')_Q - (\varphi_w'')_{Q-1}\right| < \epsilon$$

Enthalpy Change Across Boundary Layer	Q			
	$\epsilon = 10^{-6}$	$\epsilon = 10^{-5}$	$\epsilon = 10^{-4}$	$\epsilon = 10^{-3}$
Approximately 10 Times	5	3	3	2
3 Times or Less	3	2	1	1

The effect of step length in x on the solution appears to be identical to that reported by the authors in References 2 and 3 for the incompressible boundary layer. The details will not be repeated here; but, briefly, not only must the size of Δx be considered in selecting the spacing in the x-direction, but also the quantity $x/\Delta x$. The latter appears in the terms containing the x-derivatives in the following way. From the momentum equation the term containing the x-derivative of φ' is replaced by a finite-difference term of the form

$$x\left[\varphi'\frac{\partial\varphi'}{\partial x}\right] \simeq x\left[\varphi'\left(\frac{\varphi_n' - \varphi_{n-1}'}{x_n - x_{n-1}}\right)\right]$$

$$= \frac{x}{\Delta x}\ \varphi'\ \Delta\varphi'$$

As Δx approaches zero $\Delta\varphi'$ approaches zero in an exact solution; but in the computer program roundoff errors exist and, furthermore, these errors are multiplied by the quantity $x/\Delta x$. Therefore as Δx approaches zero the error in the solution is not necessarily decreased. This type of roundoff error is observed as Δx becomes small in the present method. It does not occur for values of $x/\Delta x$ less than about 25. The maximum error that has been observed is one in the fifth significant digit for $x/\Delta x \simeq 25$. The error grows as $x/\Delta x$ becomes larger. Of course, this roundoff error is a function of the number of significant digits, eight, that are carried in the computer program and is not inherent in the method of solution. It can be reduced by using ''double precision'' routines, that is, sixteen significant digits would be carried instead of the present eight. In all of the calculations presented in this report Δx was selected so that the quantity $x/\Delta x$ was less than 25. Therefore it is believed that the results are free of this type of roundoff error.

In particular cases care in selecting two of the other input quantities is necessary to prevent erroneous results. If g_w is known, two trial values of g_w' must be input; or if g_w' is known, then two trial values of g_w must be input. In the method of solution these two trial values are used to obtain two solutions of the energy equation (see Section 6.6). Then, because the equation is linear, the correct solution is found by combining the two solutions to meet the outer boundary conditions. If the trial values at the wall are far from the correct solution, the trial values of ψ and ψ' can become very large near the outer edge of the boundary layer. This is the same phenomenon that occurs when η_∞ is selected too large, and that is discussed above. In one example when solving for g_w' which had a correct value of approximately 0.4, trial values of 0.0 and 1.0 were input. At the the outer edge of the boundary layer they led to values of ψ of around -10^9 and $+10^{10}$, respectively. When the two solutions were combined, in order to satisfy the outer boundary condition (see equations 6.56 and 6.57), the large trial values led to roundoff errors in the second significant digit of ψ. This roundoff error can be eliminated by selecting trial values of g_w' (or g_w) near to the correct value, within one significant digit. Selection is done by either experience or a trial run. The magnitude of the roundoff error can be easily seen by inspecting values of ψ and ψ' near η_∞.

7.3 Flow on a Flat Plate with Variable Temperature

Chapman and Rubesin developed a method for calculating exactly the compressible laminar boundary layer on a flat plate with variable wall temperature (Reference 15). The method requires that the surface temperature distribution be expressible as a polynomial in surface distance, that the viscosity varies linearly with temperature through the boundary layer, and that the Prandtl number be constant. One of the examples presented by Chapman and Rubesin was calculated by the present method with the same assumptions for fluid properties. The distribution of surface temperature is given by

$$\frac{T_w}{T_e} - \frac{T_{ad}}{T_e} = \frac{T_{ad}}{T_e}\,(0.25 - 0.83\,x + 0.33\,x^2) \qquad (7.8)$$

where $T_{ad}/T_e = 1 + 0.169\,M_\infty^2$ is the wall recovery temperature and T_e is the temperature at the edge of the boundary layer. Since constant c_p is assumed the wall enthalpy distribution has the same form as the temperature. The external flow has a Mach number of 3.0. Results of the two calculations are compared in figure 9 in the form of

$$-\frac{g_w'}{(g_w)_{ad}} = \frac{q\,x}{k_e \sqrt{\frac{u_e\,x'}{\nu_e}}\;T_{ad}} \qquad (7.9)$$

versus x. The latter quantity is the parameter used by Chapman and Rubesin. Greatest disagreement between the two methods is 5 in the fourth significant digit. Furthermore, this difference is consistent for the whole length of flow; the values calculated by the present method are (0.4 ± 0.1) percent less than the values calculated by Chapman and Rubesin. In the present method inputs were selected in such a way that the calculation was accurate to five decimal places. In using the method of Chapman and Rubesin the calculation depended on parameters given to four figures in Reference 15. Therefore the two calculations might be expected to agree to at least four decimal places. But Chapman and Rubesin do not specifically state that all four digits presented are significant. The value of recovery factor they calculated is presented to only three figures, a recovery factor = 0.845. This affects the values of the other quantities — temperature and heat transfer —

calculated by their method. Recovery factor calculated by the present method for the flow is 0.8475. The ratio of recovery temperature calculated by the present method to that by Chapman and Rubesin is 1.0018.

7.4 Effect of Fluid-Property Laws on Recovery Factor

Effect of the various fluid-property laws on recovery factor was studied for flow over a flat plate and flow over a cone at Mach numbers from 1.0 to 10.0. Recovery factor r_f had its usual definition

$$\frac{T_{ad}}{T_e} = \frac{h_{ad}}{h_e} = 1 + r_f \frac{\gamma - 1}{2} M_e^2 \qquad (7.10)$$

Relation (7.10) is exact only if c_p is constant. Fluid-property laws studied included: first, a viscosity proportional to temperature and an arbitrary but constant Prandtl number, and second, the "exact" property laws of Cohen (see Section 6.3). The assumption of viscosity proportional to temperature in the boundary layer gives a value of $C = \rho\mu/\rho_e\mu_e$ of 1.0, since density is inversely proportional to temperature across the boundary layer. Recovery factor versus Mach number is shown in figure 10a for the various laws. Cohen's relations are not used below a Mach number of 2.0 because they are not valid below that Mach number for the altitude assumed, 50,000 ft. They are not valid for $h/h_{ref} < 0.0152$, where h_{ref} is Cohen's reference enthalpy, 2.119×10^8 ft^2/sec^2. The assumptions of viscosity proportional to temperature, $C = 1.0$, and a constant Prandtl number of 0.72, which are often used in boundary-layer work, give recovery factors that are within 3.3 percent of those calculated with the more nearly exact properties. The calculated recovery factors for a cone are identical to those for the flat plate with indentical boundary conditions.

Variation of the calculated recovery factors with Prandtl number at the wall is shown in figure 10b. The approximate relation that is often assumed in boundary-layer theory

$$r_f = \sqrt{Pr} \qquad (7.11)$$

is also shown.

7.5 Comparison of Present Method with that of Flügge-Lotz and Blottner

Recently Flügge-Lotz and Blottner developed an implicit finite-difference method for calculating the compressible laminar boundary layer (Reference 6). Fluid-property relations that were used included an arbitrary but constant Prandtl number and one of two relations for viscosity. Either Sutherland's viscosity law or a viscosity that varied linearly with temperature was used, and examples for both are given in Reference 6. Since, as of now, the present method is programed to use either Cohen's "exact" relation for viscosity or a linear variation with temperature, results of the two methods can be compared directly only for the examples in Reference 6 that use the linear viscosity law. These examples consist of a flat plate at Mach number 3.0 with an insulated wall and with a heated wall such that $T_w/T_{ad} = 2.0$. Because the boundary conditions are independent of x, the flows can also be calculated by similar-flow methods. Flügge-Lotz and Blottner compare their results with the similar solution of Low (Reference 16). The results of the present method are compared with the same method.

The shear parameter f_w'' calculated by the present method agrees with that calculated by Low's method within the accuracy with which his method can be used. His method uses parameters presented to only four decimal places. For the heated plate Low's method gives $f_w'' = 0.33205$ as compared to 0.332057 obtained by the present method. Flügge-Lotz and Blottner compare their results with Low's in graphical form, and it appears that values of f_w'' agree to at least four decimal places a short distance downstream of the start of the calculation. At the start the agreement between the two methods is not so close. In the method of Flügge-Lotz and Blottner the form of the equation is singular at $x = 0$, and the calculation must be started at some point downstream of $x = 0$. Furthermore, the initial profile must be specified at this starting point. Flügge-Lotz and Blottner used the similar profile of Low to get started, and they state in Reference 6 "Since the initial profiles are only accurate to four decimal places, there are initially errors in the boundary-layer calculations and characteristics. These errors appear to decrease as the computations proceed."

7.5 Comparison of Present Method with that of Flügge-Lotz and Blottner

Recently Flügge-Lotz and Blottner developed an implicit finite-difference method for calculating the compressible laminar boundary layer (Reference 6). Fluid-property relations that were used included an arbitrary but constant Prandtl number and one of two relations for viscosity. Either Sutherland's viscosity law or a viscosity that varied linearly with temperature was used, and examples for both are given in Reference 6. Since, as of now, the present method is programed to use either Cohen's "exact" relation for viscosity or a linear variation with temperature, results of the two methods can be compared directly only for the examples in Reference 6 that use the linear viscosity law. These examples consist of a flat plate at Mach number 3.0 with an insulated wall and with a heated wall such that $T_w/T_{ad} = 2.0$. Because the boundary conditions are independent of x, the flows can also be calculated by similar-flow methods. Flügge-Lotz and Blottner compare their results with the similar solution of Low (Reference 16). The results of the present method are compared with the same method.

The shear parameter f_w'' calculated by the present method agrees with that calculated by Low's method within the accuracy with which his method can be used. His method uses parameters presented to only four decimal places. For the heated plate Low's method gives $f_w'' = 0.33205$ as compared to 0.332057 obtained by the present method. Flügge-Lotz and Blottner compare their results with Low's in graphical form, and it appears that values of f_w'' agree to at least four decimal places a short distance downstream of the start of the calculation. At the start the agreement between the two methods is not so close. In the method of Flügge-Lotz and Blottner the form of the equation is singular at $x = 0$, and the calculation must be started at some point downstream of $x = 0$. Furthermore, the initial profile must be specified at this starting point. Flügge-Lotz and Blottner used the similar profile of Low to get started, and they state in Reference 6 "Since the initial profiles are only accurate to four decimal places, there are initially errors in the boundary-layer calculations and characteristics. These errors appear to decrease as the computations proceed."

The agreement of heat-transfer values calculated by the present method with those of Low's similar method is not so good as that for the shear parameter. For the heated plate at Mach 3.0, the present method gave a value of g'_w of -0.29416 as compared to -0.29367 obtained from Low's parameters. Since Low presents his data to four decimal places, better agreement might be expected. The disagreement may be due to the difference in the recovery factor calculated and used by Low, $r_f = 0.8477$, and that calculated by the present method, 0.84746. Flügge-Lotz and Blottner also compare their heat-transfer values with Low's values calculated for the same flow. Close observation of their graphs at a point downstream of the initial x-station appears to show that their results are around 0.2 percent higher than Low's (see figures 6(b) and 7(b) of Reference 6). This is about the same percentage difference that appears between the present method and Low's, that is,

$$\frac{\text{Present method } g'_w}{\text{Low's } g'_w} = 1.002$$

Velocity and enthalpy profiles as calculated by the three methods — Low, Flügge-Lotz and Blottner, and present — agree to three decimal places at the one station, $x = 1.10$, where data exist so that such a comparison could be made. This is within the accuracy with which the profiles are presented in Reference 6.

7.6 Comparison of Heat Transfer Calculated by the Present Method with that Measured on a Circular Cylinder

Few experimental data on compressible boundary layers are available for comparison with the prediction of theories. Exceptions are a few heat-transfer data. Reference 17 presents experimental data on heat transfer measured on circular cylinders with their axes normal to the flow at several Mach numbers. Comparison of the measured heat transfer with that calculated by the present method is shown in figure 11. The external velocity and onset flow conditions used in the calculation were obtained from Reference 17. The experimental temperatures were so low that the relations for fluid properties given by Cohen (see Section 6.3) are invalid. Therefore, the simple assumptions of constant Prandtl number (0.72) and a viscosity proportional to temperature through the boundary layer were assumed.

As discussed by the authors of Reference 17, the magnitude of the experimental error is not known; but it may be as great as the difference between the calculated and measured results in figure 11. They point out that the experimental data at $M = 4.15$ are known to include experimental error not present at the other Mach numbers, and, furthermore, that the error in instrumentation tends to increase the indicated heat transfer rearward of 40°. They also state that "for $\alpha \gtrsim 90°$ the accuracy of all the data becomes questionable because of the very small convective heat rates compared with radiation and other sources of error." To avoid confusion with experimental points, calculated points are not indicated in the figure, but the step size was 5° except near the stagnation point, where step lengths of 1° were used. Smaller steps were used here in order to converge on the heat-transfer rate at the stagnation point. Values calculated are believed to be accurate to three decimal places. Experimental data were obtained at $g_w \simeq 1.0$, 0.8, and 0.7. The calculated curves shown are for $g_w = 0.8$, but calculations at the other two enthalpies were very similar. A g_w of 0.70 gives values of $[g_w/(g_{ad} - g_w)]/[g_w/(g_{ad} - g_w)]_{stag}$ that are from 0.7 to 1.2 percent higher than those shown.

7.7 Boundary Layer in an Axisymmetric Convergent-Divergent Rocket Nozzle

As an example of internal axisymmetric flow the boundary layer inside a rocket nozzle was calculated. The flow involves both large pressure gradients and heat transfer. It is similar to the flow calculated by C. B. Cohen and E. Reshotko in Reference 18, but an exact comparison between the two calculations can not be made because there is insufficient information on the flow properties and the nozzle dimensions of Reference 18. Radius, surface distance, and the velocity and Mach number at the center of the nozzle are plotted in figure 12 against the axial distance. These local flow conditions were obtained by means of simple one-dimensional flow relations. Stagnation pressure is assumed to be 500 pounds per square inch and stagnation temperature as 4000°R, which leads to a total enthalpy $H_e = 27.246 \times 10^6$ ft^2/sec^2. The nozzle wall is assumed cooled to a uniform temperature of 800°R, which corresponds to an enthalpy ratio of $g_w = 0.17625$.

Results of the calculation are presented in figure 13. The skin-friction coefficient c_f, defined by equation (6.115), and the ratio of Stanton number to skin friction coefficient, defined by equations (6.120) and (6.121), are shown. Calculations denoted by "exact properties" were obtained by using the relations of N.B.Cohen described in Section 6.3. A calculation was also made by using the simple assumptions of constant Prandtl number and viscosity proportional to local enthalpy. Because of the high enthalpies involved, a Prandtl number of 0.78 was chosen. Figure 13 shows that these simple assumptions for fluid properties lead to results that seriously overestimate both skin friction and heat transfer at the higher Mach number. At the lower Mach numbers, the effect is reversed, that is, the simple assumptions gave lower skin friction and heat transfer than those calculated for exact properties. This study and those in previous sections indicate that the exact-property relations should be used if the local enthalpy exceeds 4×10^6 ft^2/sec^2.

Stagnation-point flow is assumed at the start of the flow ($x = 0$). Because $u_e = 0$, here, the skin friction coefficient c_f is singular and, of course, can not be presented at the stagnation point in figure 13. The shear parameter f_w'' and also the gradient of g at the wall, g_w', are finite here and are

$$f_w'' = 0.38084 \; ; \quad g_w' = 0.16523 \qquad \text{for exact properties}$$

$$f_w'' = 0.73507 \; ; \quad g_w' = 0.38177 \qquad \text{for } C = 1.0, \; Pr = 0.78$$

7.8 Boundary Layer on a Spherically Blunted Cone at Mach Numbers of 3.0 and 9.0

Boundary layers were calculated on a reentry-type body that consists of a 15° half-angle cone blunted with a spherical nose. The conical and spherical surfaces join in such a way that there is no discontinuity in body slope. The velocity distribution outside the boundary layer was calculated by a computer program that consists of (1) a solution of the blunt-body problem from the stagnation point to a point past the sonic point and (2) a solution by the method of characteristics in the supersonic flow region. The method of

characteristics is started just aft of the sonic point by using local velocities and pressures given by the blunt-body solution as an initial boundary condition. Variation of the inviscid velocity and Mach number with axial distance is shown in figure 14. Surface distance and local radius are also shown. Though the velocity varies smoothly in going from the blunt-body solution to the characteristics solution, there is a large change in velocity gradient, du_e/dx, just aft of the point where the change in methods occurs, $x = 0.9$. This results in large changes in the parameter $P = (x/u_e)(du_e/dx)$ just aft of this point, which produces large changes in the calculated values, as will be seen below.

Boundary layers on the body were calculated at the two speeds, M = 3.0 amd 9.0, at three altitudes, 50,000, 100,000 and 250,000 ft., for three body temperatures. Results for M = 3.0 are shown in figure 15 (a, b, c). Results are independent of altitude to three decimal places; therefore,only the 50,000-ft values are shown. The reason that the effect of altitude is found to be negligible is that there is only a small change in total enthalpy with altitude. Total enthalpy is given in Table VII for the three altitudes. Also, the reference velocity a_t that is used to nondimensionalize the velocity u_e is given. The velocity a_t is the velocity of sound at free-stream stagnation conditions. The total enthalpy of about 6.6×10^6 ft^2/sec^2 at the lower altitudes corresponds to a total temperature of about 1090°R. The three body temperatures presented are: $g_w = 0.357$, which gives a body temperature equal to about the static temperature of the onset flow; $g_w = 0.458$, which gives a wall temperature equal to about 50°F; and an adiabatic wall, which is calculated by setting $g_w' = 0$. Variation of the skin-friction coefficient c_f and ratio of Stanton number to the skin friction coefficient St/c_f with surface distance are shown for the flows when g_w is specified. When an adiabatic wall ($g_w' = 0$) is specified, c_f and g_w are shown. To further investigate the effect of fluid-property laws on the solution, the flows were calculated twice, once with the ''exact fluid properties'' of Cohen (Section 6.3), and again with the simple assumptions of constant Prandtl number and a linear viscosity law. It is seen that the simple assumptions greatly overestimate the skin friction and heat transfer (figure 15(a, b)) and, in the adiabatic wall case, the surface temperature (figure 15c). For the results with exact properties the figures show a ''bump'' in c_f just aft of $x = 0.90$. This is at the point, mentioned

in the last paragraph, where the method of calculating the inviscid flow results in a large gradient in u_e. This gradient causes a large variation in the local enthalpy h in this region, which produces a large variation in Prandtl number (see figure 2). Even though there is a large change in local flow conditions it is believed that the calculated values are accurate to three decimal places, because in accuracy studies where the present method was used to calculate flows with discontinuities in P, and also in g_w and f_w, such accuracy was obtained downstream of the discontinuity.

Results for $M = 9.0$, shown in figure 16(a, b, c), have a variation similar to those at the lower speed. As was also the case for the flow at Mach number 3.0, altitude has a small effect on the calculated values. A change from 50,000 ft to 250,000 ft causes at most a change of 4 in the third significant figure of the values calculated. Total enthalpy and the reference velocity used in the calculations are given in Table VII. The total enthalpy of about 4.0×10^7 ft^2/sec^2 corresponds to a total temperature of about 6700°R. Since some dissociation would occur at this high a temperature, there would be some change in the fluid properties. But the magnitude of this change and its effect on the solution are left for a later report. It will be simple to study the effect of equilibrium dissociation by means of the present method of solution, since all that will be necessary is to replace the functions for Prandtl number given in Section 6.3 by similar functions for an effective Prandtl number that includes dissociation. Such a Prandtl number is presented in Reference 7. The three body temperatures in figure 16 are: $g_w = 0.083124$, which gives a wall temperature of about 560°R or 100°F; $g_w = 0.40$, which gives a wall temperature of around 2000°R; and the adiabatic wall, which is given by $g'_w = 0$. Again the simpler fluid-property laws — those of a viscosity that varies linearly with temperature and a constant Prandtl number — give results that differ greatly from those obtained with the ''exact properties''. Values of St/c_f are indeterminate at the stagnation point, but values of f''_w, g_w, and g'_w are finite and are given in Table VIII.

TABLE VII

ALTITUDE, TOTAL ENTHALPY, AND REFERENCE VELOCITY USED IN CALCULATION OF FLOWS OVER THE SPHERICALLY BLUNTED CONE

Altitude ft	Static Temperature °R	Mach 3		Mach 9	
		$H_e \times 10^{-7}$ ft^2/sec^2	$a_t = u_\infty$ ft/sec	$H_e \times 10^{-7}$ ft^2/sec^2	$a_t = u_\infty$ ft/sec
50,000	390.0	0.65523	1620.5	4.03180	4016.5
100,000	392.4	0.65893	1625.0	4.05386	4027.4
250,000	451.8	0.75894	1743.6	4.66769	4321.5

TABLE VIII

STAGNATION POINT VALUES OF f_w'', g_w, AND g_w' FOR THE SPHERICALLY BLUNTED CONE

M_∞	Altitude ft	f_w''		g_w		g_w'	
		Exact Properties	Pr = 0.72 C = 1.0	Exact Properties	Pr = 0.72 C = 1.0	Exact Properties	Pr = 0.72 C = 1.0
3.0	50,000	1.7989	1.3119	1.0	1.0	0.0*	0.0*
3.0	50,000	0.9851	0.9828	0.3570*	0.3570*	0.4205	0.4076
3.0	50,000	1.1365	1.0369	0.4580*	0.4558*	0.3878	0.3475
9.0	50,000	0.9261	1.3119	1.0	1.0	0.0*	0.0*
9.0	50,000	0.3155	0.8275	0.08312*	0.08312*	0.1883	0.5603
9.0	50,000	0.6091	1.0060	0.400*	0.400*	0.2117	0.3822
9.0	250,000	0.9261	1.3119	1.0	1.0	0.0*	0.0*
9.0	250,000	0.3185	0.8275	0.08312*	0.08312*	0.1854	0.5603
9.0	250,000	0.6113	1.0060	0.400*	0.400*	0.2162	0.3822

*Input values

7.9 Transverse Curvature Effect in Axially Symmetric Flow

In all the examples presented so far, the transverse curvature terms have been neglected. These terms become of importance when the boundary layer has a thickness of about the same magnitude as the body radius. There are two of these terms: the first term, which includes T, on the right-hand side of both the momentum equation (6.35) and the energy equation (6.46) and the term that contains $N = \frac{P+1}{2} + R$ in both equations. The transverse curvature parameter T is defined by (6.32) and the radius parameter R by (6.33b).

Transverse curvature effects were investigated by Probstein and Elliott, Reference 19. The study was restricted to similar flow and essentially expanded the stream function f and the enthalpy function g in a power series in ξ, where

$$\xi = \sqrt{\frac{\nu_e}{u_e r_o}} \frac{\cos\alpha}{r_o^{3/2}} \left[\int_0^x r_o^2 \, dx\right]^{1/2}$$

$$\sim \frac{\delta^* \cos\alpha}{r_o} \tag{7.12}$$

That is,

$$f(\xi, \eta) = f_o(\eta) + \xi f_1(\eta) + \xi^2 f_2(\eta) \ldots$$

$$= \sum_{j=0}^{\infty} \xi^j f_j(\eta) \tag{7.13}$$

and there is a similar function for enthalpy. The expansion parameter was assumed to be small with respect to unity. Substituting their asymptotic expansions into the momentum and energy equations, and equating to zero all terms with the same power in ξ, Probstein and Elliot obtained a double infinity of ordinary differential equations. They found all these equations except the zeroth order momentum equation to be linear, because a $Pr = 1.0$ and a viscosity proportional to temperature had been assumed. They obtained solutions of the zeroth- and first-order equations. They forced the equations to be similar, that is, independent of x, by assuming ξ to be constant. As discussed by them, this assumption requires that the boundary-layer thickness be directly proportional to the body radius. They present solutions for

only two types of bodies — a cone and a cylinder with axes aligned with the flow. Their assumption of similarity — that δ^* varies as the body radius — is a poor approximation for these two bodies, for in reality the thickness grows nearly parabolically with x, as $\sqrt{x}$.

The present method was used to calculate the boundary layer on the same two types of bodies. Assumptions on the fluid properties are the same as those used by Probstein and Elliott. Results are presented in terms of the parameters used by them,

$$\frac{r_o}{x}\sqrt{Re}\;\frac{f_w'' - (f_w'')_{T=0}}{(f_w'')_{T=0}} \tag{7.14}$$

for the cylinder, and

$$\tan\alpha\sqrt{Re}\;\frac{f_w'' - (f_w'')_{T=0}}{(f_w'')_{T=0}} \tag{7.15}$$

for the cone, where $Re = u_e x/\nu_e$; α is the angle between the normal to surface and the radius, but is also the half angle of the cone here; and the subscript $T = 0$ denotes the solution with no transverse curvature effect. For the cylinder the radius parameter R is zero, and for the cone it is given exactly by (6.33b)

$$R = \frac{\dfrac{x}{r_o}\dfrac{dr_o}{dx}}{1 + T_w\displaystyle\int_0^\eta \frac{\rho_e}{\rho}\,d\eta} \tag{6.33b}$$

since $\cos\alpha$ is constant. Calculations for a large range in Reynolds numbers, up to 10^7, at Mach numbers from 1.0 to 10.0, wall enthalpy ratios h_w/h_e from 1.0 to 10.0, and, for the case of cone flow, α of from 5° to 20° showed that the parameters (7.14) and (7.15) asymptotically approached a constant as the solution proceeded downstream. It was found that the asymptotes depended mostly only on Mach number and body temperature and were nearly independent of Reynolds number, body radius, and, in the case of the cone, the cone angle. Sample solutions are shown in figures 17 and 18 for a cylinder and cone, respectively. Probstein and Elliott's solutions for the same flows are indicated in the figures and give values of the parameters plotted that are

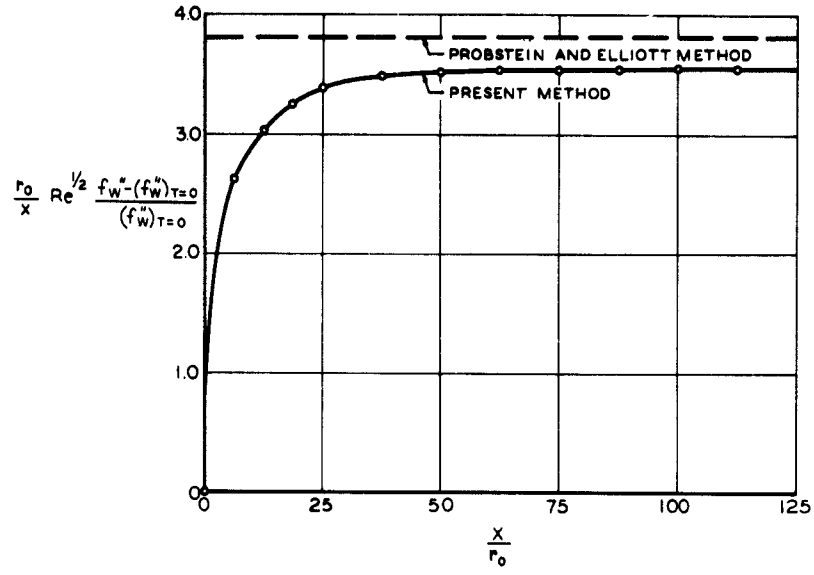

Figure 17.– Effect of transverse curvature on shear parameter for flow over a circular cylinder with axis aligned with the flow. $M_e = 5.0$; $h_w/h_e = 1.0$; $Pr = 1.0$.

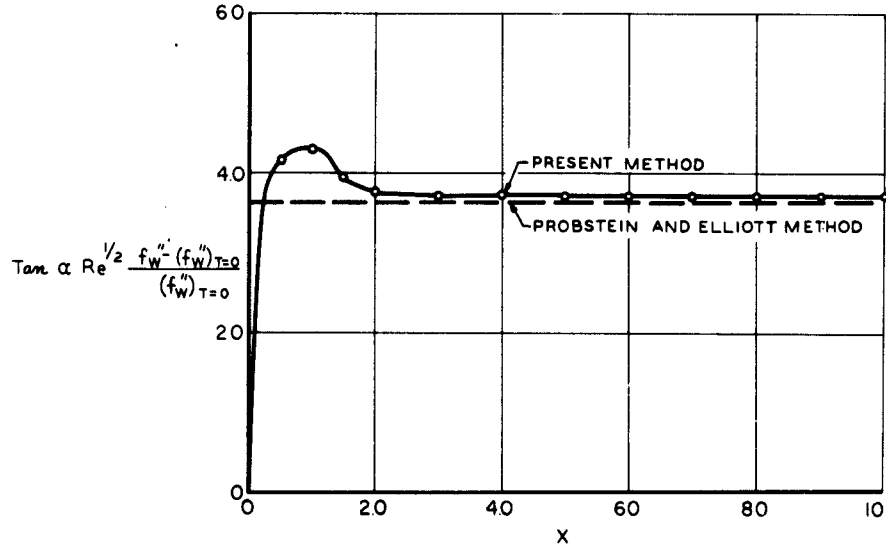

Figure 18.– Effect of transverse curvature on shear parameter for flow over a cone with axis aligned with the flow. $M_e = 5.0$; $h_w/h_e = 5.0$; $Pr = 1.0$; $\alpha = 10°$; $Re = 10^4/ft$.

independent of x. Because of the similarity requirement assumed by Probstein and Elliott, the disagreement between the two methods is not surprising. In the calculations by the present method, solutions were required to converge to four significant digits.

Effects of Mach number and wall temperature on the asymptotic values of the shear parameter are shown in figure 19 for the cone. The Probstein-Elliott values are also shown. Although the values given by the two methods of solution differ, the effects of Mach number and wall temperature are similar. Since a Prandtl number of 1.0 is assumed for the flows studied, Reynolds analogy holds exactly, and therefore the effect of transverse curvature on heat transfer is identical to its effect on wall shear, that is,

$$\frac{f_w'' - (f_w'')_{T=0}}{(f_w'')_{T=0}} = \frac{g_w' - (g_w')_{T=0}}{(g_w')_{T=0}} \qquad (7.16)$$

As was pointed out by Probstein and Elliott, transverse curvature behaves like an external favorable pressure gradient, that is, it increases both local shear and heat transfer and tends to delay both separation and transition.

7.10 Effect of Discontinuities in Surface Temperature and in Wall Mass Transfer on Wall Shear and Heat Transfer

In Reference 2 the authors investigated solutions of the incompressible boundary layer in the region where a discontinuity in the pressure gradient parameter P occurred. The purpose of the investigation was to learn how rapidly the boundary layer adjusts to local changes in pressure outside the boundary layer. The answer to this question is of great importance in application of local-similarity methods that give approximate solutions of the boundary-layer equations. In local-similarity methods solutions are obtained by a step-by-step procedure, in which each x-wise segment of the flow is approximated by one of the family of similar flows. The method assumes that the local boundary-layer profiles are functions of local boundary conditions only. For the method to be accurate the boundary layer must adjust to the local boundary conditions very rapidly.

In the investigation of the incompressible boundary layer in the region of a discontinuity in P, it was found that this adjustment to local boundary conditions was surprisingly slow (Reference 2). Study of the same adjustment for compressible flow by means of the present method shows that it is nearly identical to that found earlier for incompressible flow. Also, the present method was used to find how rapidly the boundary layer adjusted to discontinuities both in wall temperature and in mass transfer at the surface for supersonic flow. These effects are presented in this Section.

First, the effect of discontinuities in wall temperature g_w on a flat plate at Mach number 3.0 are presented. Prandtl number is assumed to be 0.72. The wall temperature g_w is constant forward of $x = 1.0$ and then abruptly changes to another value downstream of $x = 1.0$. Three values of the wall temperature were studied: $h_w = h_{ad}$, giving a value of $g_w = 0.90134$; $h_w = 2\ h_{ad}$, giving $g_w = 1.80268$; and $h_w = h_e$, giving $g_w = 0.35714$. In figure 20a calculated values of g_w' are shown for the flows when g_w is initially the adiabatic value and then abruptly changes to the higher or lower temperature downstream of $x = 1.0$. For comparison, the calculated values are also shown for the case when the plate is adiabatic for the whole length of flow. The latter is a similar flow and therefore independent of x. A positive value of g_w' means that heat is being transferred to the surface; a negative value means that heat is being transferred from the surface to the air. The figure shows that g_w' abruptly changes just aft of the discontinuity in g_w and slowly approaches an asymptotic value as the flow proceeds downstream. This asymptotic value, which is indicated in the figure, is the same as that which would be obtained by a similar solution using the local boundary conditions downstream of the discontinuity. It is seen that the calculated value of g_w' overshoots the asymptotic value just downstream of the discontinuity and slowly approaches the value from the opposite side from which it started. That is, in figure 20a for the case when $g_w = 0.35714$ downstream, the calculated value of g_w' at first greatly exceeds its asymptotic value and then approaches it from above as the calculation proceeds downstream. Step size in x used in the calculation was selected in such a way as to give calculated values accurate to three decimal places downstream of the discontinuity. Local similarity methods would give a constant value of g_w' for the whole

length of flow downstream of the discontinuity, and, furthermore, this value would be the asymptotic value indicated in the figure.

Similar plots for flows where g_w is initially 0.35714 and 1.80268 and then abruptly changes to the other two values are shown in figures 20b and 20c, respectively. The adjustment of g_w' to the local boundary conditions is like that shown in figure 20a. As was the case in the adjustment of f_w'' to local changes in P, the adjustment of g_w' to the local value of g_w is surprisingly slow. Since flat-plate flow, P = 0, is assumed for the flows shown in figure 20 (a, b, and c), the term containing ρ_e/ρ in the momentum equation (6.37) drops out, and the calculated values of f, f', and f'' are independent of g_w.

Enthalpy profiles for two of the flows with discontinuity in g_w are shown in figure 21. It is seen that the enthalpy values adjust to the local boundary conditions more rapidly near the wall than they do at the outer edge of the boundary layer. Asymptotic profiles for the two flows are also shown.

Discontinuities in mass transfer at the surface were also investigated. Two external flows were studied. First flat-plate flow similar to that described in the previous paragraphs is assumed: P = 0.0, M_e = 3.0, Pr = 0.72. It is assumed that air is blowing out of the surface forward of x = 1.0 in such a way that f_w is equal to a constant. Aft of x = 1.0 the surface is impermeable. Although there is a discontinuity in the suction velocity v_w the stream function f_w is a continuous function since it is an integral of v_w over x (see equation 6.16). Two different blowing quantities are assumed forward of x = 1.0: f_w = -0.5 and -0.1. The resulting variation of f_w downstream of the discontinuity in v_w is shown in figure 22a. Effects of the mass transfer and its discontinuity on the calculated values of f_w'' and g_w are shown in figures 22b and 22c, respectively, for the case of an insulated plate. It is seen that blowing decreases both f_w'' and g_w.

The effect of blowing cold air at the front of a nearly insulated plate is shown in figure 23. The same blowing quantities used in the previous paragraph are assumed (figure 22a). The air blown from the surface is assumed to

have the same temperature as the free stream, $h_w = h_e$, giving a value of $g_w = 0.35714$ forward of $x = 1.0$. Aft of $x = 1.0$, the surface is solid and has a temperature close to the adiabatic temperature. Effects of the blowing and its discontinuity on g_w' are shown in figure 23b. For comparison values of g_w' for the case of no blowing ($f_w = 0$) are also plotted. Since flat-plate flow ($P = 0$) is assumed, the term containing ρ_e/ρ in the momentum equation disappears, and the calculated values of f, f', and f_w'' are independent of g_w. Therefore the variation of f_w'' with x for this case of blowing cold air on a hot plate is the same as that shown in figure 22b for the case of blowing on an insulated plate.

The opposite effect, that of blowing hot air at the front of a cold plate, is shown in figure 24. Three different blowing quantities are assumed forward of $x = 1.0$: $f_w = -0.1, -0.5$, and -1.0. The first two of these are identical to those used on the plates described in the two previous paragraphs and shown in figure 22a. The blowing air is assumed to have a temperature nearly equal to the adiabatic temperature, $g_w = 1.0$. Downstream of blowing ($x > 1.0$) the surface has a temperature equal to the static temperature outside the boundary layer. Again the variation of g_w' with distance is shown. The effect of blowing on the velocity and enthalpy profiles for this flow is shown in figure 25. The adjustment of the profiles to the discontinuities in mass transfer and temperature is typical of that observed for all flows where such discontinuities occurred.

The effect of blowing air out of the surface at the front of a body is applicable to some forms of ablation cooling. In practice, when ablation cooling is used, the body is usually blunt and thus the flow is initially like that of a stagnation-point flow rather than the flat-plate flow that was assumed in the preceding paragraphs. Therefore the effect of blowing has also been studied on a body that is initially blunt. The flow is assumed to be stagnation-point flow ($P = 1.0$) for $x \leq 1.0$ and then to change abruptly to a constant pressure flow ($P = 0.0$) for $x > 1.0$. This assumption of an abrupt change from stagnation-point flow to constant-pressure flow would not be a bad approximation to the flow over the reentry type body, a spherically blunted cone, studied in Section 7.8 and shown in figure 14. The mass-transfer distributions are assumed to be the same as those studied in the flat-

plate flow. Also the onset flow is the same. Effect of the discontinuities in P and v_w on an insulated body is shown in figure 26. Variation of the shear parameter f''_w with distance is shown in figure 26c and of the wall enthalpy g_w with distance in figure 26d. Note that even though the pressure gradient parameter P, the suction parameter f_w, and the heat-transfer parameter g'_w are constants in the stagnation-point flow region, $x < 1.0$, the wall enthalpy, and thus f''_w, change because of the variation in u_e. The effect of blowing cold air initially out of the blunt body is shown in figure 27. Aft of the discontinuities in both P and v_w, the surface is assumed to have a temperature equal to the total temperature of the flow. Adjustment of the velocity and enthalpy profile to the change in P, v_w, and g_w is shown in figure 28 for one of the mass-transfer distributions of figure 27.

In conclusion, the study of discontinuities in the boundary conditions — P, g_w, and f_w — shows surprisingly slow adjustment of the boundary layer to these local conditions. It appears that local similarity methods give erroneous results for flows where rapid variation in the external or wall boundary condition occurs.

7.11 Concluding Statement

The large number of calculations and their comparison with other methods and experiment establish the fact that the method is rapid, highly accurate, and powerful. About 0.25 minutes of computing time on the IBM 7090 computer are required to calculate the velocity and enthalpy profiles at one station accurate to four significant digit. Since a typical flow requires from 20 to 30 stations, computer time averages between 5 and 7 minutes for solving a given problem. The method appears capable of solving any flow problem for which the boundary-layer equations themselves remain valid. It is now being extended to handle flows where dissociation (both equilibrium and nonequilibrium) occurs. Also effects of both catalytic and noncatalytic walls will be included.

APPENDIX A

DEVELOPMENT OF THE BOUNDARY-LAYER EQUATIONS FOR COMPRESSIBLE LAMINAR FLOW INCLUDING THE EFFECT OF TRANSVERSE CURVATURE

In this Appendix the boundary-layer equations are developed for axially symmetric flow for the coordinate system of Section 6.1. The effects of transverse curvature are included.

Continuity Equation

The continuity equation is

$$\frac{\partial \rho}{\partial t} + \text{div}\ (\rho\, \overline{V}) = 0 \tag{A1}$$

The first term is of course zero for steady flow.

Before writing (A1) in the x,y coordinate system, consider the general orthogonal coordinates. Let

$X,\quad Y,\quad Z,$ ⇔ any Cartesian coordinates

$\alpha_1,\quad \alpha_2,\quad \alpha_3,$ ⇔ any orthogonal coordinates

Let the elements of length in the direction of increasing α_1, α_2, and α_3 be $h_1\alpha_1$, $h_2\alpha_2$, and $h_3\alpha_3$, respectively, so that

$$(ds)^2 = h_1^2(d\alpha_1)^2 + h_2^2(d\alpha_2)^2 + h_3^2(d\alpha_3)^2 \tag{A2}$$

The quantities h_1, h_2, and h_3 are defined by

$$\left.\begin{aligned} h_1 &= \sqrt{\left(\frac{\partial X}{\partial \alpha_1}\right)^2 + \left(\frac{\partial Y}{\partial \alpha_1}\right)^2 + \left(\frac{\partial Z}{\partial \alpha_1}\right)^2} \\ h_2 &= \sqrt{\left(\frac{\partial X}{\partial \alpha_2}\right)^2 + \left(\frac{\partial Y}{\partial \alpha_2}\right)^2 + \left(\frac{\partial Z}{\partial \alpha_2}\right)^2} \\ h_3 &= \sqrt{\left(\frac{\partial X}{\partial \alpha_3}\right)^2 + \left(\frac{\partial Y}{\partial \alpha_3}\right)^2 + \left(\frac{\partial Z}{\partial \alpha_3}\right)^2} \end{aligned}\right\} \tag{A3}$$

Now consider the coordinate system of figure 1. It is redrawn in figure A1, to show that

$$d\alpha_1 = dx$$
$$d\alpha_2 = dy$$
$$d\alpha_3 = d\varphi$$

where here φ is the azimuthal angle. If the second order effect of longitudinal curvature were to be retained as well as that of transverse curvature, $d\alpha_1 = dx/(1 + ky)$ where k is the local curvature, that is, the reciprocal of the local radius of curvature. For most flows of interest in aerodynamics the effect of longitudinal curvature is usually much smaller that that of transverse curvature, and it will be neglected in the present study. Since the problem is axisymmetric, all quantities are independent of φ. Now from (A3)

$$\left.\begin{aligned} h_1 &= h_2 = 1 \\ h_3 &= r \end{aligned}\right\} \qquad (A4)$$

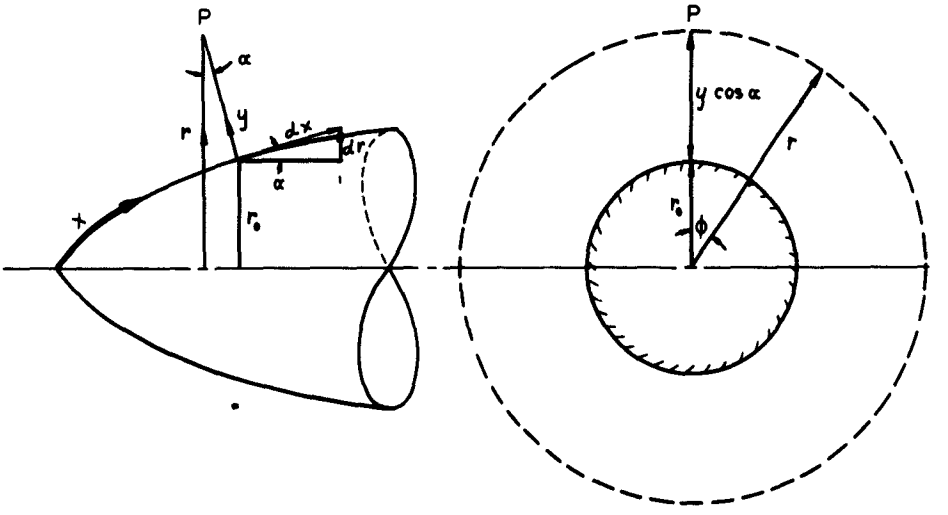

Figure A1.– Coordinate system for axially symmetric body.

From vector analysis and the relation

$$\overline{V} = \overline{i}\, u + \overline{j}\, v \tag{A5}$$

the continuity equation can be written

$$\frac{\partial \rho}{\partial t} + \text{div}\ (\rho\, \overline{V}\ ) = \frac{\partial \rho}{\partial t} + \frac{1}{r}\left\{\frac{\partial}{\partial x}\,(r\,\rho\,u) + \frac{\partial}{\partial y}\,(r\,\rho\,v)\right\} = 0 \tag{A6}$$

Momentum Equation

The Navier-Stokes equation of motion in vector notation is (from page 50 of Howarth, Reference 5):

$$\begin{aligned}\rho\left(\frac{\partial \overline{V}}{\partial t} - \overline{V} \times \text{curl}\ \overline{V} + \frac{1}{2}\,\text{grad}\ \overline{V}^{\,2}\right) = {} & \rho\,\overline{F} - \text{grad}\ p + \frac{4}{3}\,\text{grad}\ (\mu\Delta) + \text{grad}\ (\overline{V} \cdot \text{grad}\ \mu) \\ & - \overline{V}\,\nabla^2\mu + \text{grad}\ \mu \times \text{curl}\ \overline{V} - \Delta\ \text{grad}\ \mu \\ & - \text{curl curl}\ \mu\ \overline{V}\end{aligned} \tag{A7}$$

In order to apply the boundary-layer assumptions, consider the x and y components of (A7) separately. The x-wise or $\overline{i}$ component in the orthogonal coordinate system is:

$$\begin{aligned}\rho\left[\frac{\partial u}{\partial t} + u\frac{\partial u}{\partial x} + v\frac{\partial u}{\partial y}\right] = {} & \rho\,\overline{X} - \frac{\partial p}{\partial x} \\ & + \frac{4}{3}\left[\frac{\partial}{\partial x}\left(\mu\frac{\partial u}{\partial x}\right) + \frac{\partial}{\partial x}\left(\mu\frac{u}{r}\frac{\partial r}{\partial x}\right) + \frac{\partial}{\partial x}\left(\mu\frac{\partial v}{\partial y}\right)\right. \\ & \left. + \frac{\partial}{\partial x}\left(\mu\frac{v}{r}\frac{\partial r}{\partial x}\right)\right] + \frac{\partial}{\partial x}\left(u\frac{\partial \mu}{\partial x}\right) + \frac{\partial}{\partial x}\left(v\frac{\partial \mu}{\partial y}\right) \\ & - u\left[\frac{1}{r}\frac{\partial r}{\partial x}\frac{\partial \mu}{\partial x} + \frac{\partial^2 \mu}{\partial x^2} + \frac{1}{r}\frac{\partial r}{\partial y}\frac{\partial \mu}{\partial y} + \frac{\partial^2 \mu}{\partial y^2}\right] \\ & + \frac{\partial \mu}{\partial y}\frac{\partial v}{\partial x} - \frac{\partial \mu}{\partial y}\frac{\partial u}{\partial y} - \frac{\partial \mu}{\partial x}\frac{\partial u}{\partial x} - \frac{u}{r}\frac{\partial \mu}{\partial x}\frac{\partial r}{\partial x} \\ & - \frac{\partial \mu}{\partial x}\frac{\partial v}{\partial y} - \frac{v}{r}\frac{\partial \mu}{\partial x}\frac{\partial r}{\partial y} - \frac{1}{r}\frac{\partial}{\partial y}\left(r\frac{\partial \mu v}{\partial x}\right) \\ & + \frac{1}{r}\frac{\partial}{\partial y}\left(r\frac{\partial \mu u}{\partial y}\right)\end{aligned} \tag{A8}$$

where $\overline{X}$ is a body force.

Now make the usual order of magnitude analysis of (A8). Let u_e, ρ_e and x be of order unity, that is, u_e, ρ_e, $x = O(1)$. Then since

$$R_x = \frac{\rho_e u_e x}{\mu_e}, \qquad \mu_e = O\left(\frac{1}{R_x}\right)$$

Also since,

$$\frac{\delta}{x}\sqrt{R_x} = O(1), \qquad \delta = O\left(\frac{1}{\sqrt{R_x}}\right)$$

Similarly, the magnitude of the other components of (A8) may be found. They are summarized in the table below.

ORDER	QUANTITY
$O(\delta^{-2})$	$\frac{\partial^2 u}{\partial y^2}$
$O(\delta^{-1})$	$\frac{\partial u}{\partial y}$.
$O(1)$	$r,\ u,\ x,\ \rho,\ \frac{\partial u}{\partial x},\ \frac{\partial u}{\partial t},\ \frac{\partial^2 u}{\partial x^2},\ \frac{\partial v}{\partial y}$
$O(\delta)$	$v,\ y,\ \frac{\partial v}{\partial t},\ \frac{\partial v}{\partial x},\ \frac{\partial^2 v}{\partial x^2}$
$O(\delta^2)$	$\nu = \mu/\rho$

If only terms of order (δ) or larger—that is, terms of order (δ), (1), (δ^{-1}), (δ^{-2})—are retained, then eq.(A8) reduces to the following equation,

$$\rho\left[\frac{\partial u}{\partial t} + u\frac{\partial u}{\partial x} + v\frac{\partial u}{\partial y}\right] = \rho\,\overline{X} - \frac{\partial p}{\partial x} + \frac{\mu}{r}\frac{\partial r}{\partial y}\frac{\partial u}{\partial y} + \frac{\partial \mu}{\partial y}\frac{\partial u}{\partial y} + \mu\frac{\partial^2 u}{\partial y^2} \qquad \text{(A9)}$$

The y or $\overline{j}$ component of equation (A7) is

$$\rho\left[\frac{\partial v}{\partial t} + u\frac{\partial v}{\partial x} + v\frac{\partial v}{\partial y}\right] = \rho\bar{Y} - \frac{\partial p}{\partial y}$$
$$+ \frac{4}{3}\left[\frac{\partial \mu}{\partial y}\left(\frac{\partial u}{\partial x} + \frac{u}{r}\frac{\partial r}{\partial x} + \frac{\partial v}{\partial y} + \frac{v}{r}\frac{\partial r}{\partial y}\right) + \mu\left\{\frac{\partial^2 u}{\partial x \partial y} + \frac{\partial}{\partial y}\left(\frac{u}{r}\frac{\partial r}{\partial x}\right)\right.\right.$$
$$\left.\left. + \frac{\partial^2 v}{\partial y^2} + \frac{\partial}{\partial y}\left(\frac{v}{r}\frac{\partial r}{\partial y}\right)\right\}\right] + \frac{\partial u}{\partial y}\frac{\partial \mu}{\partial x} + u\frac{\partial^2 \mu}{\partial x \partial y} + \frac{\partial v}{\partial y}\frac{\partial \mu}{\partial y} + v\frac{\partial^2 \mu}{\partial y^2}$$
$$- v\left[\frac{1}{r}\frac{\partial r}{\partial x}\frac{\partial \mu}{\partial x} + \frac{\partial^2 \mu}{\partial x^2} + \frac{1}{r}\frac{\partial r}{\partial y}\frac{\partial \mu}{\partial y} + \frac{\partial^2 \mu}{\partial y^2}\right] - \frac{\partial \mu}{\partial x}\left[\frac{\partial v}{\partial x} - \frac{\partial u}{\partial y}\right]$$
$$- \frac{\partial \mu}{\partial x}\left[\frac{\partial u}{\partial x} + \frac{u}{r}\frac{\partial r}{\partial x} + \frac{\partial v}{\partial y} + \frac{v}{r}\frac{\partial r}{\partial y}\right] + \frac{1}{r}\frac{\partial r}{\partial x}\left[\frac{\partial(\mu v)}{\partial x} - \frac{\partial(\mu u)}{\partial y}\right]$$
$$+ \frac{\partial}{\partial x}\left[\frac{\partial(\mu v)}{\partial x} - \frac{\partial(\mu u)}{\partial y}\right] \qquad \text{(A10)}$$

If terms of order unity are retained, (A10) reduces to

$$\bar{Y} = \frac{1}{\rho}\frac{dp}{dy} \qquad \text{(A11)}$$

For the flow under consideration there are no body forces and the flow is steady. The momentum equations (A9) and (A11) then become

$$\rho\left[u\frac{\partial u}{\partial x} + v\frac{\partial u}{\partial y}\right] = -\frac{\partial p}{\partial x} + \frac{\mu}{r}\frac{\partial r}{\partial y}\frac{\partial u}{\partial y} + \frac{\partial}{\partial y}\left(\mu\frac{\partial u}{\partial y}\right) \qquad \text{(A12)}$$

$$\frac{1}{\rho}\frac{\partial p}{\partial y} = O(\delta) \qquad \text{(A13)}$$

The latter says that the total change of pressure through the boundary layer normal to the surface is of order δ^2. Therefore it will be neglected, and the partial derivative of pressure with respect to x, $\partial p/\partial x$, is replaced by the total derivative, dp/dx, in eq.(A12).

Energy Equation

The basic form of the energy equation for an orthogonal coordinate system is given by Howarth, page 55, Reference 5. In his notation

$$\rho\frac{Dh}{Dt} = \Phi + \frac{Dp}{Dt} + \frac{\partial}{\partial x_\alpha}\left(k\frac{\partial T}{\partial x_\alpha}\right) \qquad \text{(A14)}$$

where

h = enthalpy = $\int c_p\, dT$

Φ = dissipation function = rate of work done by viscous forces

and by definition

$$\frac{D}{Dt} = \left(\frac{\partial}{\partial t} + \overline{V} \cdot \nabla\right) \tag{A15}$$

$$\frac{\partial}{\partial x_\alpha}\left(k \frac{\partial T}{\partial x_\alpha}\right) = \text{div } (k \text{ grad } T) \tag{A16}$$

The dissipation term in vector coordinates is given by

$$\frac{\Phi}{\mu} = \text{div grad } \overline{V}^2 - 2 \text{ div}(\overline{V} \times \text{curl } \overline{V}) - 2 \overline{V} \cdot \text{grad}(\text{div } V) + (\text{curl } \overline{V})^2 - \frac{2}{3} (\text{div } \overline{V})^2 \tag{A17}$$

An order of magnitude analysis as was made above for the momentum equation gives, if terms of only the highest order are retained,

$$\rho\left[\frac{\partial h}{\partial t} + u \frac{\partial h}{\partial x} + v \frac{\partial h}{\partial y}\right] = \frac{\partial p}{\partial t} + u \frac{\partial p}{\partial x} + \mu \left(\frac{\partial u}{\partial y}\right)^2 + \frac{1}{r} \frac{\partial}{\partial y}\left(r\, k \frac{\partial T}{\partial y}\right) \tag{A18}$$

The last term can be written in terms of enthalpy by the relation

$$k \frac{\partial T}{\partial y} = \frac{k}{c_p} \frac{\partial h}{\partial y} = \mu \frac{k}{\mu c_p} \frac{\partial h}{\partial y} = \frac{\mu}{Pr} \frac{\partial h}{\partial y} \tag{A19}$$

where Pr is the Prandtl number. Substitution of (A19) in (A18) gives

$$\rho\left[\frac{\partial h}{\partial t} + u \frac{\partial h}{\partial x} + v \frac{\partial h}{\partial y}\right] = \frac{\partial p}{\partial t} + u \frac{\partial p}{\partial x} + \mu \left(\frac{\partial u}{\partial y}\right)^2 + \frac{1}{r} \frac{\partial}{\partial y}\left[r \frac{\mu}{Pr} \frac{\partial h}{\partial y}\right] \tag{A20}$$

Now if steady flow is assumed and if the momentum equation (A12) is used to replace the term $u \frac{\partial p}{\partial x}$, (A20) may be written

$$\begin{aligned} &\rho\left[u\left(\frac{\partial h}{\partial x} + u \frac{\partial u}{\partial x}\right) + v\left(\frac{\partial h}{\partial y} + u \frac{\partial u}{\partial y}\right)\right] \\ &= \frac{1}{r} \frac{\partial r}{\partial y}\left[\frac{\mu}{Pr}\left(\frac{\partial h}{\partial y} + u \frac{\partial u}{\partial y}\right) + \left(\mu - \frac{\mu}{Pr}\right) u \frac{\partial u}{\partial y}\right] \\ &\quad + \frac{\partial}{\partial y}\left[\frac{\mu}{Pr}\left(\frac{\partial h}{\partial y} + u \frac{\partial u}{\partial y}\right) + \left(\mu - \frac{\mu}{Pr}\right) u \frac{\partial u}{\partial y}\right] \end{aligned} \tag{A21}$$

Now introduce total enthalpy H

$$H = h + \frac{1}{2} u^2$$

and substitution in (A21) gives

$$\rho\left[u\frac{\partial H}{\partial x}+v\frac{\partial H}{\partial y}\right]=\frac{1}{r}\frac{\partial r}{\partial y}\left[\frac{\mu}{Pr}\frac{\partial H}{\partial y}+\mu\left(1-\frac{1}{Pr}\right)u\frac{\partial u}{\partial y}\right]$$
$$+\frac{\partial}{\partial y}\left[\frac{\mu}{Pr}\frac{\partial H}{\partial y}+\mu\left(1-\frac{1}{Pr}\right)u\frac{\partial u}{\partial y}\right] \qquad (A22)$$

APPENDIX B

COMPUTER PROGRAM FOR SOLVING THE BOUNDARY-LAYER EQUATIONS

(IBM 7090 Computer)

Input*

1. The constants:

H_e	$u_\infty^2/2h_{ref}$	C_1
h_{ref}	$\Delta\eta$	C_2 (Appendix B)
n-MAX	$R'_e = \rho_\infty u_\infty/\mu_\infty$	C_3
f'''_{w_o}	K (Section 6.5)	P-MAX (Section 6.9)
L-MAX (Section 6.9)		Q-MAX (Section 6.9)
ϵ_1 (Appendix B)	ϵ_2 (Appendix B)	

2. The Table:

TABLE 1 A

Page 1

n	x	r_o	P	R	$\left(\frac{u_e}{u_\infty}\right)^2$	$\frac{\rho_w v_w}{\rho_\infty u_\infty}$	$\frac{p_e}{p_\infty}$

Page 2

n	g_w	g'_{w_1}	g'_w	g_{w_1}	f'''_{w_o}	cos α	η_∞	p	Print

*Not all of the notation used here are defined in Section 4.0 PRINCIPAL NOTATION, but if not, they are defined when applicable here.

Computation

1. Determine local value of P_n and R_n if they are not inputs.
   (a) If $n = 0$, P_o and R_o are always inputs
   (b) If $n \neq 0$, calculate using (6.13), (6.14), (6.97), (6.98)
2. Calculate C_∞ by (6.26).
3. Set $n = 0$.

(A) →

4. Set $Q = 0$, $i = 0$.
5. Form table of ρ_e/ρ and C versus η.
   If $n = 0$, calculate g_o
   (a) If g_w is input, $g_o = g_w - (g_w - 1)\frac{\eta}{\eta_\infty}$

   (b) If g'_w is input, $g_o = g'_w(\eta - \eta_\infty) + 1$
   Calculate ρ_e/ρ and C using (6.23), (6.24), (6.25) and $f'_o = \eta/\eta_\infty$
   If $n \neq 0$, use table of ρ_e/ρ and C from n-1 station

(B) →

6. If $Q \neq 0$, use values of ρ_e/ρ and C determined from the last solution of the energy equation.
7. Solve momentum equation.
   (a) If $n = 0$, use (6.95)
   If $n \neq 0$, use (6.37)
   If $p = 0$, use (6.58) for x-wise derivatives
   If $p = 1$, use (6.59) for x-wise derivatives
   (b) Find values of φ''_w to be used for the first try.
   If $Q = 0$ and $n = 0$, then $\varphi''_w = f''_{w_o}$
   If $Q = 0$ and $n \neq 0$, then $\varphi''_w = \varphi''_{w_{n-1}}$

(C) →

   If $Q \neq 0$, then $\varphi''_w = \varphi''_{w_{Q-1}}$
   (c) Calculate momentum equation, testing
   (1) If $\varphi' > K$, stop calculation and store φ''_w as a high solution

(2) If $\varphi' < -K$ and $\varphi'' < 0$, stop calculation and store φ''_w as a low solution

(3) If $\eta = \eta_\infty$ and
if $\varphi'(\eta_\infty) < 0$, store as low solution
if $\varphi'(\eta_\infty) > 0$, store as high solution

(4) Denote solution as $\varphi'(\eta_\infty)_i$

(D) →

8. Set $i = i + 1$ and reenter at (C), using:

(a) If φ''_{w_i} is high, then $\varphi''_{w_{i+1}} = \varphi''_{w_i} - C_1$

(b) If φ''_{w_i} is low, then $\varphi''_{w_{i+1}} = \varphi''_{w_i} + C_1$

9. Repeat procedures (C) and (D) until at least one high and one low value of φ''_{w_i} are known. Enter at (E).

(E) →

10. Reenter at (C), using:

$$\varphi''_{w_i} = \frac{\left[\varphi''_w\right]_{High} + \left[\varphi''_w\right]_{Low}}{2}$$

where $\left[\varphi''_w\right]_{High}$ = lowest high solution

$\left[\varphi''_w\right]_{Low}$ = highest low solution

11. Repeat procedures (C) and (E) until either:

(a) there are three trial solutions extending to η_∞ within the bounds of $-K < \varphi'(\eta_\infty) < K$
Interpolate by means of (6.43) and (6.44) for solution that causes $\varphi'(\eta_\infty) = 0$

(b) $\left[\varphi''_w\right]_{High} - \left[\varphi''_w\right]_{Low} < \epsilon_1$. If so, determine the maximum value of η common to the last three trial solutions. Denote this η as η-MAX. Interpolate by means of (6.43) and (6.44) for solution that causes $\varphi'(\eta_\infty) = 0$, treating η-MAX as η_∞.

12. Compare Q :

(a) If $Q = 0$, enter at (F)

(b) If $0 < Q < Q_{MAX}$, compare $\left(\varphi_w''\right)_Q$:

(1) If

$$\left|\left[\varphi_w''\right]_Q - \left[\varphi_w''\right]_{Q-1}\right| > \epsilon_2$$

enter at (F)

(2) If

$$\left|\left[\varphi_w''\right]_Q - \left[\varphi_w''\right]_{Q-1}\right| \leq \epsilon_2$$

enter at (G)

(c) If $Q = Q\text{-MAX}$, enter at (G)

(F) →

13. Set $L = 0$.

(a) Determine table of C and Pr

(1) If $Q = 0$, $L = 0$, $n = 0$, use g_o from step 5 to determine C and Pr by (6.23), (6.25), (6.27a), (6.27b), (6.27c)

(2) If $Q = 0$, $L = 0$, $n \neq 0$, use C and Pr from n-1 station

(3) If $Q \neq 0$, $L = 0$, use C and Pr from Q-1 solution

(H) →

(4) If $L \neq 0$, use C and Pr from L-1 solution

14. Solve energy equation.

(a) If $n = 0$, use (6.96)

If $n \neq 0$, use (6.49)

(b) Calculation depends on whether g_w' or g_w is input

If g_w' is input,

(1) Calculate, first using $\psi_w' = g_w'$ and $\psi_{w_1} = g_{w_1} - 1$. Denote solution as ψ_1

(2) If $\psi_1(\eta_\infty) > 0$, solve for ψ_2, using $\psi_{w_2} = g_{w_1} - 1 - C_2$

(3) If $\psi_1(\eta_\infty) < 0$, solve for ψ_2, using $\psi_{w_2} = g_{w_1} - 1 + C_2$

(4) Determine correct values of ψ and ψ', using (6.56), (6.57a), (6.57b)

(c) If g_w is input,

(1) Calculate, first using $\psi'_{w_1} = g'_{w_1}$. Denote solution as ψ_1

(2) If $\psi_1(\eta_\infty) > 0$, solve for ψ_2, using $\psi'_{w_2} = g'_{w_1} - C_2$

(3) If $\psi_1(\eta_\infty) < 0$, solve for ψ_2, using $\psi'_{w_2} = g'_{w_1} + C_2$

(4) Determine correct values of ψ and ψ', using (6.56), (6.57a), (6.57b)

15. Calculate values of C and Pr and store as C_L and Pr_L, using (6.23), (6.25), (6.27a), (6.27b), (6.27c).

16. Test L.

(a) If L < L-MAX, set L = L + 1 and enter at (H)

(b) If L = L-MAX, set the tables

$$C_L = C_Q$$

$$Pr_L = Pr_Q$$

and solve for $(\rho_e/\rho)_Q$ using (6.24). Set $\varphi''_w = [\varphi''_w]_Q$

Set Q = Q + 1. Enter at (C).

(G) →

17. Denote values of $(C\,\varphi'')'$, φ'', φ', φ, ψ, ψ', ρ_e/ρ, C, and Pr as n values, that is, $(C\,\varphi'')' = (C\,\varphi'')'_n$, etc.

18. Determine values of f_n, f'_n, f''_n, g_n and g'_n by (6.36), (6.45).

19. Calculate: Y versus η by (6.106), Δ^* by (6.107), θ by (6.111), c_f^* by (6.116), and St_∞ / c_f by (6.121).

20. Go to next n-station by setting n = n + 1 and entering at (A).

21. Stop calculation when n > n-MAX.

Print Out

1. Input constants and table.
2. The table

n	f''_w	g_w	g'_w	Δ^*	θ	c_f^*	$\frac{St_\infty}{c_f}$	Pr_w

3. For every station, the table

η	f	f'	f''	$(C\varphi'')'$	g	g'	Y

4. If ''print'' is indicated in table of input, the following is printed out for every trial solution:

Station No. ———

η	π	Ψ	Ψ'	π'	C	Pr

η	φ	φ'	φ''	$(C\varphi'')'$	C	ρ_e/ρ

REFERENCES

1. Smith, A. M. O. and Clutter, D. W.:-Solution of the Incompressible Laminar Boundary Layer Equations. Douglas Aircraft Co. Report No. ES 40446, July 29, 1961.
2. Smith, A. M. O. and Clutter, D. W.:-Solution of the Incompressible Laminar Boundary Layer Equation. Douglas Aircraft Co. Engineering Paper No. 1525, January 1, 1962.
3. Smith, A. M. O. and Clutter, D. W.:-Solution of Prandtl's Boundary-Layer Equations. Douglas Aircraft Co. Engineering Paper No. 1530, February 2, 1962.
4. Van Dyke, M.:-Second-Order Compressible Boundary-Layer Theory with Application to Blunt Bodies in Hypersonic Flow. Stanford University Department of Aeronautical Engineering Report SUDAER No. 112, July 1961.
5. Howarth, L.:-Modern Developments in Fluid Dynamics. Vol. 1, Oxford 1953.
6. Flügge-Lotz, I. and Blottner, F.G.:-Computation of the Compressible Laminar Boundary-Layer Flow Including Displacement-Thickness Interaction Using Finite-Difference Methods. Stanford University Division of Engineering Mechanics Technical Report No. 131, January 1962.
7. Cohen, N. B.:-Correlation Formula and Tables of Density and Some Transport Properties of Equilibrium Dissociating Air for Use in Solution of the Boundary-Layer Equations. NASA TN D-194, February 1960.
8. Hartree, D. R. and Womersley, J. R.:- A Method for the Numerical or Mechanical Solution of Certain Types of Partial Differential Equations. Proc. Royal Soc. Series A, Vol. 161, No. 906, p.353, August 1937.
9. Hartree, D. R.:-A Solution of the Laminar Boundary-Layer Equation for Retarded Flow. British R and M No. 2426, 1949.
10. Hartree, D. R.:-The Solution of the Equations of the Laminar Boundary Layer for Schubauer's Observed Pressure Distribution for an Elliptic Cylinder. British R and M No. 2427, 1949.
11. Collatz, L.:-The Numerical Treatment of Differential Equations. Third Edition. Springer-Verlag 1960.
12. Hildebrand, F. B.:-Introduction to Numerical Analysis. McGraw Hill, 1956.
13. Hayes, Wallace D., and Probstein, Ronald F.:-Hypersonic Flow Theory. Academic Press, 1959.

14. Cohen, C. B., and Reshotko, E.:-Similar Solutions for the Compressible Laminar Boundary Layer with Heat Transfer and Pressure Gradient. NACA Report 1293, 1956.

15. Chapman, D. R. and Rubesin, M. W.:-Temperature and Velocity Profiles in the Compressible Laminar Boundary Layer with Arbitrary Distribution of Surface Temperature. J. Aero. Sci. Vol. 16, 547 (1949).

16. Low, G. M.:-The Compressible Laminar Boundary Layer with Heat Transfer and Small Pressure Gradient. NACA TN 3028, October 1953.

17. Beckwith, I.E., and Cohen, N. B.:-Application of Similar Solutions to Calculation of Laminar Heat Transfer on Bodies with Yaw and Large Pressure Gradient in High-Speed Flow. NASA TN D-625, January 1961.

18. Cohen, C. B. and Reshotko, E.:-The Compressible Laminar Boundary Layer with Heat Transfer and Arbitrary Pressure Gradient. NACA Report 1294, 1956.

19. Probstein, R. F. and Elliott, D.:-The Transverse Curvature Effect in Compressible Axially Symmetric Laminar Boundary-Layer Flow. J. of Aeronautical Sciences, Vol. 23, No. 3, March 1956, pp. 208-224, 236.

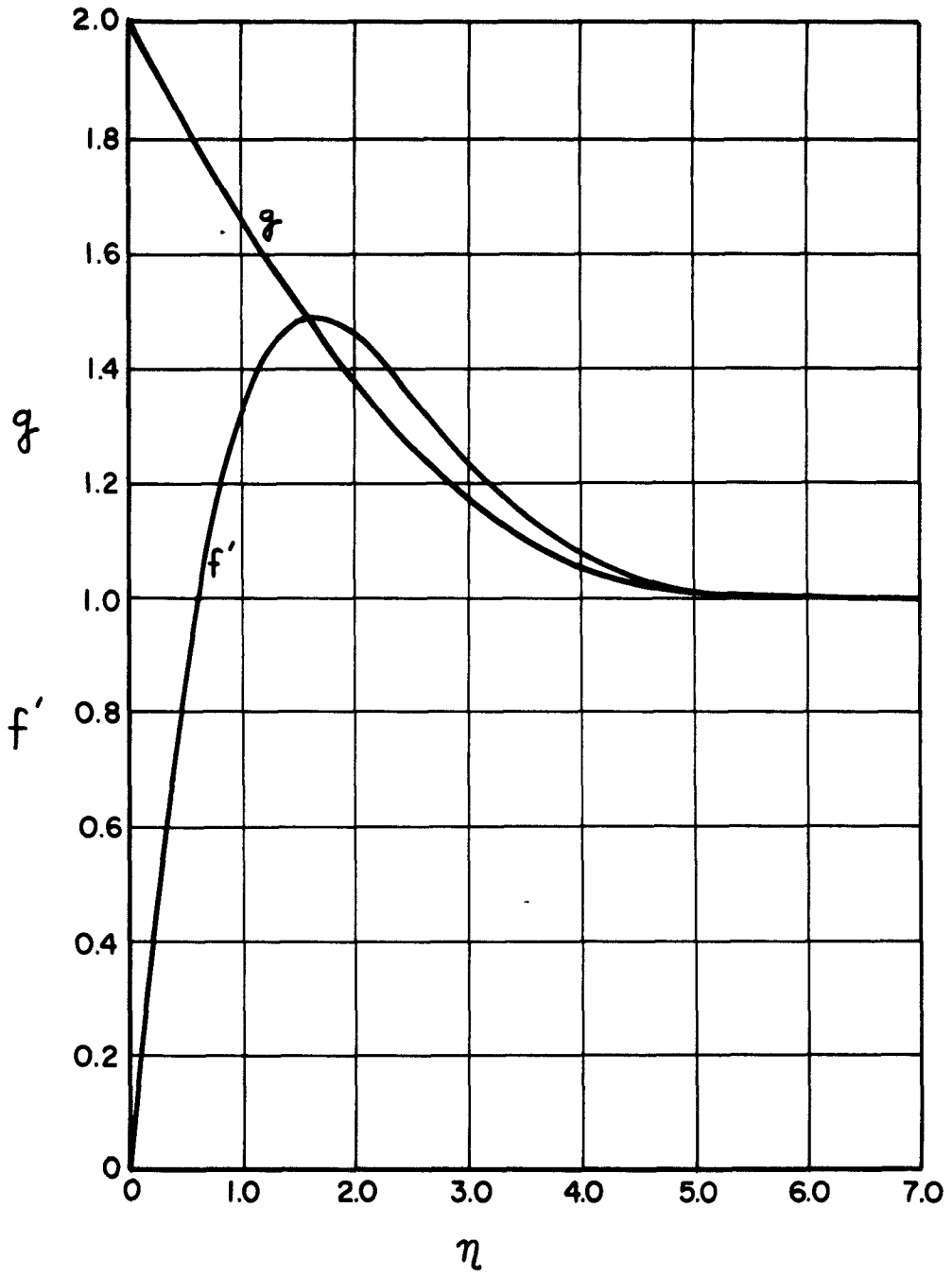

Figure 8.– Velocity and enthalpy profiles at Mach number = 3.0 for the similar flow described by P = 1/3, R = 0, g_w = 2.0. Velocity overshoot shown.

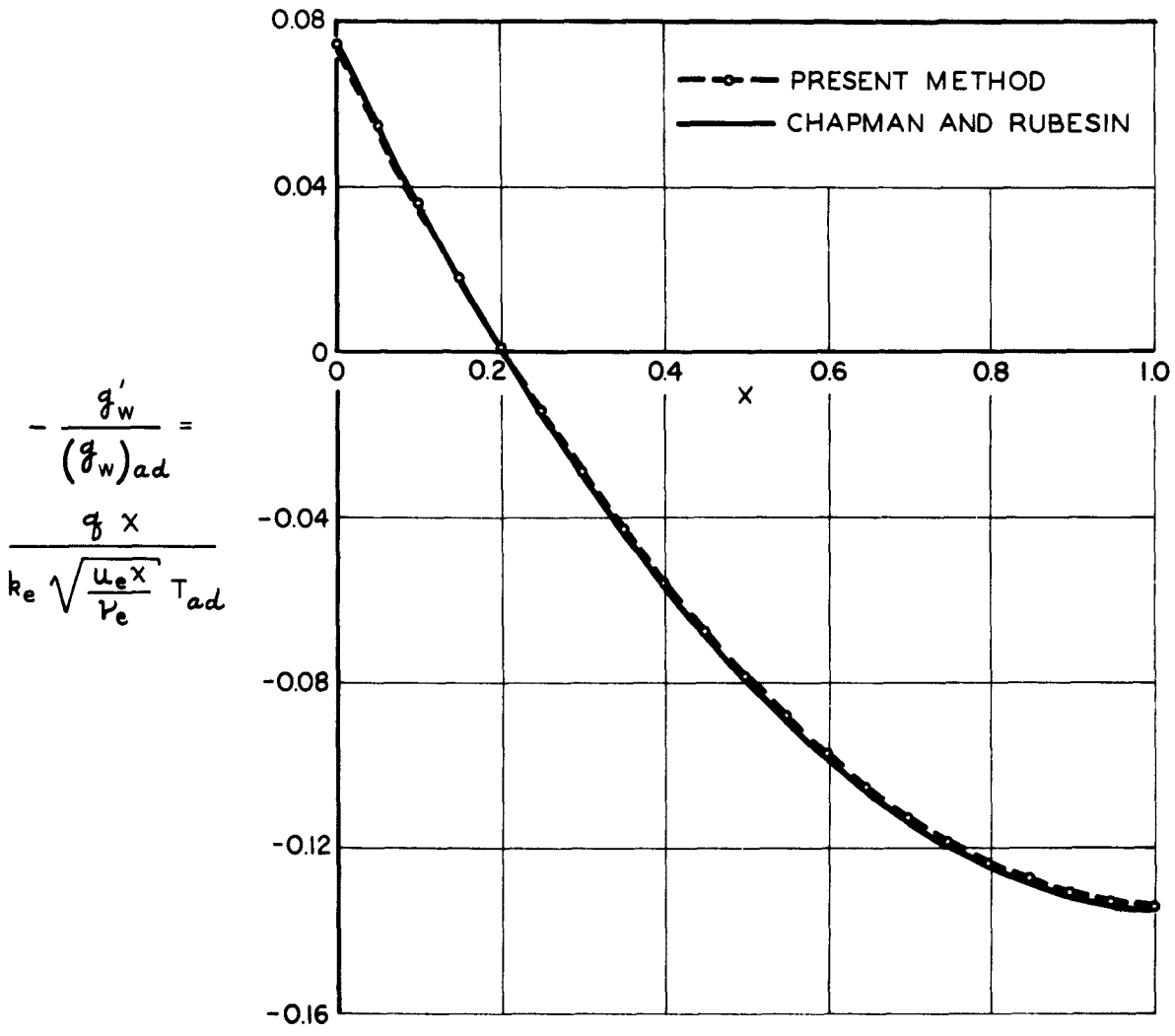

Figure 9.- Heat transfer on a flat plate with variable surface temperature. Mach number = 3.0, Pr = 0.72.

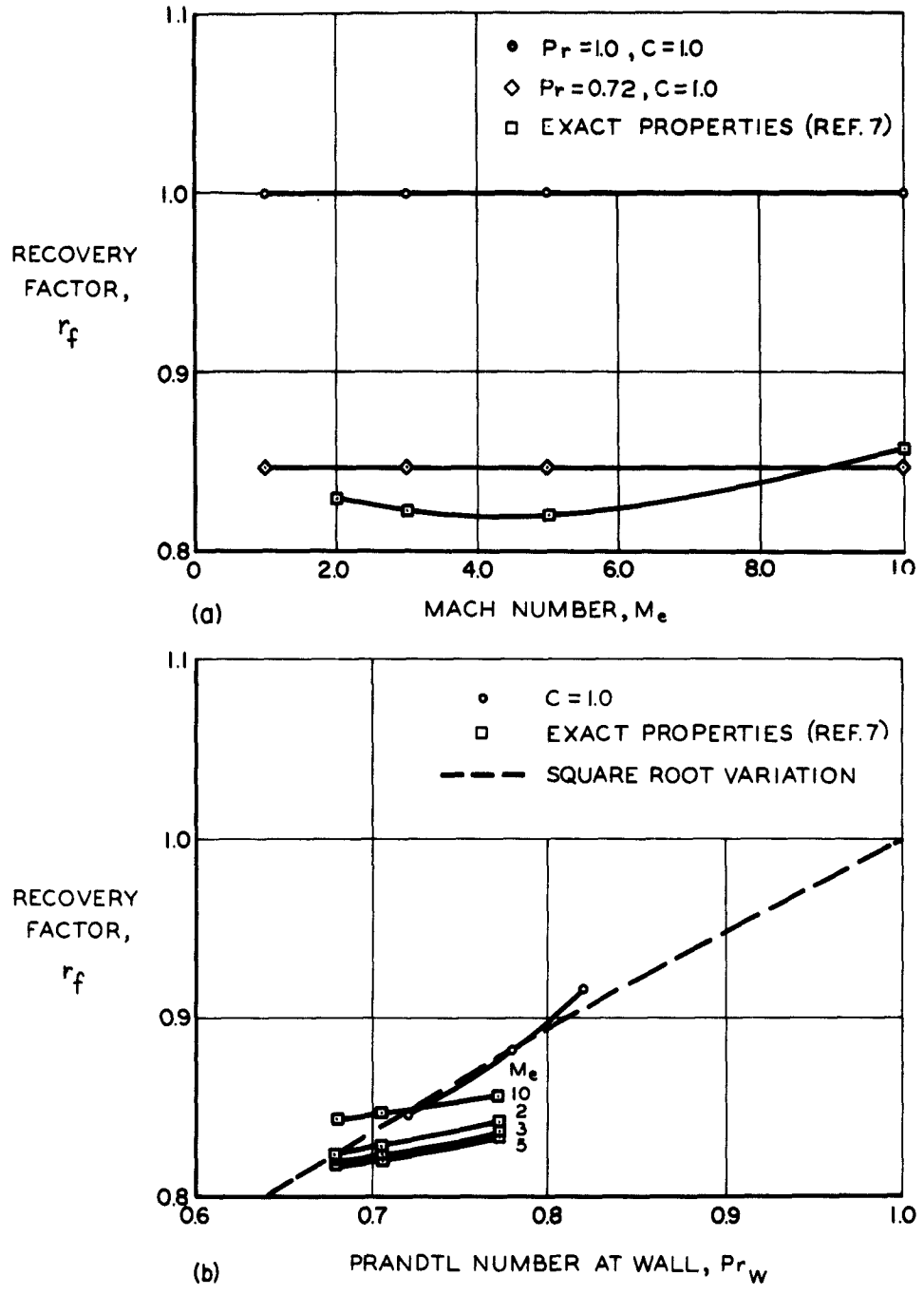

Figure 10.–Dependence of recovery factor on fluid-property laws.
(a) Recovery factor versus Mach number.
(b) Recovery factor versus Prandtl number.

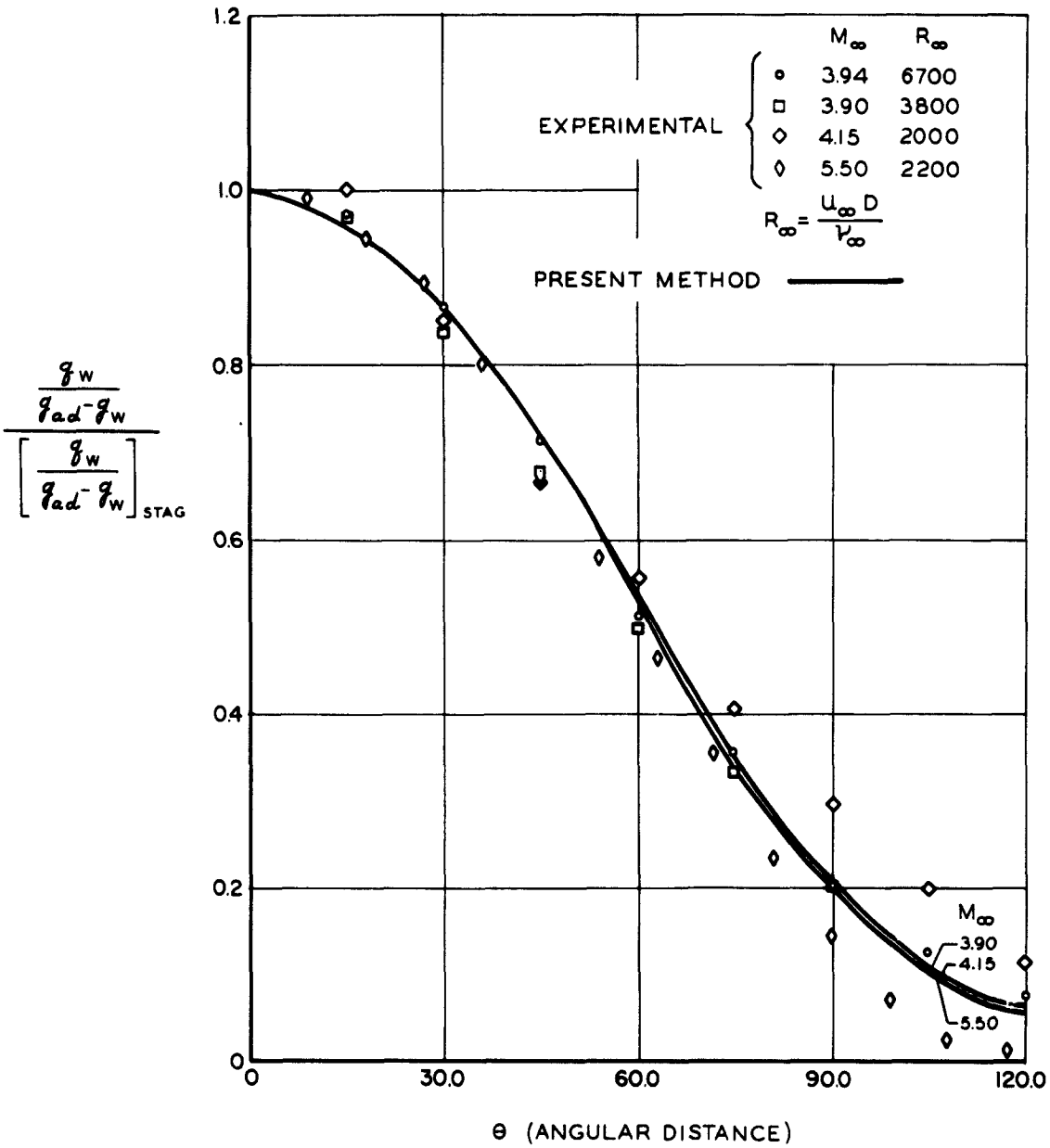

Figure 11.–Comparison of heat transfer calculated by the present method with that measured in the wind tunnel for a circular cylinder.

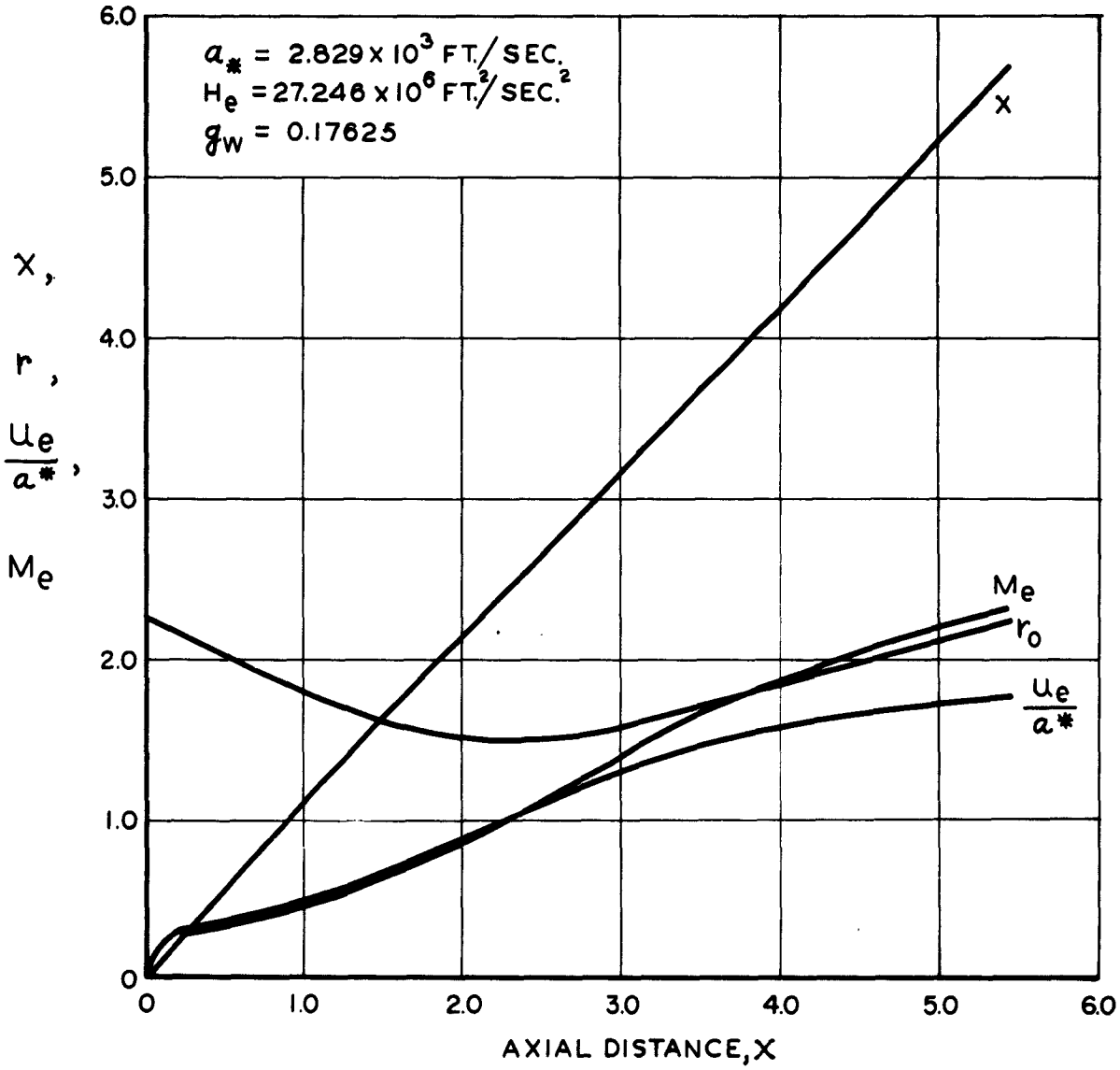

Figure 12.–Variation of surface distance x, body radius r_o, u_e/a^*, and M_e with axial distance for the rocket nozzle problem. $H_e = 27.246 \times 10^6$ ft^2/sec^2; $g_w = 0.17625$; Pr = 0.78.

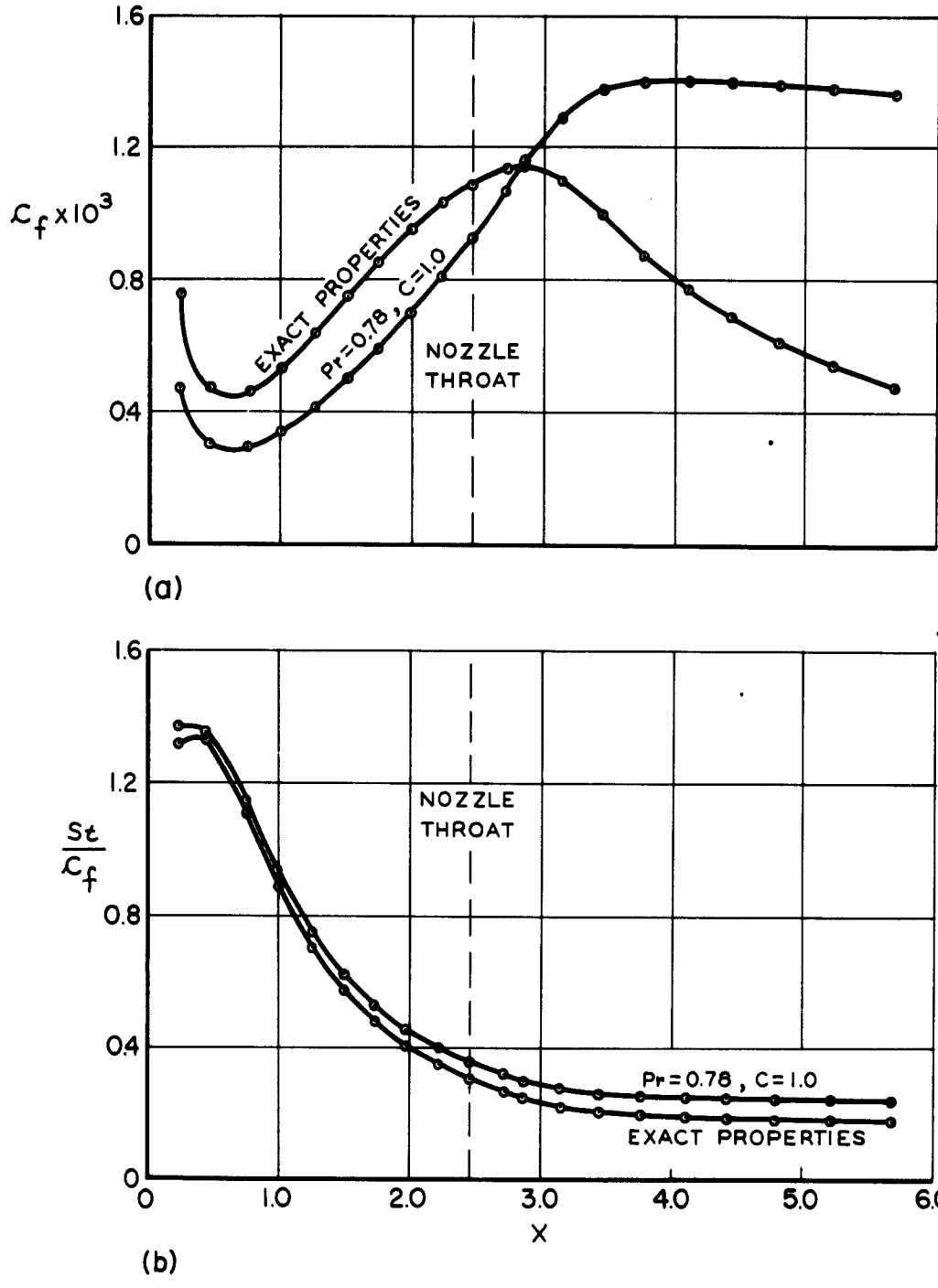

Figure 13.–Results of calculation for the rocket nozzle.
(a) Skin friction. (b) Ratio of Stanton number to skin friction.

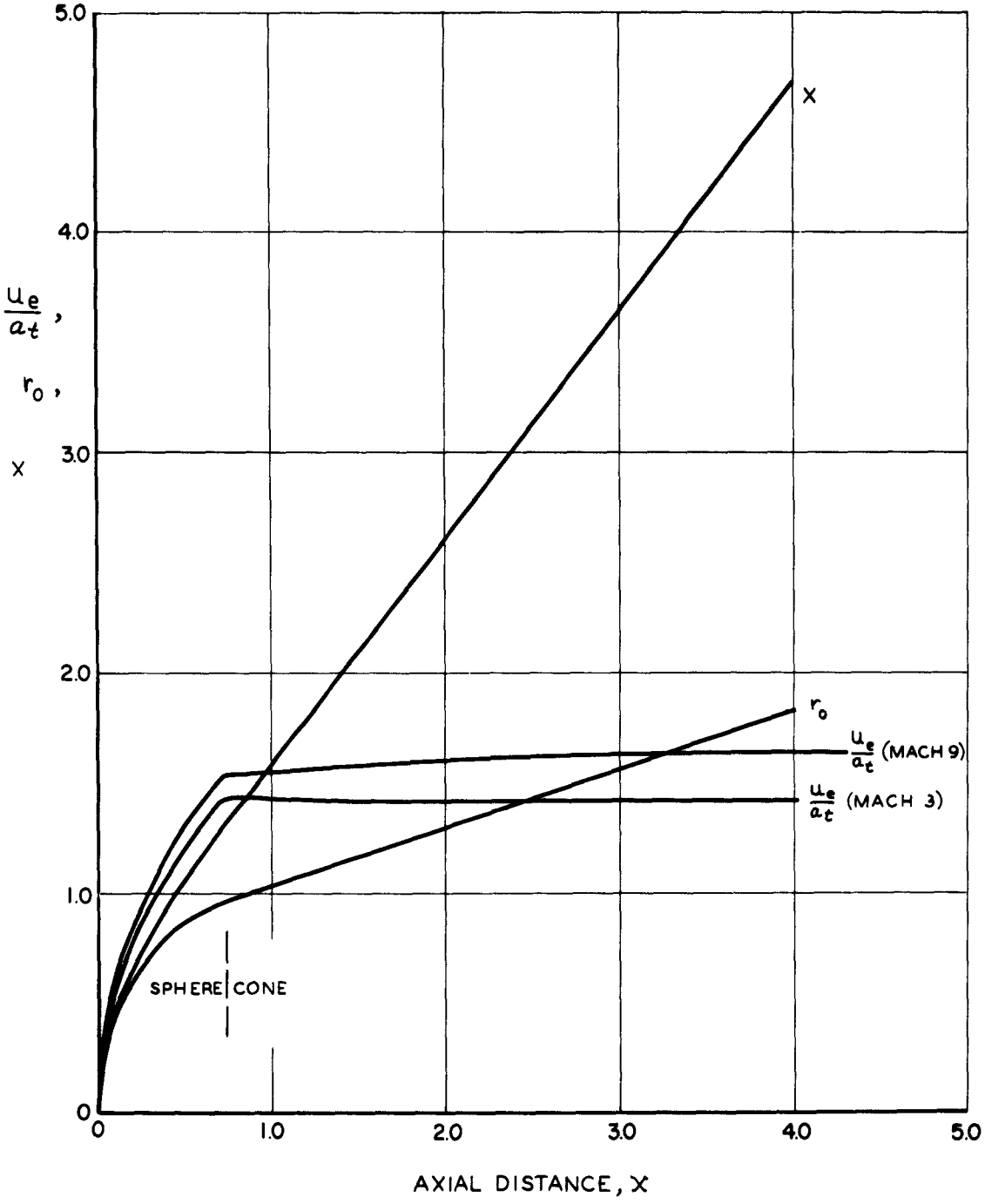

Figure 14.–Variation of local velocity, body radius and surface distance with axial distance for a spherically blunted cone. $M_\infty = 3.0$ and 9.0.

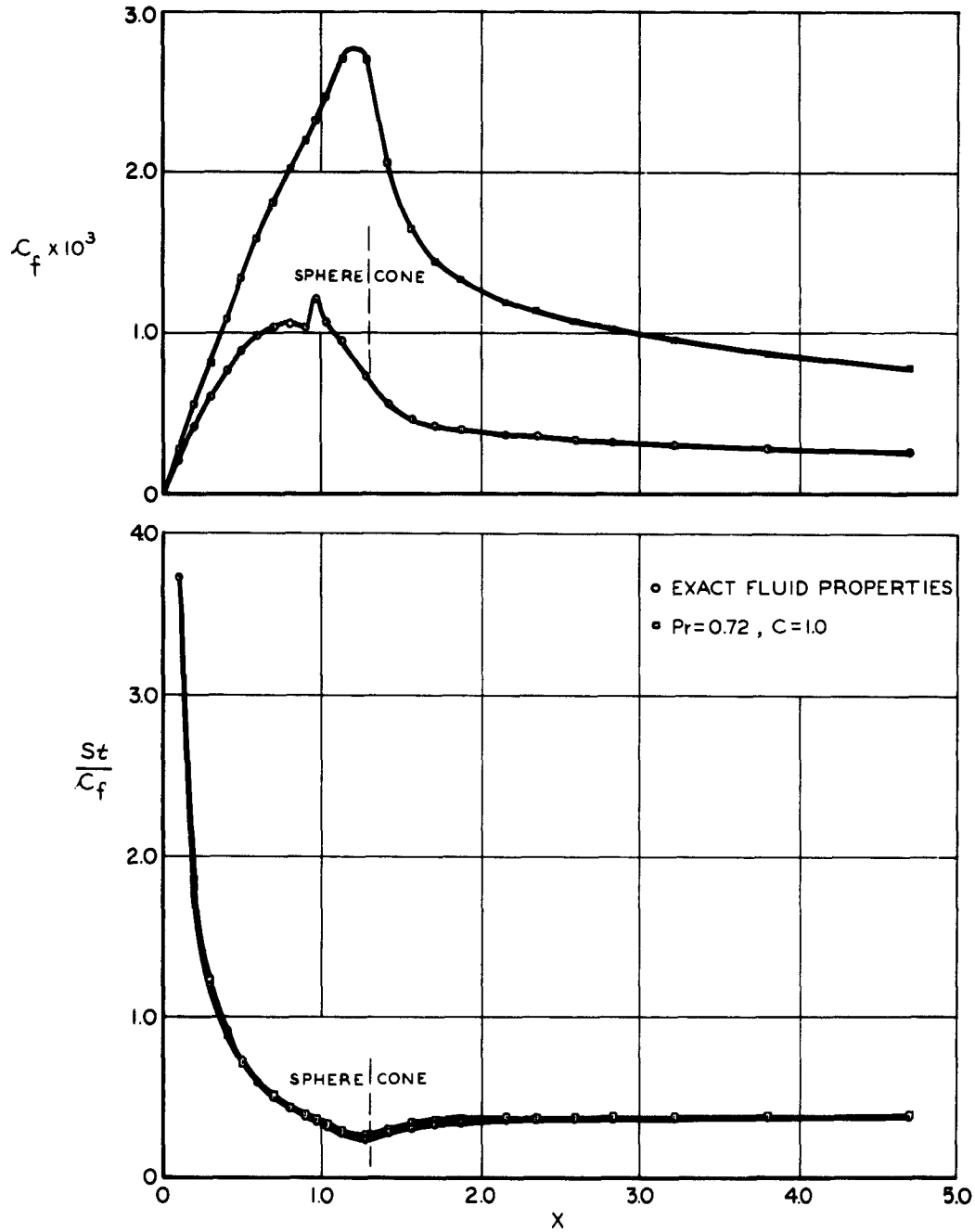

Figure 15.–Results of calculations for the spherically blunted cone at Mach number = 3.0 and 50,000-ft. altitude. (a) Skin friction and Stanton number for $g_w = 0.357$.

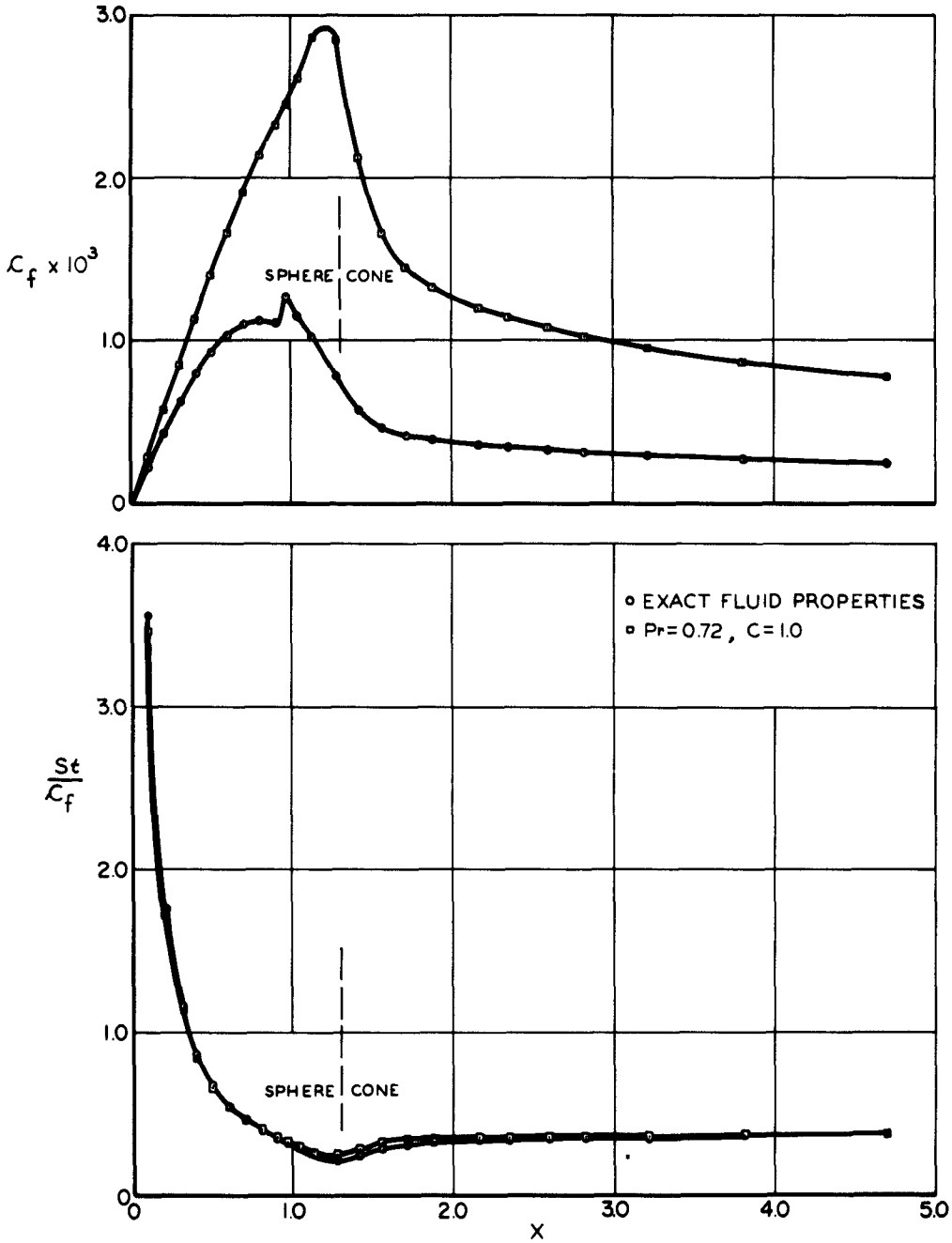

Figure 15.– Continued. (b) Skin friction and Stanton number for $g_w = 0.400$.

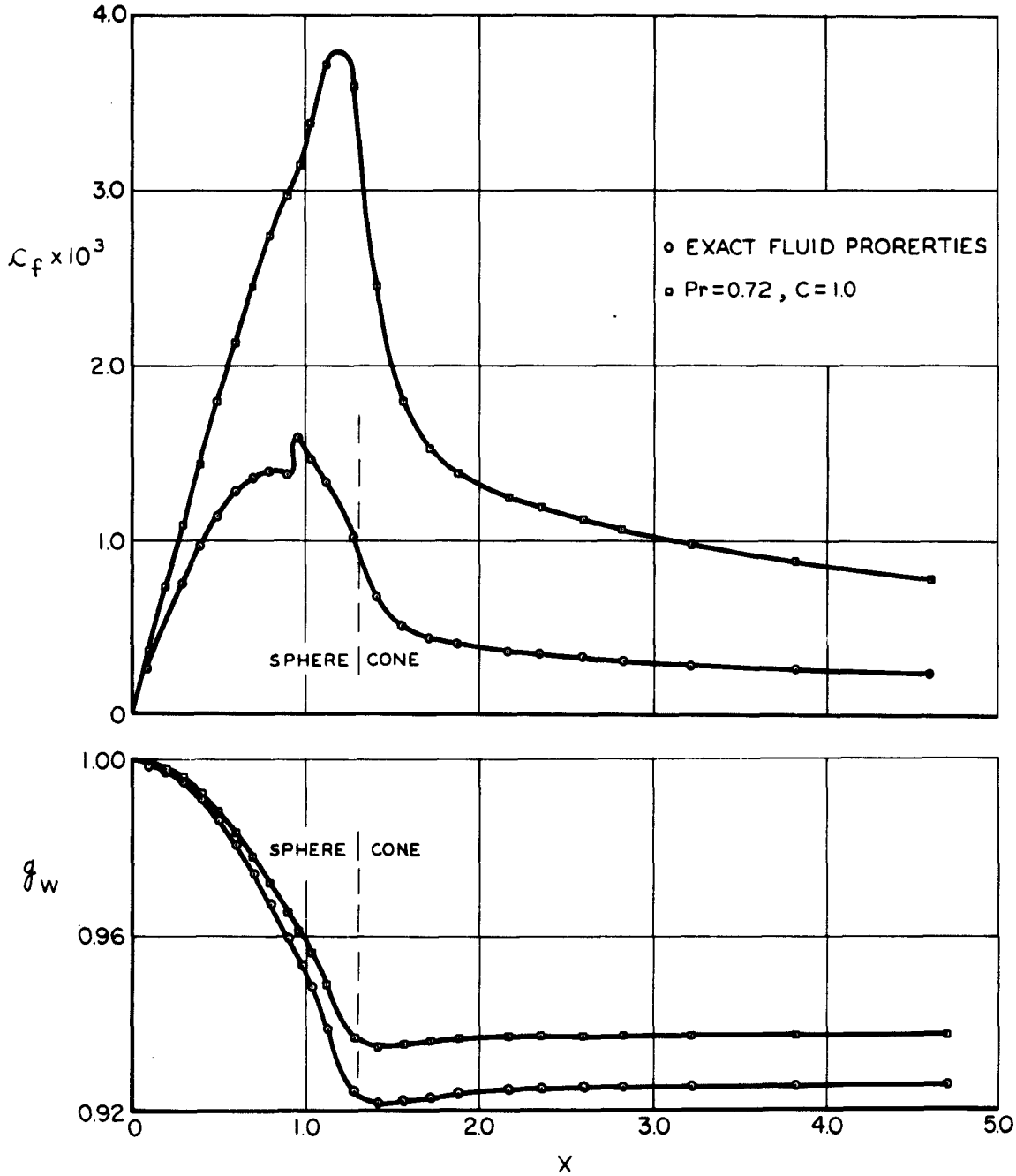

Figure 15.– Concluded. (c) Skin friction and wall enthalpy for $g'_w = 0.0$.

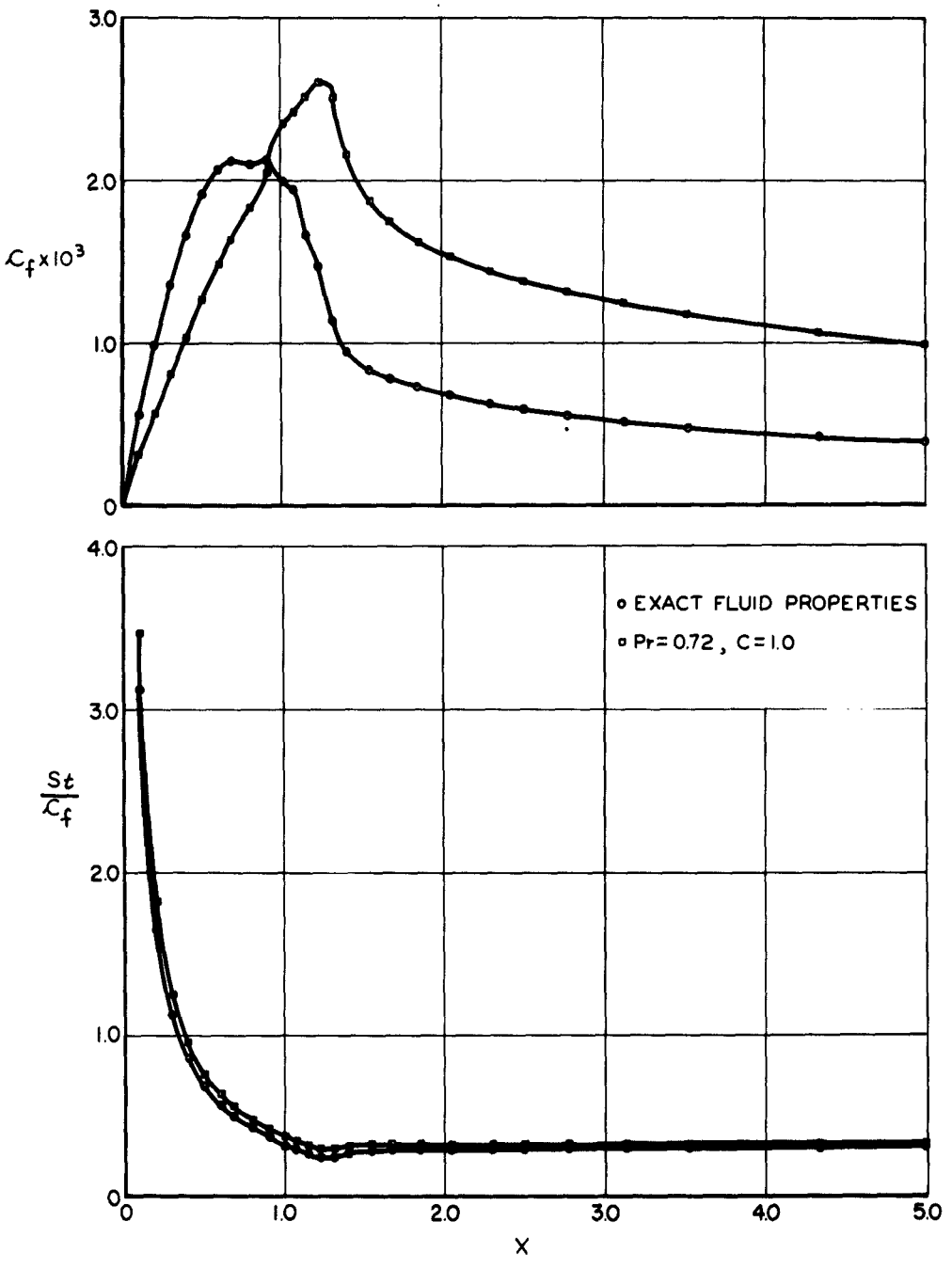

Figure 16.– Results of calculations for the spherically blunted cone at Mach number = 9.0 and 50,000-ft. altitude. (a) Skin friction and Stanton number for $g_w = 0.083124$.

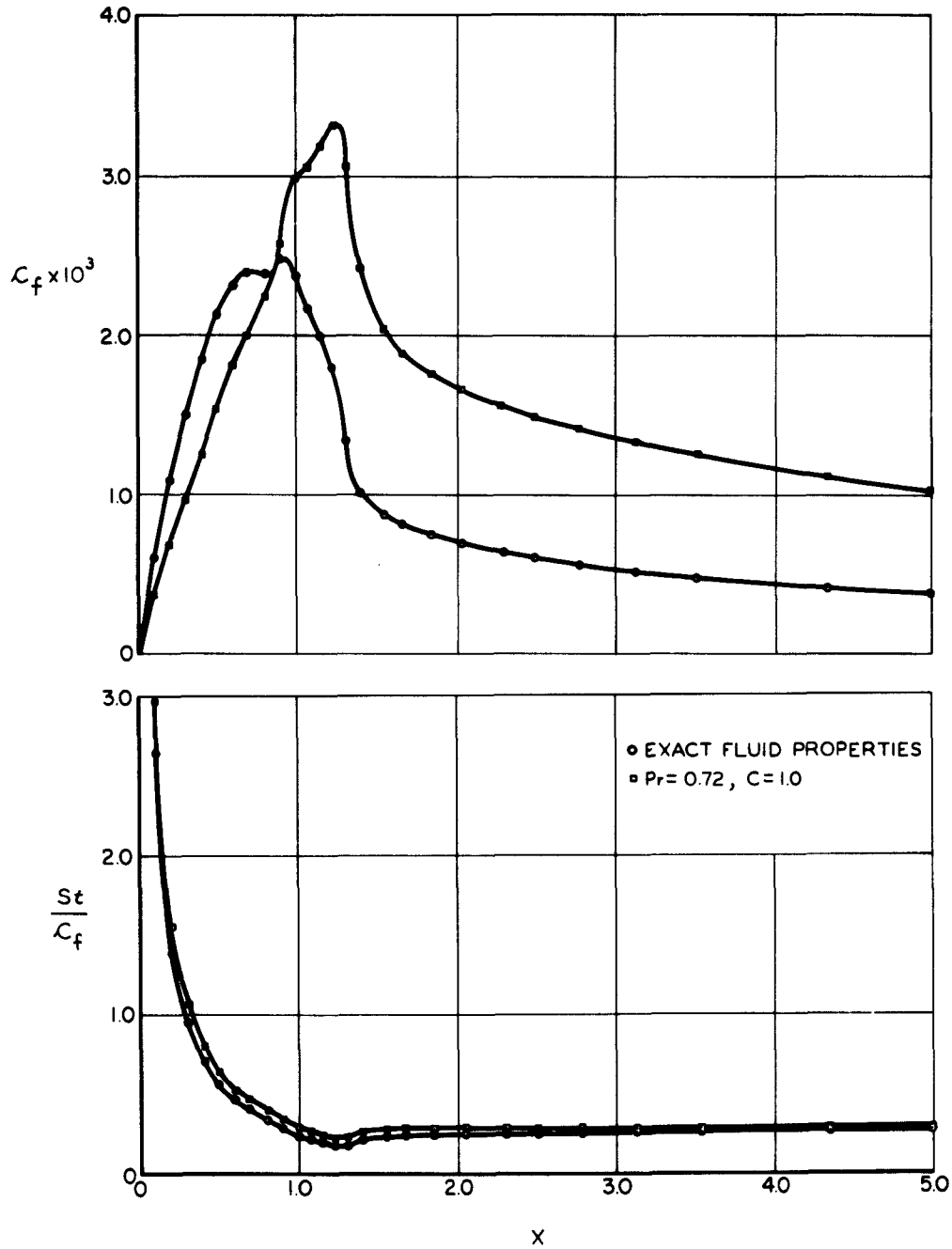

Figure 16.– Continued. (b) Skin friction and Stanton number for $g_w = 0.400$.

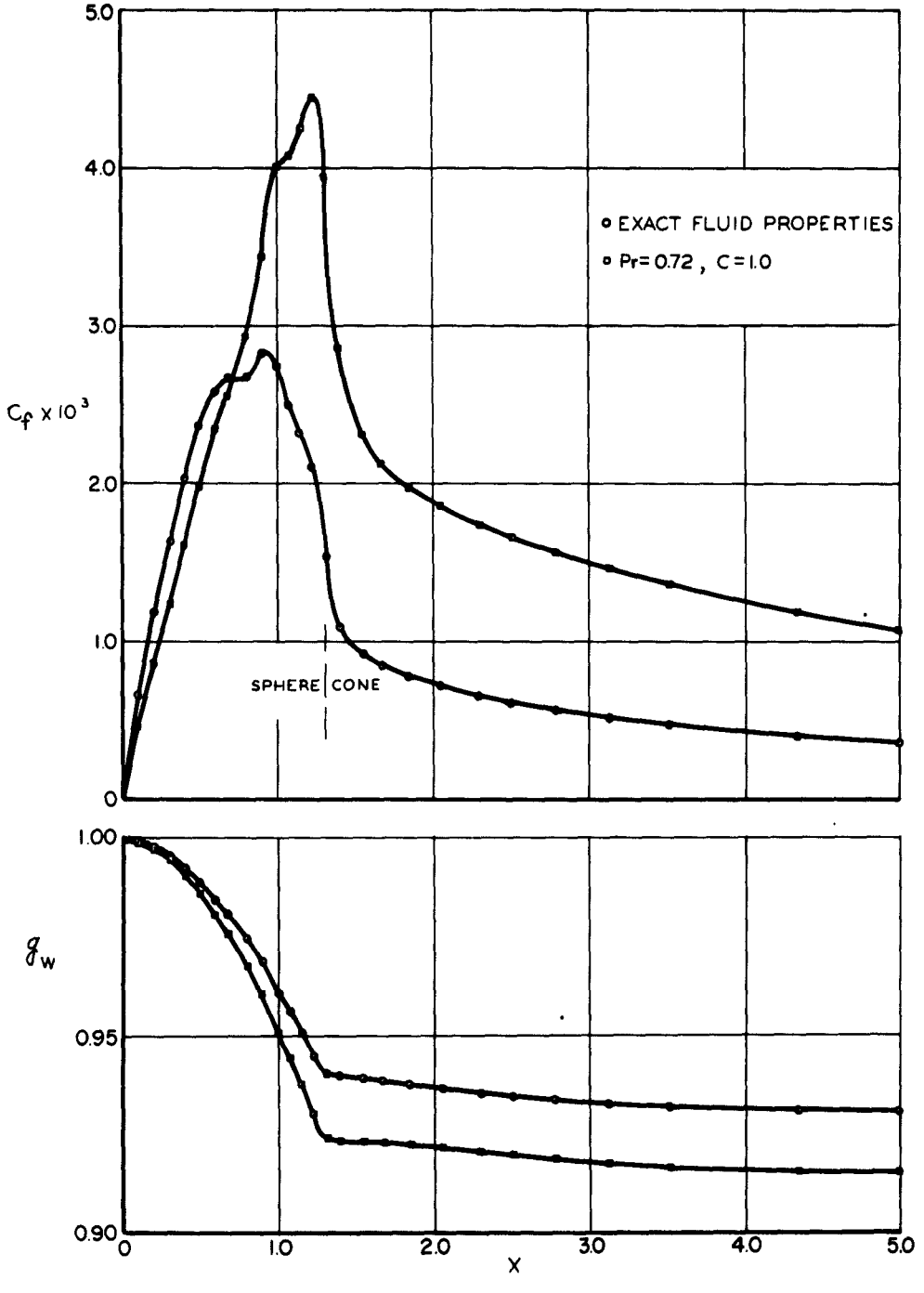

Figure 16.– Concluded. (c) Skin friction and wall enthalpy for $g'_w = 0.0$.

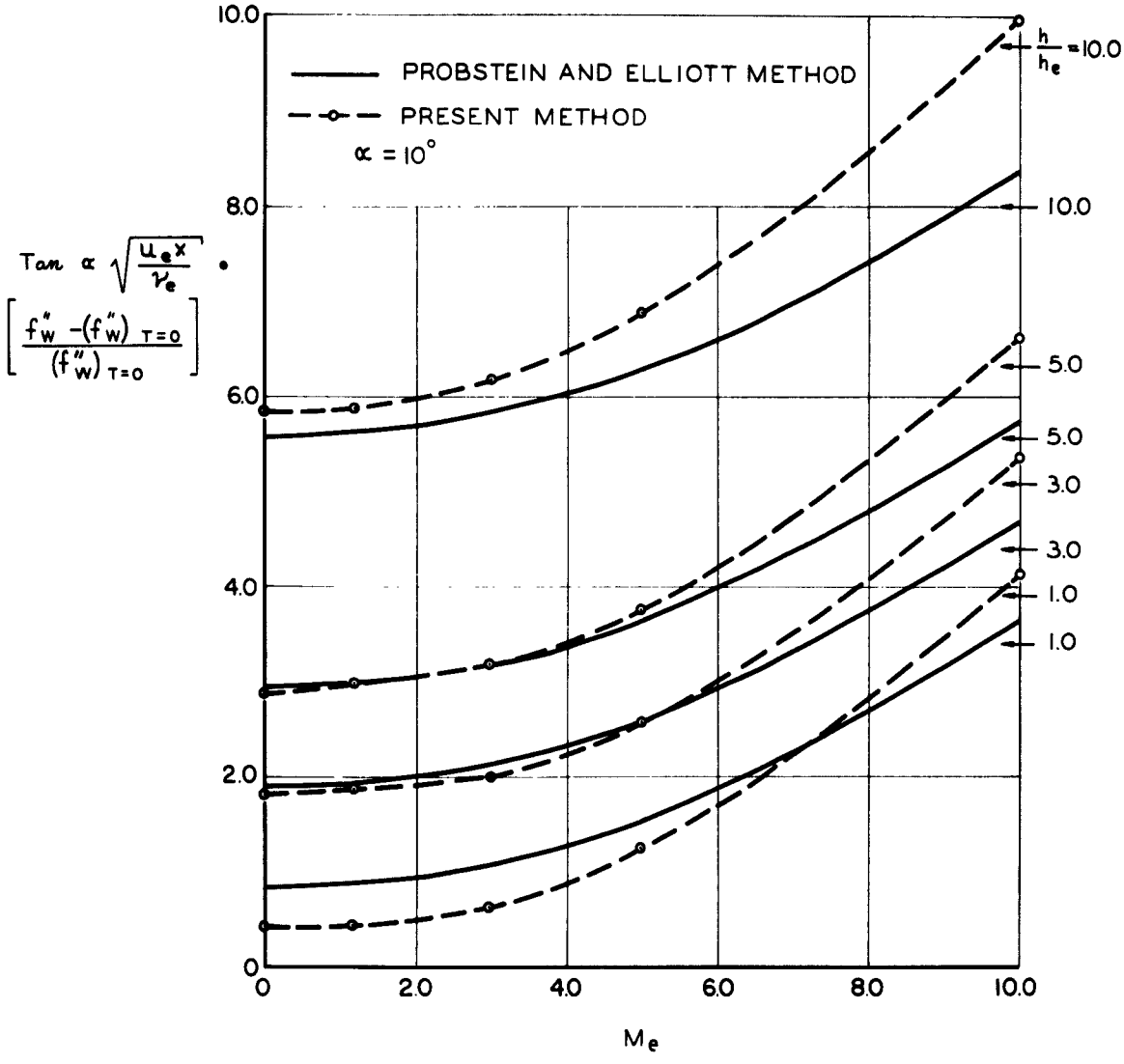

Figure 19.– Transverse curvature effect on shear parameter for flow over a cone for Pr = 1.0, γ = 1.4. Comparison of present method with first-order effect of Probstein and Elliott. Pr = 1.0; C = 1.0; α = 10°; Re = 10^4/ft.

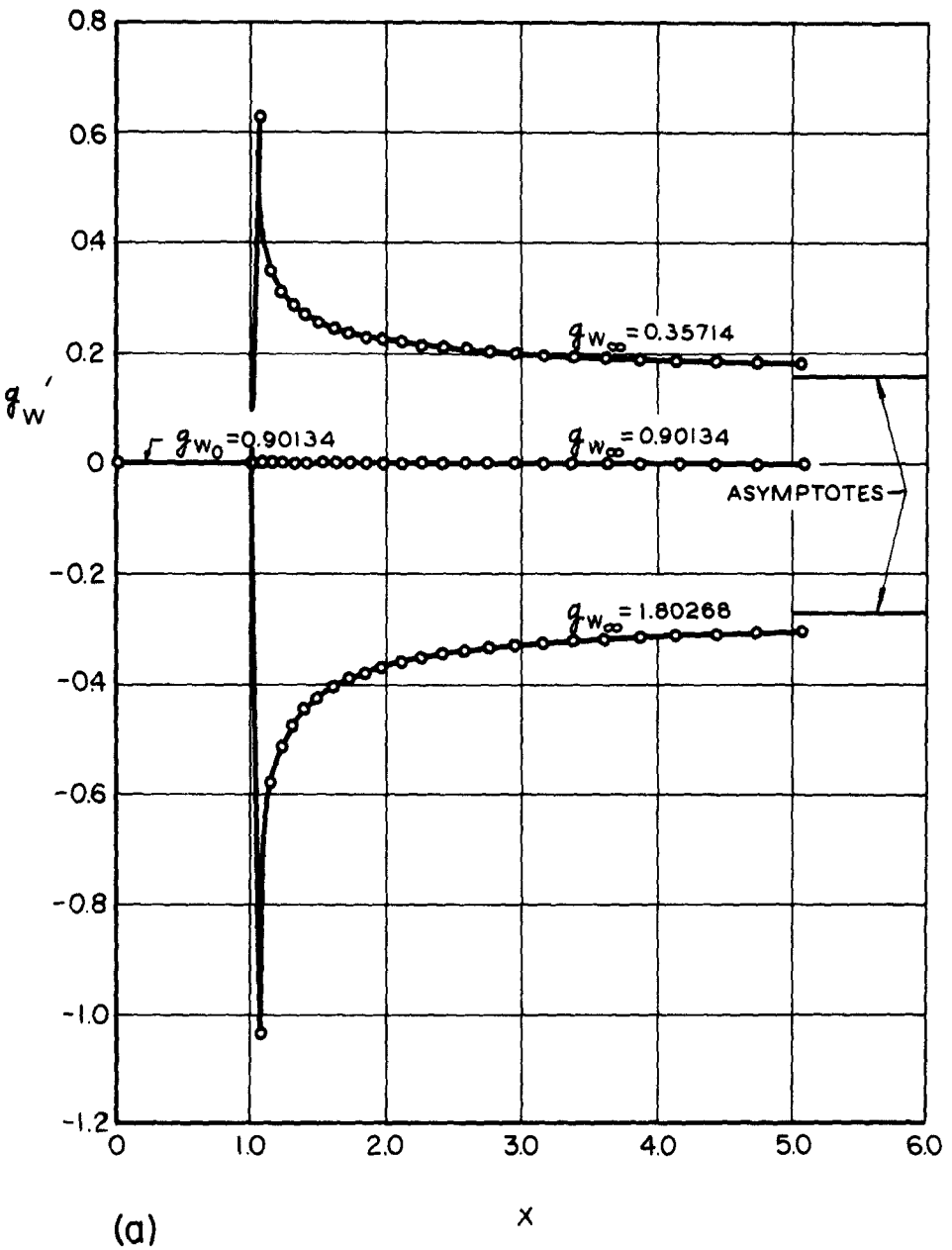

Figure 20.- Effect of discontinuities in g_w on the solution of flow over a flat plate at Mach number = 3.0. Pr = 0.72; C = 1.0; $g_w = g_{w_0}$ for $x \leq 1.0$; $g_w = g_{w_\infty}$ for $x > 1.0$. Positive value of g_w' means that heat is being transferred to surface. Negative value means that heat is being transferred from surface to the air. (a) $g_{w_0} = 0.90134$; $g_{w_\infty} = 0.35714$, 0.90134, and 1.80268.

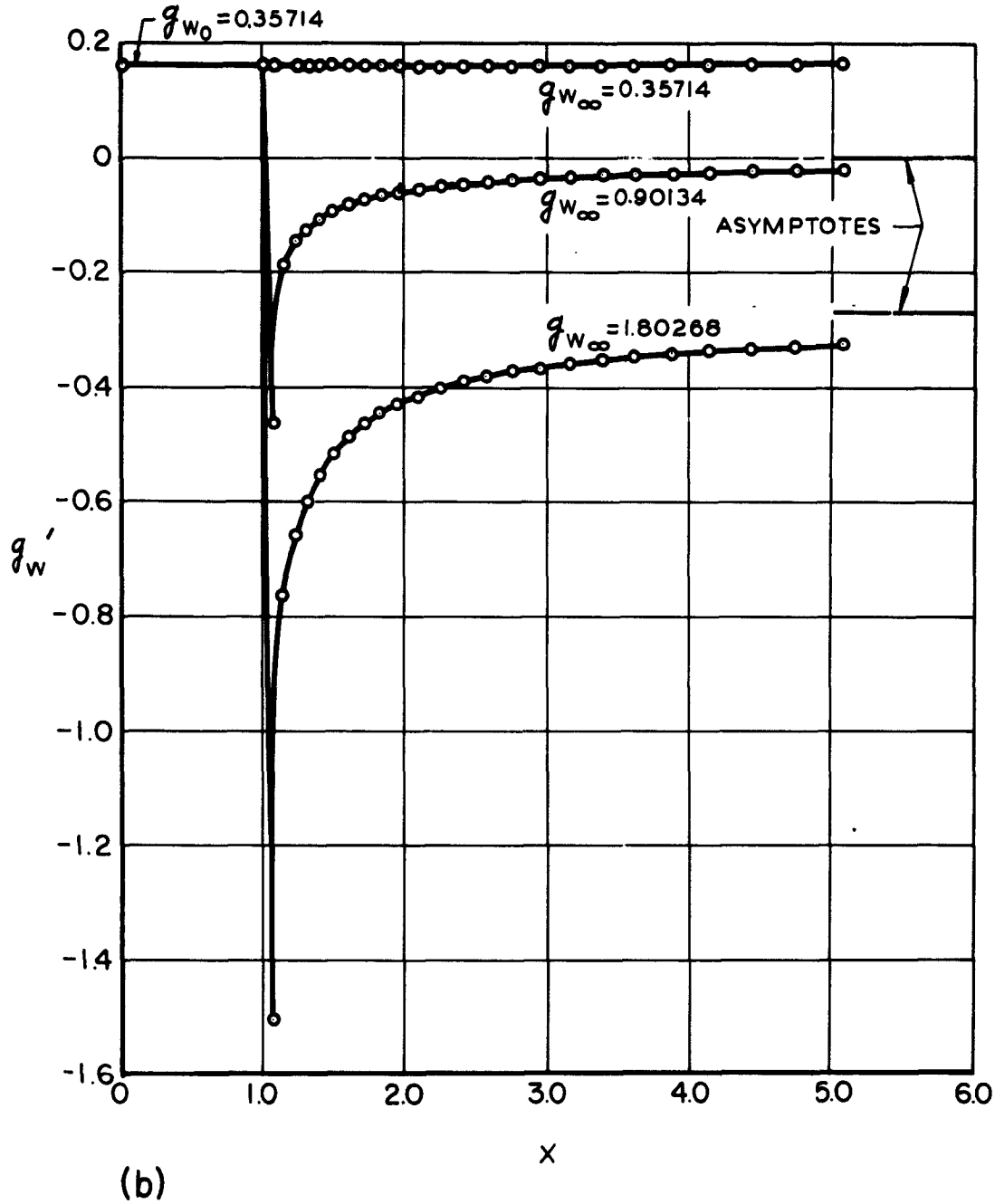

Figure 20.– Continued. (b) $g_{w_o} = 0.35714$; $g_{w_\infty} = 0.35714$, 0.90134, and 1.80268.

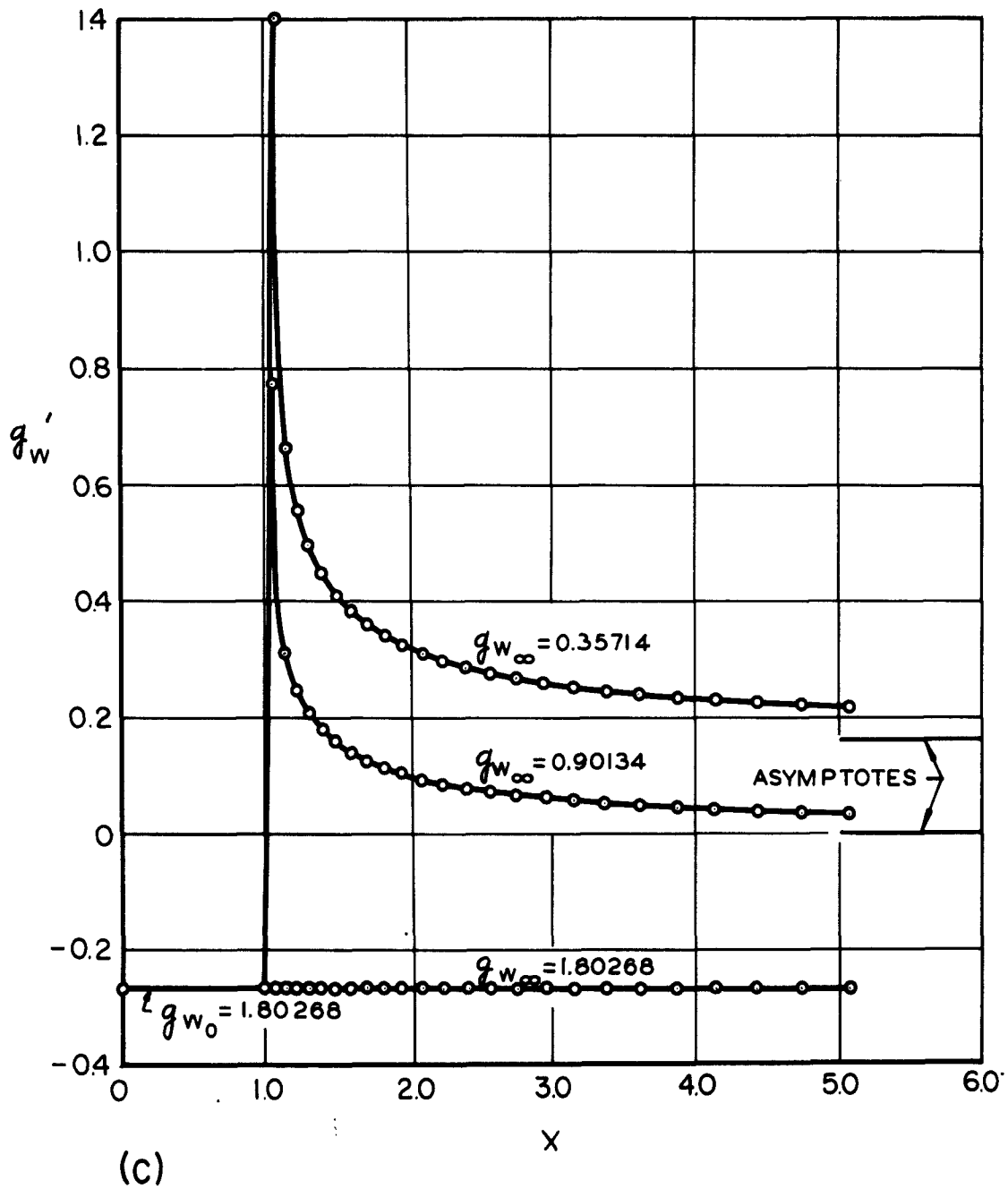

Figure 20.– Concluded. (c) $g_{w_0} = 1.80268$; $g_{w_\infty} = 0.35714$, 0.90134, and 1.80268.

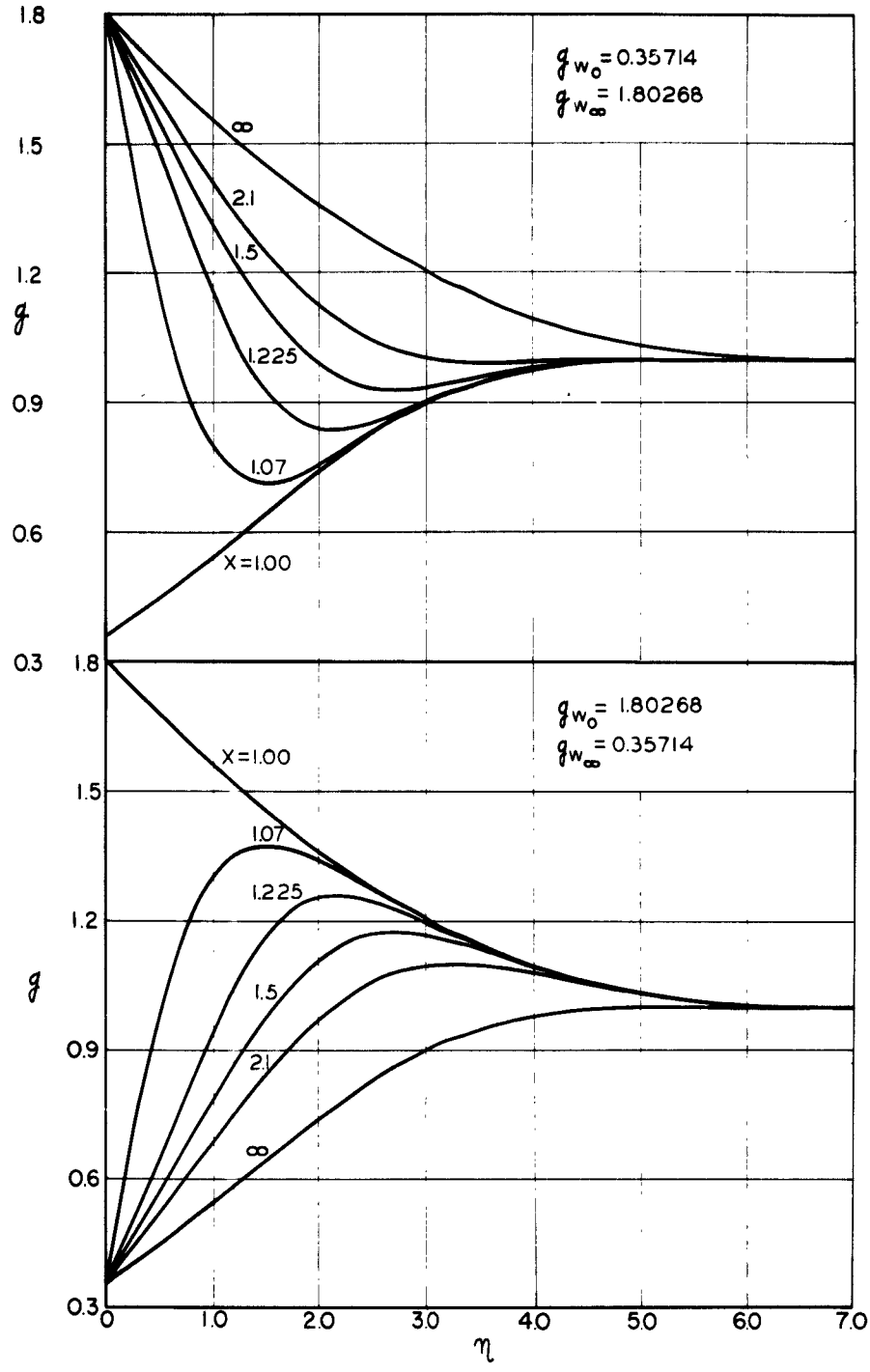

Figure 21.- Enthalpy profiles for two of the flows shown in figure 20.

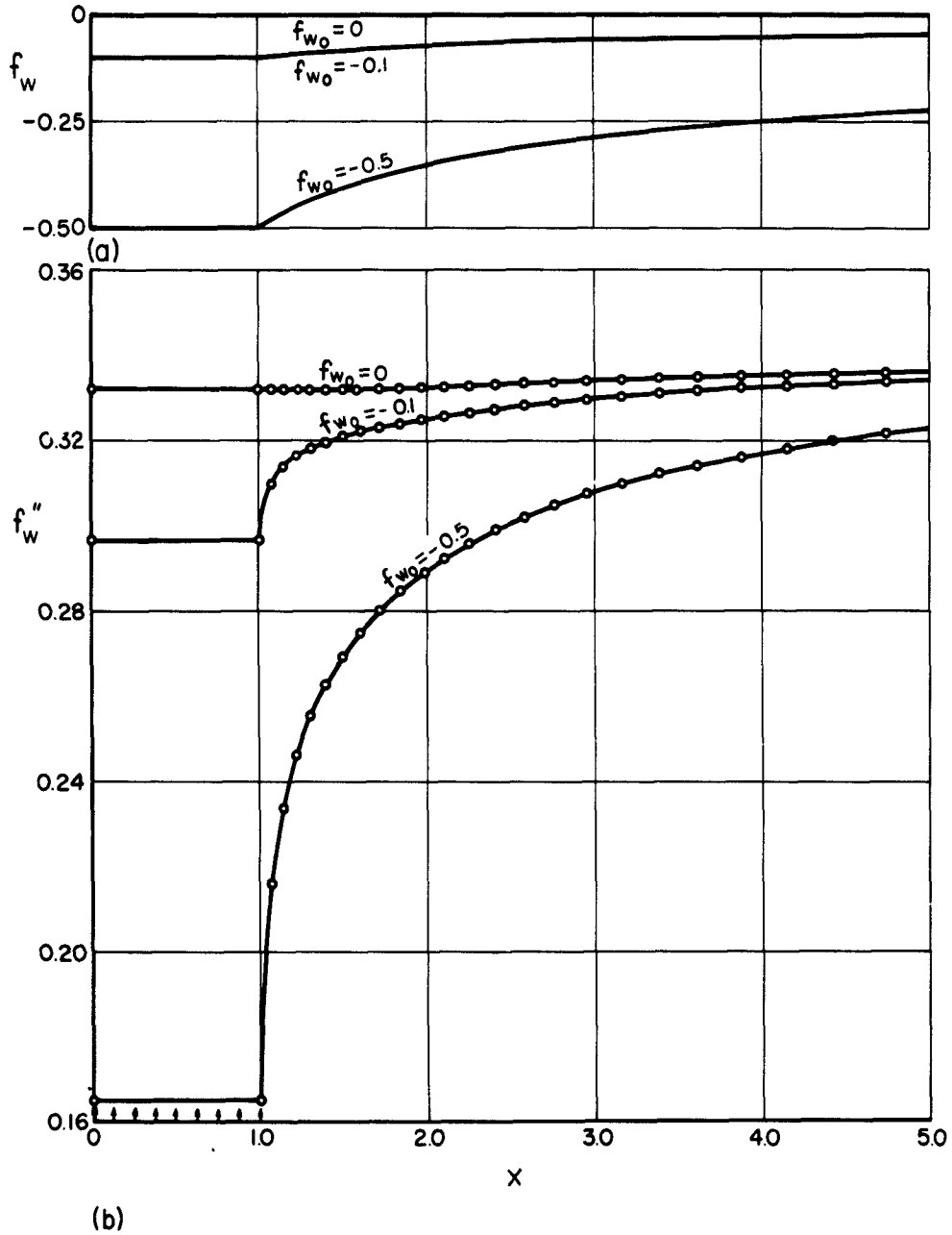

Figure 22.– Effect of discontinuities in mass transfer on the solution of flow over an insulated flat plate ($g'_w = 0.0$). $M_\infty = 3.0$; $Pr = 0.72$; $C = 1.0$. Arrows indicate direction of air flow out of surface.
(a) Mass-transfer quantity f_w versus x. (b) Shear parameter f''_w versus x.

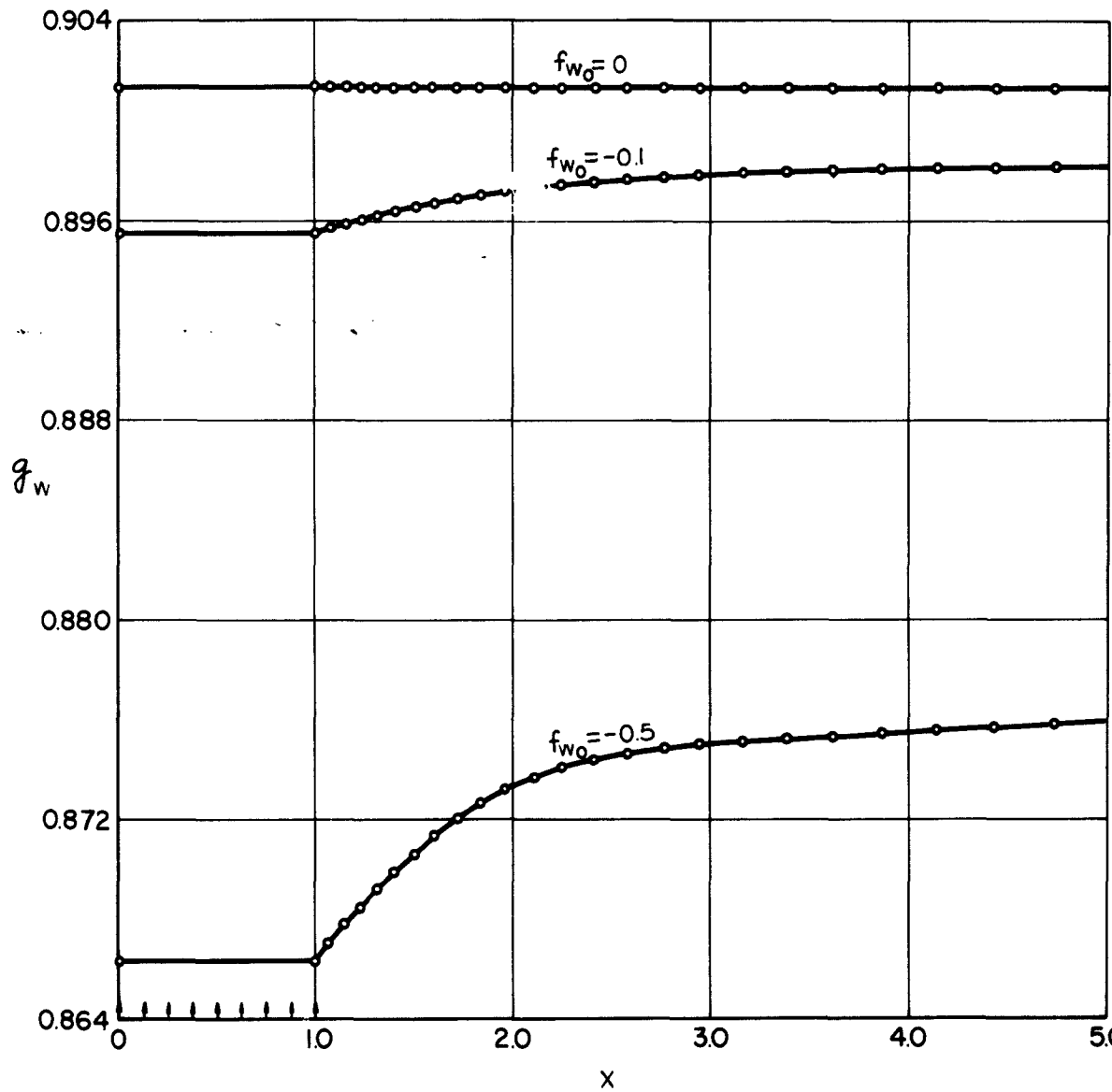

Figure 22.– Concluded. (c) Wall enthalpy g_w versus x.

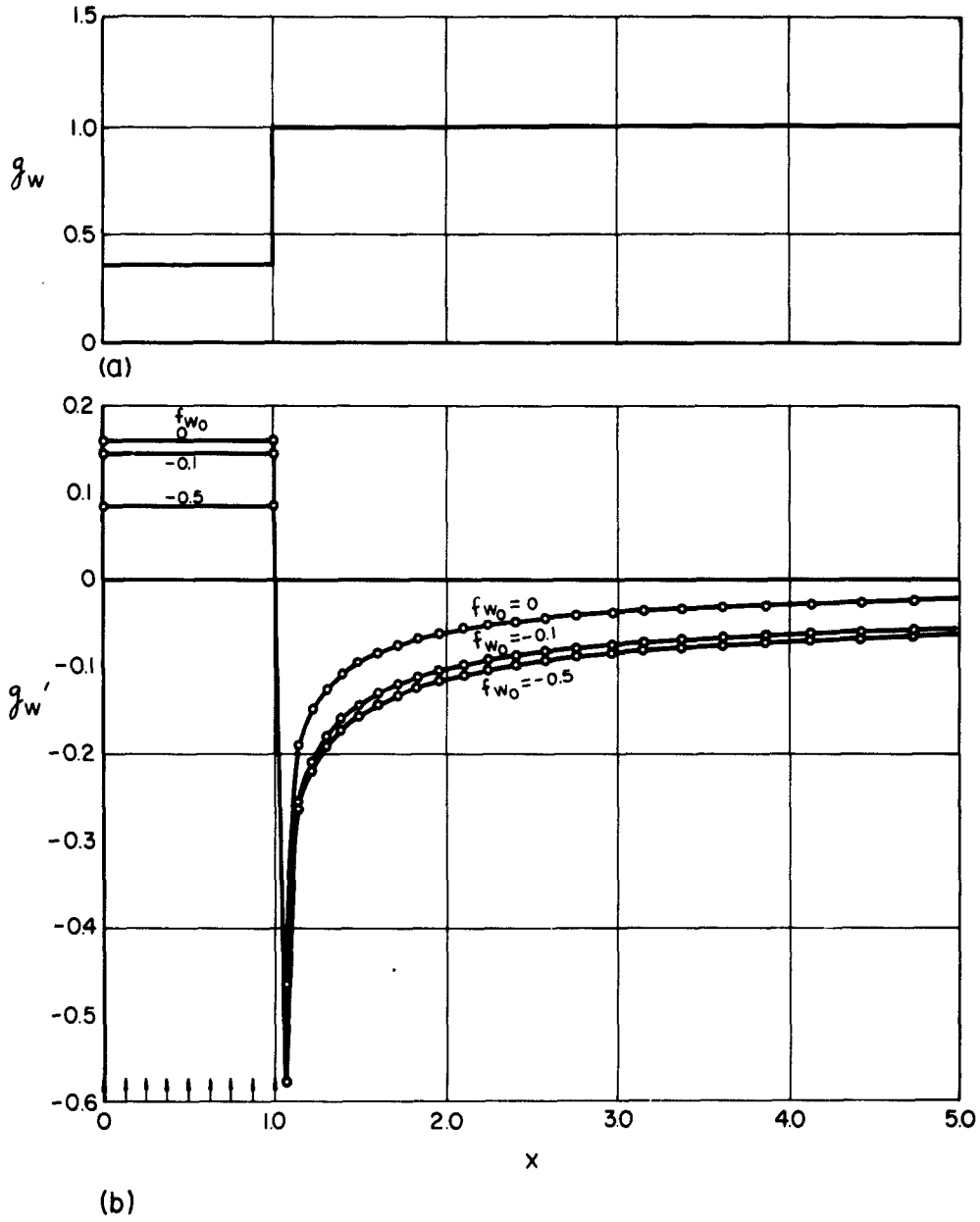

Figure 23.- Effect of blowing cold air at the front of a hot flat plate. External conditions and mass-transfer distributions are the same as shown in figure 22. Also variation of f''_w with x is the same. (a) Wall enthalpy g_w versus x. (b) Heat-transfer parameter g'_w versus x.

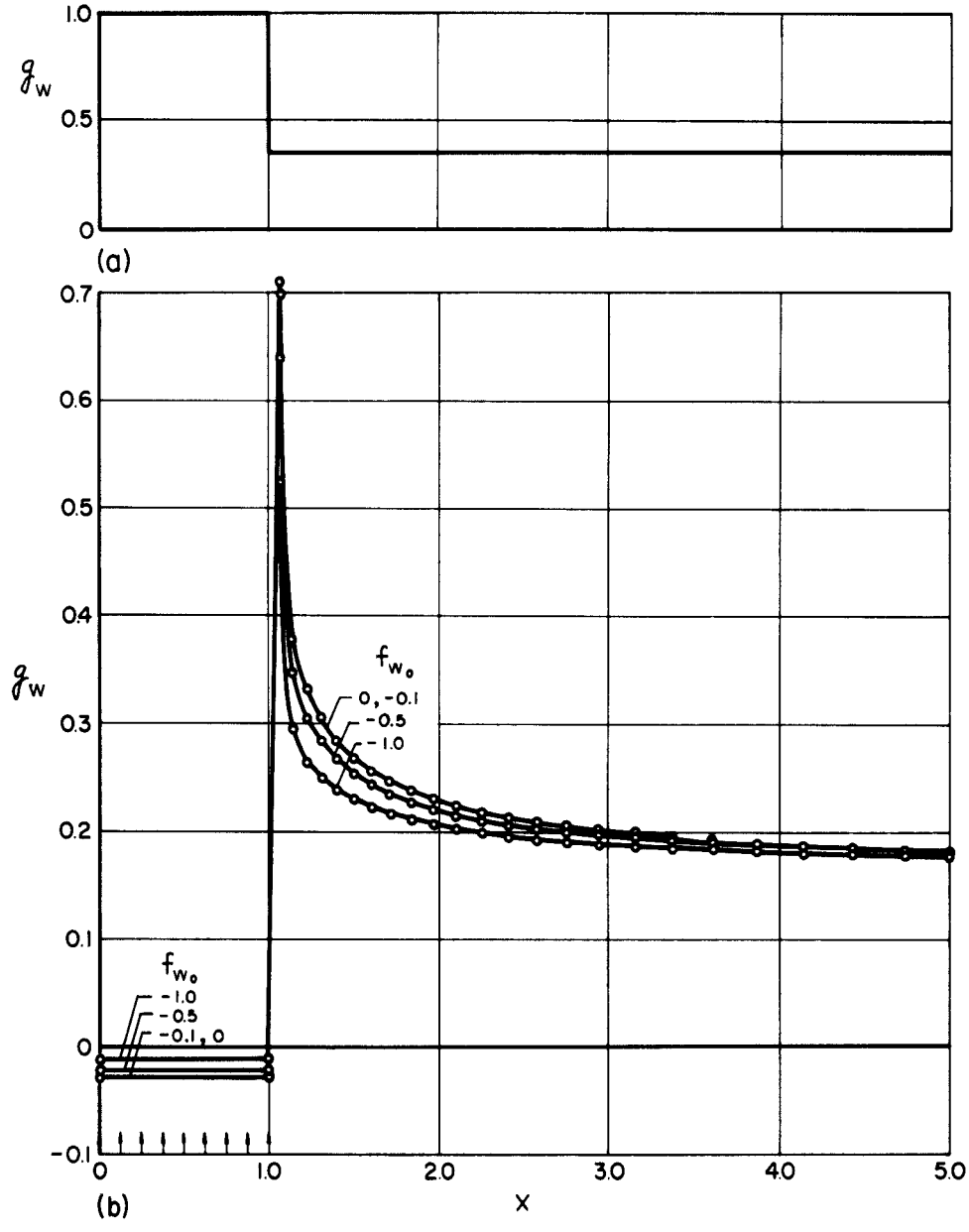

Figure 24.– Effect of blowing hot air at the front of a cold flat plate. External conditions and mass-transfer distributions are the same as shown in figure 22. Also a variation of f''_w with x is the same. (a) Wall enthalpy g_w versus x. (b) Heat-transfer parameter g'_w versus x.

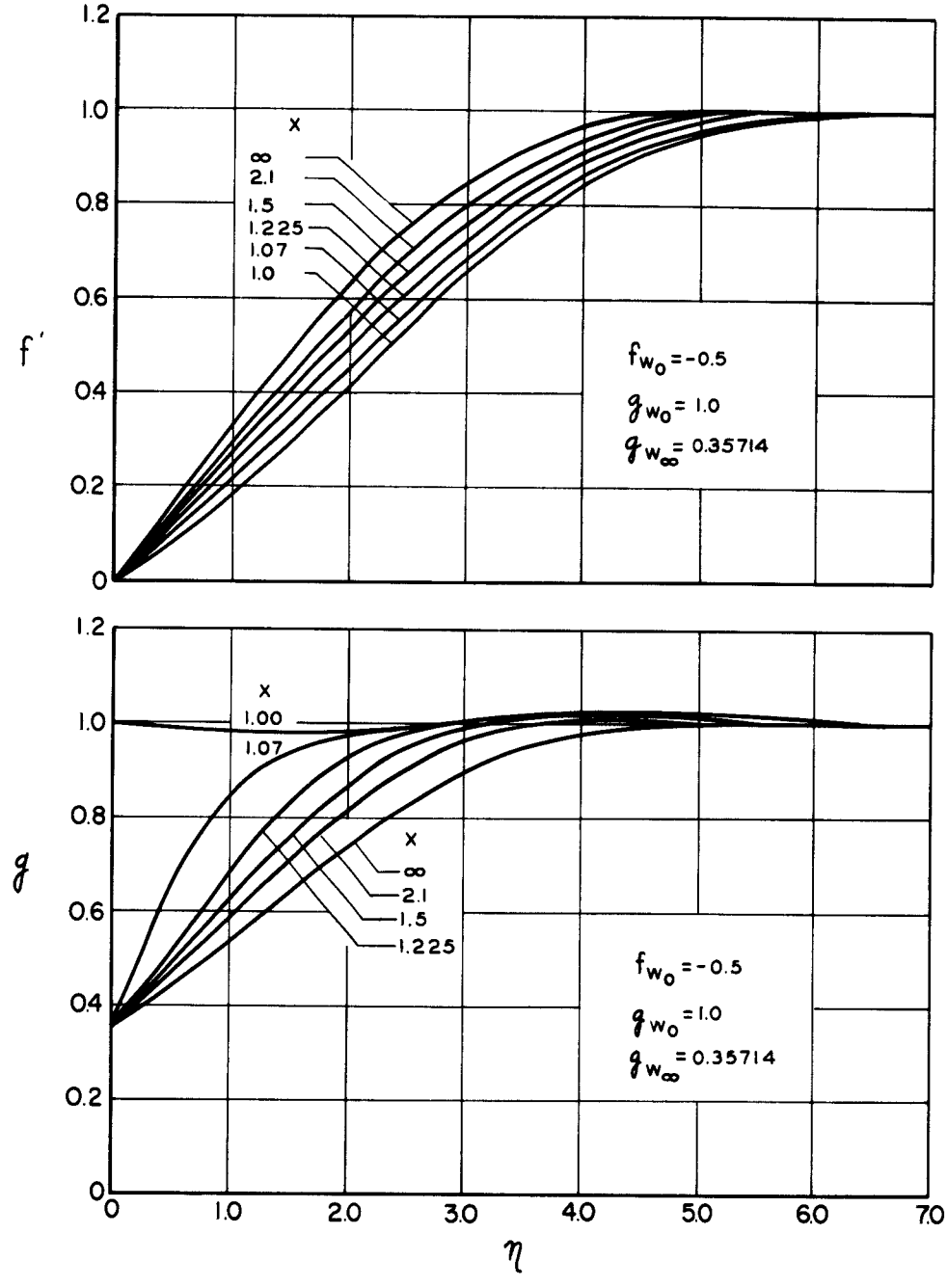

Figure 25.–Velocity and enthalpy profiles for one of the flows described in figure 24.

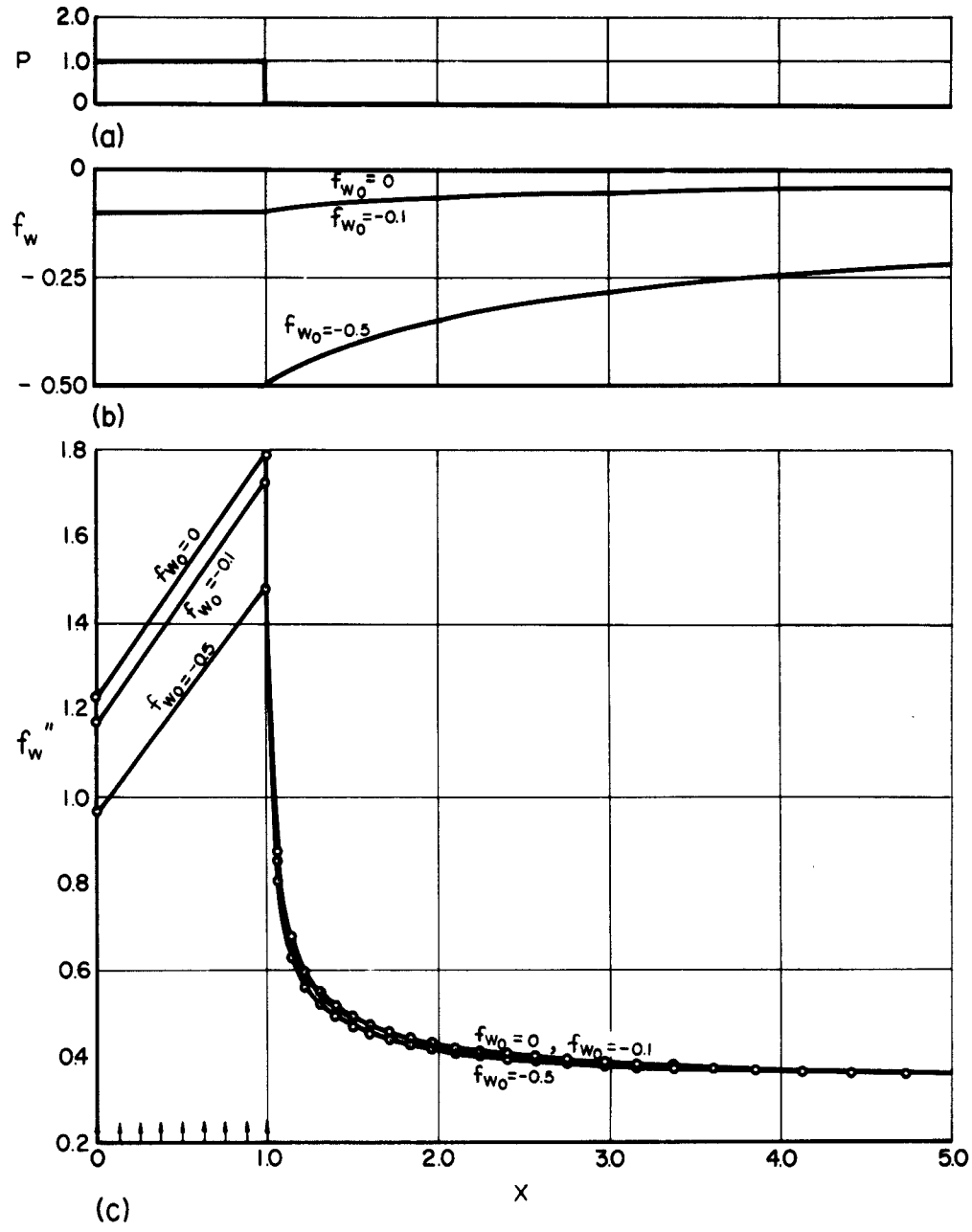

Figure 26.– Effect of blowing at the nose of an insulated blunt body on the solution downstream. $M_\infty = 3.0$; $Pr = 0.72$; $C = 1.0$; $P = 1.0$ for $x \leq 1.0$; $P = 0.0$ for $x > 1.0$. Arrows indicate direction of air flow out of surface. (a) Pressure gradient parameter P versus x. (b) Mass-transfer distribution, f_w versus x. (c) Shear parameter f_w'' versus x.

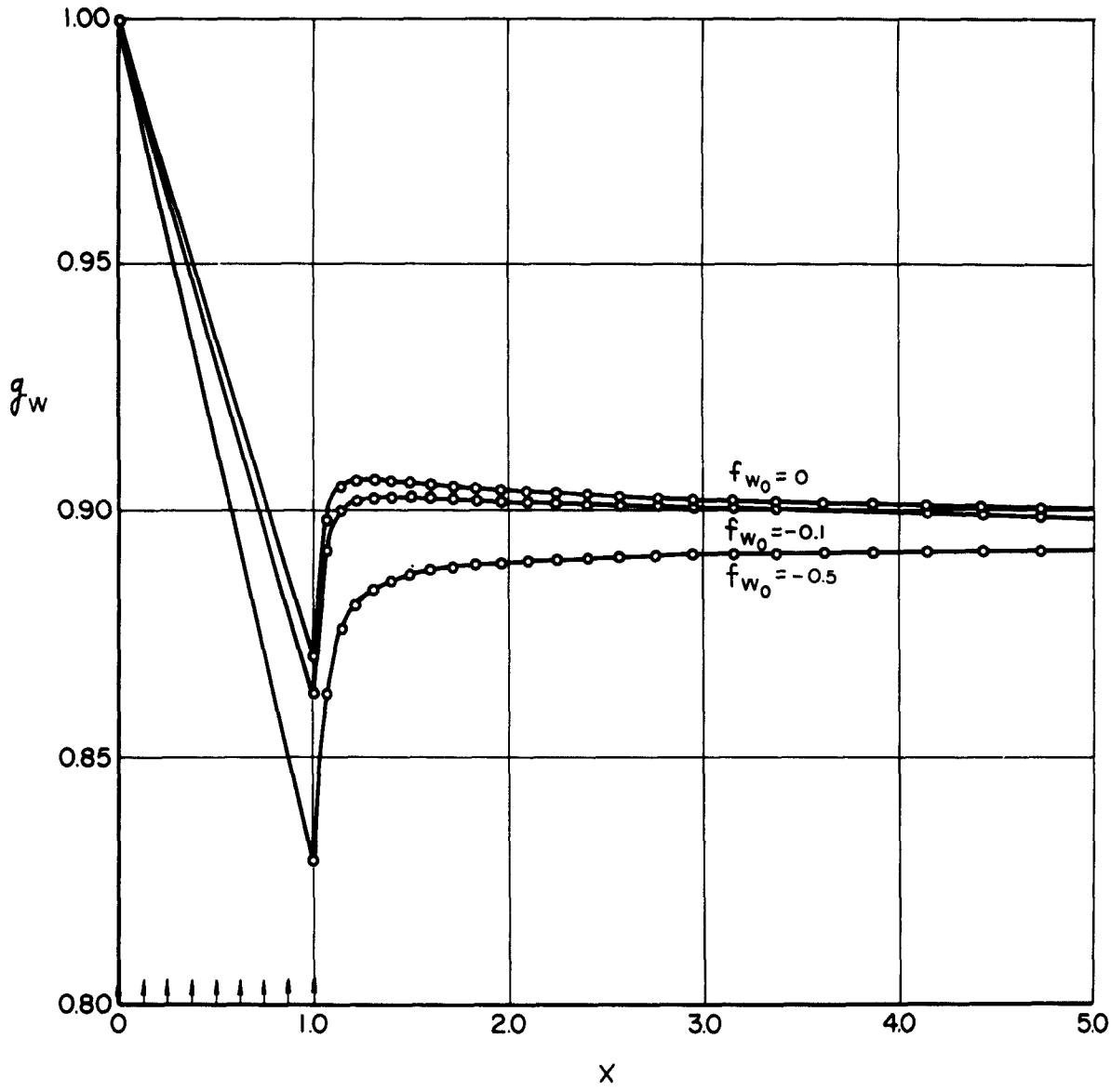

Figure 26.– Concluded. (d) Wall enthalpy, g_w versus x.

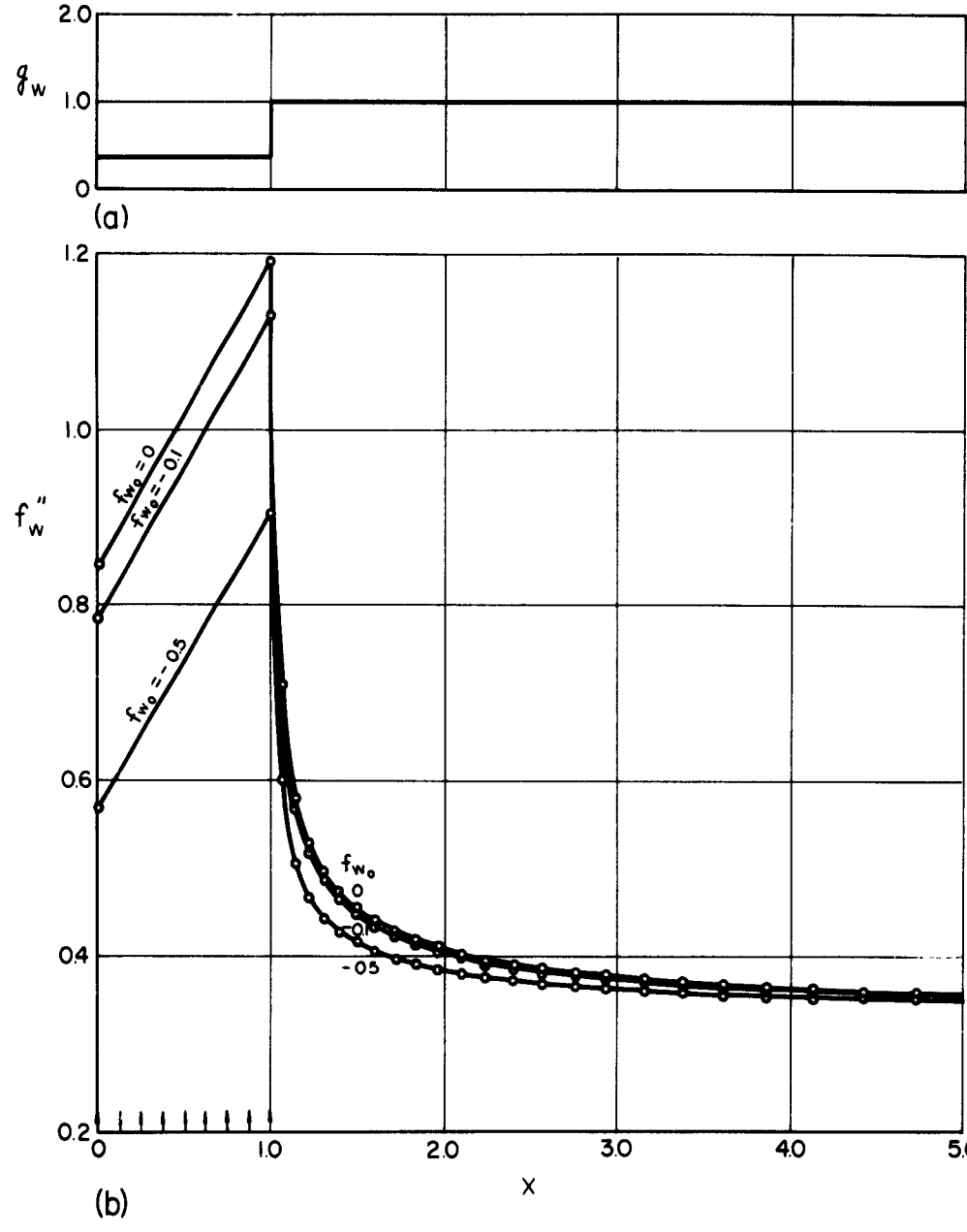

Figure 27.– Effect of blowing cold air at the nose of a hot blunt body on the solution downstream. External flow and mass-transfer distributions are the same as for the flow in figure 26. (a) Wall enthalpy g_w versus x. (b) Shear parameter f''_w versus x.

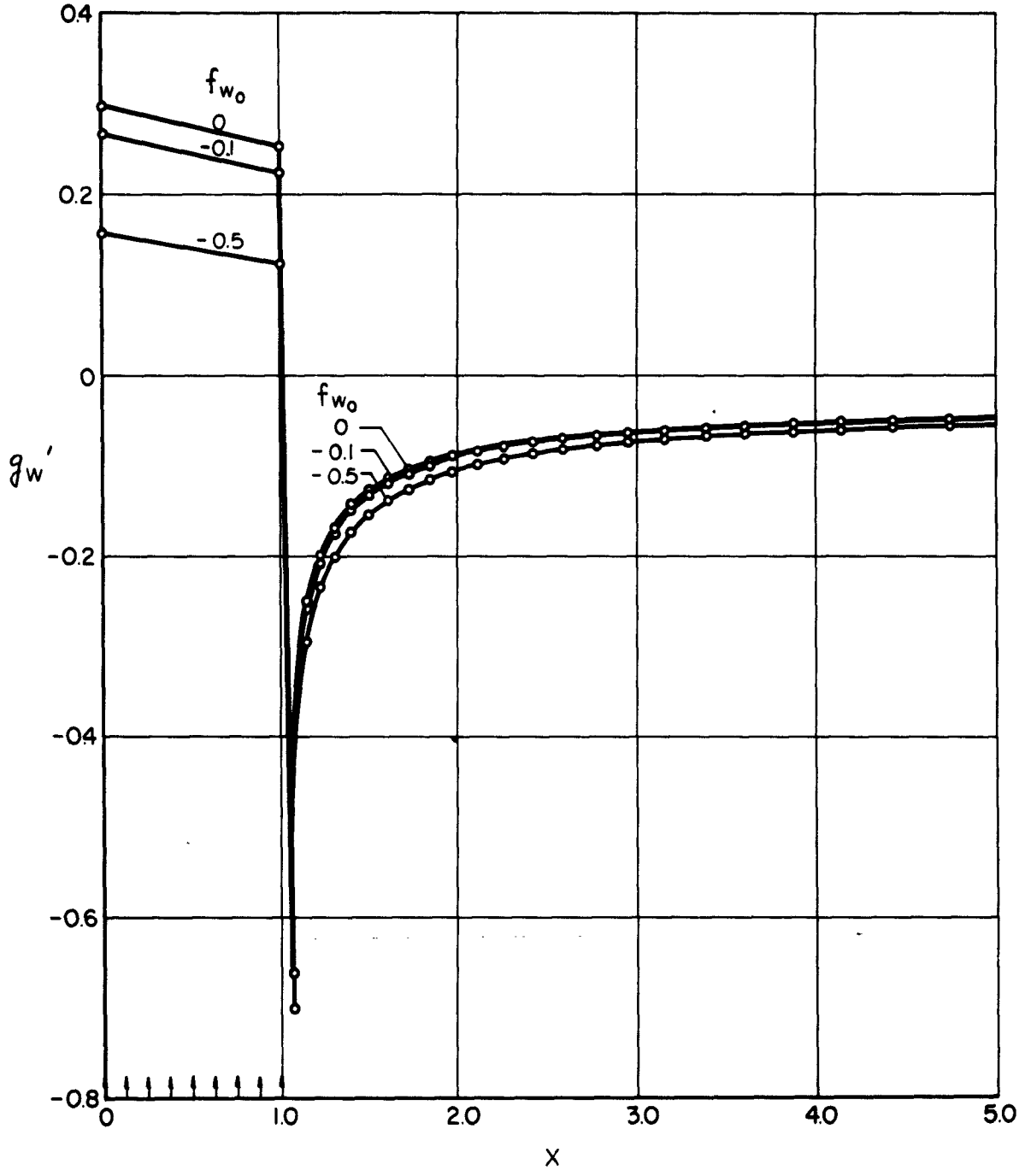

Figure 27.– Concluded. – (c) Heat-transfer parameter g'_w versus x.

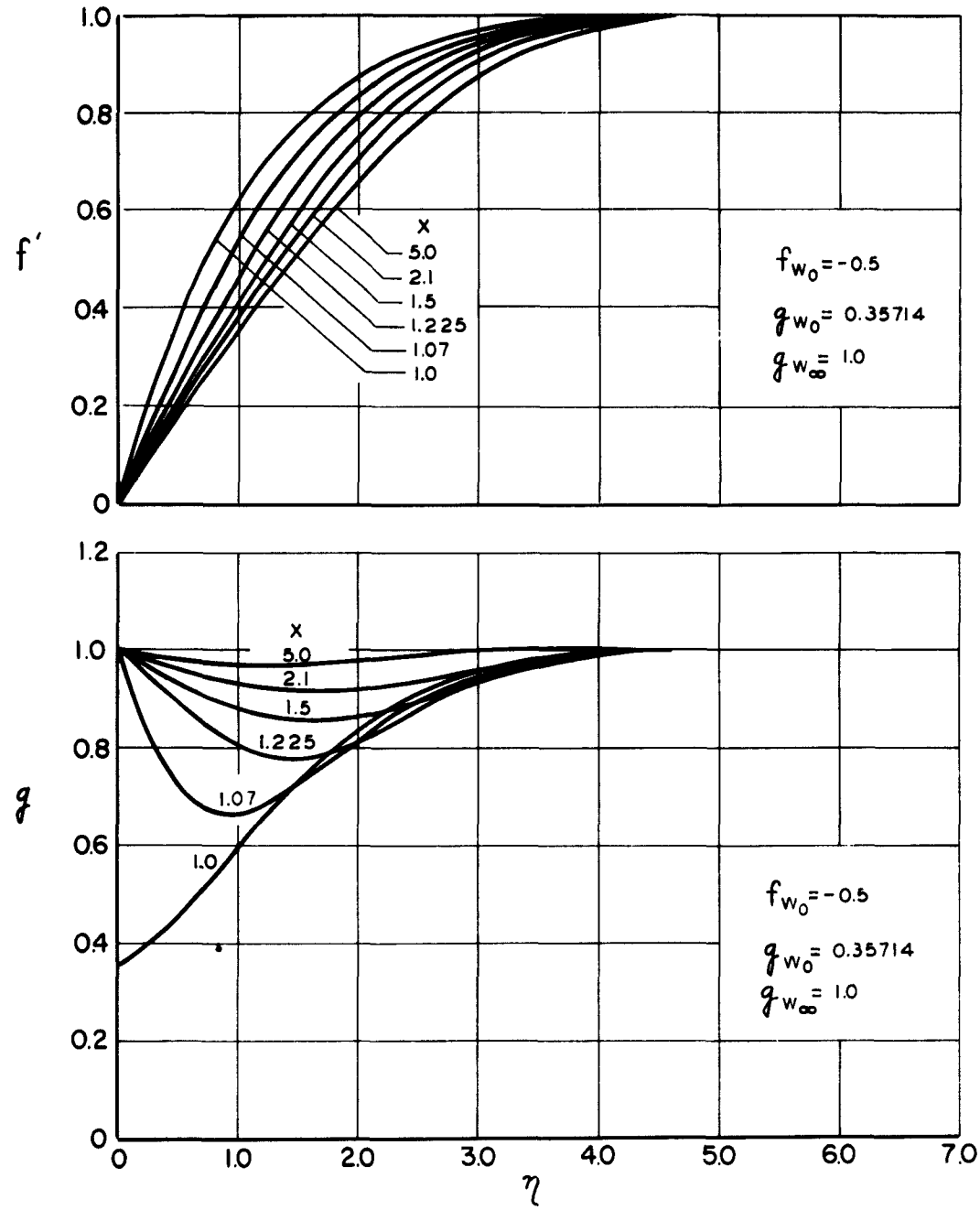

Figure 28.–Velocity and enthalpy profiles for one of the flows described in figure 27.

DISTRIBUTION LIST FOR DOUGLAS AIRCRAFT CO. REPORT NO.

LB 31088, CONTRACT NO. NOw 60-0533c

NAVY

Chief, Bureau of Naval Weapons
Department of the Navy
Washington 25, D. C.
Attn: Code RRRE-4
Code RAAD-3
Code DLI-31

Commanding Officer and Director
David Taylor Model Basin
Carderock, Maryland
Attn: Aerodynamics Laboratory

Commander
Naval Missile Center
Point Mugu, California

Commander
Naval Ordnance Test Station
Inyokern, China Lake, California
Attn: Technical Library

Commander
Naval Ordnance Test Station
Pasadena Annex
Pasadena, California
Attn: Technical Library

Commander
Naval Ordnance Laboratory
White Oak, Silver Spring, Maryland
Attn: Code HL
Code DA

Commander
Naval Weapons Laboratory
Dahlgren, Virginia
Attn: Technical Library

Chief of Naval Research
Department of the Navy
Washington 25, D. C.
Attn: Code 438
Code 461

AIR FORCE

Commander
Office of Aerospace Research
Washington 25, D. C.

Directorate of Aeromechanics
USAF Aeronautical Systems Division
Wright-Patterson Air Force Base, Ohio

Arnold Engineering Development Center
P.O. Box 162
Tullahoma, Tennessee

ARMY

Office of Ordnance Research
Department of the Army
Duke Station
Durham, North Carolina

Ballistic Research Laboratory
Aberdeen Proving Ground
Aberdeen, Maryland

OTHER GOVERNMENT AGENCIES

Commander
Armed Services Technical Information Agency
Arlington Hall Station
Arlington 12, Virginia

National Aeronautics and Space
Administration
1512 H Street N.W.
Washington 25, D. C.

Director
National Bureau of Standards
Washington 25, D. C
Attn: Fluid Mechanics Section

EDUCATIONAL INSTITUTIONS

Guggenheim Aeronautical Laboratory
California Institute of Technology
Pasadena 4, California
Attn: Dr. Clark B. Millikan

Applied Physics Laboratory
Johns Hopkins University
P.O. Box 244 - Rt. 1
Laurel, Maryland
Attn: Technical Reports Office

Department of Aeronautics
Johns Hopkins University
Baltimore 18, Maryland
Attn: Dr. F. H. Clauser

Institute for Fluid Mechanics
and Applied Mathematics
University of Maryland
College Park, Maryland
Attn: Professor J. M Burgers

Massachusetts Institute of Technology
Cambridge 39, Massachusetts
Attn: Aerophysics Laboratory

Defense Research Laboratory
University of Texas
P.O. Box 8029
Austin, Texas
Attn: Professor M. J. Thompson

INDUSTRIAL ORGANIZATIONS

Ling-Temco-Vought-Corporation
P.O. Box 1508
Dallas 22, Texas

General Dynamics/Convair
P.O. Box 1950
San Diego 12, California
Attn: Mr. C. W. Frick

Grumman Aircraft Engineering Corporation
Bethpage, Long Island, New York
Attn: Fluid Mechanics Section

Lockheed Aircraft Corporation
Burbank, California
Attn: Mr. L. A. Rodert

McDonnell Aircraft Corporation
St. Louis, Missouri
Attn: Mr. G. S. Graff

Norair Division
Northrop Corporation
1001 East Broadway
Hawthorne, California
Attn: Dr. W. Pfenninger

North American Aviation, Inc.
Aerophysics Department
12214 Lakewood Boulevard
Downey, California
Attn: Dr. E. R. Van Driest

North American Aviation, Inc.
4300 East 5th Avenue
Columbus, Ohio
Attn: Mr. R. M. Crone

Cornell Aeronautical Laboratory
4455 Genesee St.
Buffalo 21, New York

Douglas Aircraft Company. Report LB 31088
SOLUTION OF THE GENERAL BOUNDARY-LAYER EQUATIONS FOR COMPRESSIBLE LAMINAR FLOW, INCLUDING TRANSVERSE CURVATURE, by Darwin W. Clutter and A. M. O. Smith. 15 February 1963, 130 p. incl. Figs.

UNCLASSIFIED

This report describes a method of solving the title problem. The only restrictions on the method are that the flow be axially-symmetric or two-dimensional and that no dissociation of the fluid occurs. The method is described and reasons for its choice are discussed. Arbitrary fluid properties may be used. Solutions for a wide variety of flows are presented. These establish the accuracy and capabilities of the method.

Douglas Aircraft Company. Report LB 31088
SOLUTION OF THE GENERAL BOUNDARY-LAYER EQUATIONS FOR COMPRESSIBLE LAMINAR FLOW, INCLUDING TRANSVERSE CURVATURE, by Darwin W. Clutter and A. M. O. Smith. 15 February 1963, 130 p. incl. Figs.

UNCLASSIFIED

This report describes a method of solving the title problem. The only restrictions on the method are that the flow be axially-symmetric or two-dimensional and that no dissociation of the fluid occurs. The method is described and reasons for its choice are discussed. Arbitrary fluid properties may be used. Solutions for a wide variety of flows are presented. These establish the accuracy and capabilities of the method.

Douglas Aircraft Company. Report LB 31088
SOLUTION OF THE GENERAL BOUNDARY-LAYER EQUATIONS FOR COMPRESSIBLE LAMINAR FLOW, INCLUDING TRANSVERSE CURVATURE, by Darwin W. Clutter and A. M. O. Smith. 15 February 1963, 130 p. incl. Figs.

UNCLASSIFIED

This report describes a method of solving the title problem. The only restrictions on the method are that the flow be axially-symmetric or two-dimensional and that no dissociation of the fluid occurs. The method is described and reasons for its choice are discussed. Arbitrary fluid properties may be used. Solutions for a wide variety of flows are presented. These establish the accuracy and capabilities of the method.

Douglas Aircraft Company. Report LB 31088
SOLUTION OF THE GENERAL BOUNDARY-LAYER EQUATIONS FOR COMPRESSIBLE LAMINAR FLOW, INCLUDING TRANSVERSE CURVATURE, by Darwin W. Clutter and A. M. O. Smith. 15 February 1963, 130 p. incl. Figs.

UNCLASSIFIED

This report describes a method of solving the title problem. The only restrictions on the method are that the flow be axially-symmetric or two-dimensional and that no dissociation of the fluid occurs. The method is described and reasons for its choice are discussed. Arbitrary fluid properties may be used. Solutions for a wide variety of flows are presented. These establish the accuracy and capabilities of the method.